



The Roles of Hypoxia on Neuroblastoma Cell Migration and Invasion

Submitted in accordance with the requirements of the University of Liverpool for the degree of Master of Philosophy by:

Michael Rice

August 2013

Acknowledgement

I would like to express my greatest thanks to all those people who supported me throughout this challenging yet exciting year, without their help this project would never have made it off the drawing board.

I feel truly privileged to have been offered the opportunity to work with such a fantastic group of people on an intriguing and all engrossing subject. Firstly I must thank my Primary Supervisor, Professor Paul Losty, for orchestrating the team and guiding me through the intricate transition from working at the hospital bed to the laboratory bench. His knowledge and expertise have shone throughout the duration of this project, especially when submitting abstracts to conferences and journals. I would also like to thank Dr. Diana Moss for permitting me to enter her lab in order to work with chick embryos.

Dr. Violaine Sée deserves special mention as she wholly accepted me into her team and provided the most excellent advice regarding the direction of this project. Aside from impressive leadership skills Dr. Sée has an innate ability to encourage hard work whilst maintaining a most pleasant atmosphere and an excellent spirit throughout each member of the team. As such it has been an absolute pleasure to work as a member of her team.

My greatest thanks go to Dr. Anne Herrmann. I entered the laboratory a complete novice however her kind and patient style of teaching was the most effective I have ever experience. As a result I now feel completely comfortable working independently at the bench. Demonstrating a wealth of knowledge at every turn Dr. Herrmann lead by example and her hard work most certainly helped to focus my efforts. I truly believe I could not have wished for a better colleague or friend.

I would also like to thank the Royal College of Surgeons and Alder Hey Children's Hospital for generously supporting the work undertaken in this study.

Finally I would like to thank my family for the continuous support they have given me throughout my life and for always encouraging my curiosity.

Abstract

Solid tumours are predisposed to hypoxic conditions due to cellular proliferation outpacing the rate of angiogenesis. Hypoxia is associated with enhanced tumour aggression. We aimed to study how hypoxia influences the migration and invasion of Neuroblastoma, a common and highly lethal, enigmatic childhood cancer.

Fluorescently labelled Neuroblastoma cell lines were cultivated under atmospheric ('normoxic') or hypoxic conditions for 3 days before implantation upon the chorioallantoic membrane (CAM) of chick embryos and observed *in-vivo* for tumour formation and metastasis.

Tumourigenesis was successful regardless of oxygen levels. Normoxic cells failed to metastasise, conversely hypoxic cells invaded the embryo forming tumour spheres in several organs. Interestingly, 'normoxic' cell invasion was observed when implanted alongside hypoxic cells resulting in co-invasion and independent microtumour deposition. These processes were later identified as 'HIF dependent,' following pretreatment of cells with DMOG.

In conclusion we found an increase in metastatic phenotype following exposure to hypoxia via stabilisation of the HIF transcription factor. This CAM model was also utilised in order to begin to understand the molecular mechanisms underpinning the aggressive and erratic clinical behaviour of Neuroblastoma.

Abbreviations

ARNT – Aryl Hydrocarbon Receptor Nuclear Translocators

BMPs – Bone Morphogenetic Proteins; BSA – Bovine Serum Albumin; β -III Tubulin – Neuronal Class III β -Tubulin Polyclonal Antibody

Ca9 – Anti-Carbonic Anhydrase IX; CAM – Chorioallantoic Membrane; CD 56 – Neural Cell Adhesion Marker; CHD5 – Chromatin Helicase-binding Domain 5; CISH - Chromogenic in-situ Hybridization; c-kit – Mast / Stem cell growth factor receptor; C-MYC – c-Myelocytomatosis Viral Oncogene Homolog; C-TAD – Carboxy-terminal Transcriptional Activation Domain.

dHAND – heart-and neural crest derivatives-expressed protein; DLX3 – (Distal-less homeobox 3); DLX5 – (Distal-less homeobox 5); DMEM – Dulbecco's Minimum Essential Medium; DMOG – Dimethylloxalyl Glycine; DNA – Deoxyribonucleic acid

ECM – Extracellular Matrix; EMT – Epithelial to Mesenchymal Transition

FACs – Fluorescence Activated Cell sorting; FCS – Fetal Calf Serum; FIH - Factor Inhibiting HIF; FISH – Fluorescence in-situ Hybridization

GFAP – Anti-Glial Fibrillary Acidic Protein; GLUT-1 – Anti-Glucose Transport Receptor 1

H&E – Haematoxylin and Eosin; HASH-1 – human achaete-scute homolog-1; HIF-1 α – (Hypoxia-inducible factor 1 α); HIF-2 α – (Hypoxia-inducible factor 2 α); HRE – Hypoxia Response Elements

ID2 – Inhibitor of Differentiation 2; ID3 – Inhibitor of DNA Binding 3, Dominant Negative Helix-Loop-Helix Protein; IHC-F – Immunohistochemical staining of Frozen sections; IHC-P – Immunohistochemical staining of Paraffin sections; IMS – Industrial Methylated Spirits; INPC - International Neuroblastoma Pathology Criteria; INRGSS - International Neuroblastoma Risk Group Staging System; INSS - International Neuroblastoma Staging System

KIF1 β – Kinesin Family Member 1 β

LMO4 – Lim domain only protein 4

MASH-1 - Mammalian Achaete-Scute Homolog 1; MDM2 – Murine double minute 2 homolog; MEM – Minimum Essential Medium; MIBG – Iodine-131-Meta-iodobenzylguanidine; MKI - Mitosis-Karyorrhexis Index; MSX1 – (msh homeobox 1) and MSX2 – (msh homeobox 2)

NB – Neuroblastoma; NEAA - Non-essential Amino Acids; Notch-1 – Translocation-associated Notch homolog 1 {Drosophila}

O₂ – Oxygen

PAS family bHLH-PAS – Period circadian protein; Aryl Hydrocarbon Receptor Nuclear Translocator; Single-minded protein; family basic helix-loop-helix proteins; PAX3 – (Paired Box Homeotic Gene 3); PAX7 – (Paired Box Homeotic Gene 7); PHD's – Prolyl Hydroxylase Domain Proteins; Phox2A – (Paired-like homeobox 2a); Phox2B – (Paired-like homeobox 2b); p21 / WAF1 – (cyclin-dependent kinase inhibitor 1); p53 / TP53 – (Tumour protein 53); p73 – (Tumour protein 73); p300 – E1A binding protein p300

RPMI – Roswell Park Memorial Institute Medium

SD – Standard Deviation; Slug – Zinc Homolog 2 {Drosophila}; Snail – Snail Homolog 1 {Drosophila}; Snail2 – Snail Homolog 2 {Drosophila}; SMA – Smooth Muscle Actin- α ; SNS – Sympathetic Nervous System; SRC-1 – Steroid Receptor Coactivator 1

TBS – Tris Buffered Saline; TrkA – (neurotrophic tyrosine kinase receptor type A); TrkB – (neurotrophic tyrosine kinase receptor type B); TrkC – (neurotrophic tyrosine kinase receptor type C)

VEGF – (Vascular Endothelial Growth Factors)

Table of Contents

Acknowledgements	2
Abstract	3
Abbreviations	4
1. Introduction	
1.1 Neuroblastoma	7
1.1.1 Epidemiology & Screening for Neuroblastoma.....	7
1.1.2. Clinical Presentation.....	9
1.1.3. Staging, Risk Classification and Treatment.....	12
1.1.4. Metastasis and Classification in Neuroblastoma.....	15
1.1.5. Embryology.....	16
1.1.6. Pathology & Pathogenesis of Neuroblastoma.....	18
1.1.7. Genetic Features.....	21
1.2 Hypoxia	22
1.2.1. Hypoxia-inducible factor (HIF).....	23
1.2.2. Physiology and Pathophysiology of Hypoxia.....	27
1.2.3. Hypoxia and Solid Tumours.....	28
1.2.4. Hypoxia and Neuroblastoma.....	31
1.3 The Chorioallantoic Membrane and Tumour Cell Invasion	34
Introducing the Chick Chorioallantoic Membrane	34
1.3.1. Anatomy and Development of the CAM.....	35
1.3.2. Chick embryo and CAM model in Cancer studies.....	37
1.3.3. The Chick Embryo and Neuroblastoma.....	39
1.3.4. Tumour cell Migration.....	41
1.4. Study Aims	43
2. Materials and Methods	
2.1.1. Overview of Cell lines.....	44
2.1.2. Tissue Culture Protocol.....	45
2.1.3. Culture and treatment of cells prior to CAM implantation.....	45
2.2. Incubation and Fenestration of Chick embryos.....	46
2.3. Implantation of Tumour cells upon the “CAM”.....	48
2.3.1. Dissection of Mature Embryos.....	50

2.4. Paraffin embedding, Sectioning & Staining.....	51
2.5. Freezing samples, Sectioning & Staining.....	52
2.6. Imaging.....	55
3. Results	
3.1. Introduction.....	56
3.1.1. Pilot study investigating cell line survival upon the CAM.....	56
3.1.2. Implantation of Normoxic Sk-N-AS.....	58
3.1.3. Normoxic Sk-N-AS Migration & Invasion.....	61
3.1.4. MYCN amplified cell lines.....	62
3.2.0. Implantation of Hypoxic Sk-N-AS cells.....	64
3.2.1. Tumour differences – Normoxic Vs Hypoxic Preculture.....	67
3.2.2. Effects of DMOG on Sk-N-AS tumourigenesis.....	69
3.3.0. Co-application of Normoxic and Hypoxic Sk-N-AS.....	71
3.3.1. Implantation of Normoxic – Hypoxic Mixtures.....	72
3.3.2. Sk-N-AS Tumourigenesis and Invasion.....	76
3.3.3. Hypoxia unlocked tumourigenesis in MYCN amplified cell line.....	78
3.4.0. Paraffin staining of Sk-N-AS tumour samples.....	80
3.4.1. Staining for markers downstream of HIF expression.....	82
3.5.0. Tumour cell Proliferation and Intravasation - Normoxia Vs Hypoxia.....	83
3.5.1. Frozen section tumour characterisation – Hypoxia Vs Normoxia.....	88
4. Discussion	
4.1. The Chick Embryo Model.....	90
4.2. Preculture in Normoxia versus Hypoxia.....	93
4.3. Hypoxia and Metastasis.....	96
4.4. Future Work.....	100
4.5. Conclusions.....	101
5. References	
5.1. Web References.....	115

1. Introduction

1.1 Neuroblastoma

Neuroblastoma (NB) is a highly dangerous often lethal, solid heterogenous tumour which is regularly encountered in paediatric oncology. It is the most common cancer diagnosed in infants accountable for nearly one third of all infant malignancies (German Childhood Cancer Registry, Web Reference 1) and responsible for 15% of mortality occurring in paediatric oncology (Maris et al. 2007).

1.1.1 Epidemiology & Screening for Neuroblastoma

Epidemiology

The global incidence of neuroblastoma is estimated at around 10.5 cases per million children aged less than 15 years (Stiller et al. 1992). Age at diagnosis is a key feature with the vast majority of patients presenting for the first time before 5 years. Interestingly older patients (> 14 years) experience poorer survival (Castleberry. 1997) although < 10% are diagnosed beyond the age of 10.

Neuroblastoma can occur in adults, however incidence is low and steadily decreasing; 1973-77 recorded 0.47 / 1,000,000; 1998-02 recorded 0.12 / 1,000,000 (Esiashvili et al. 2007). Overall survival in adults is poor (5-year survival 36.3%) when compared to other age groups; infant 5-year survival 84.6%; 1-9 years old 47.8%; 10-19 years old 46.2% (Esiashvili et al. 2007). Due to the significant difference in survival between infant and child, age has been included in the Children's Oncology Group Prognostic Classification (Katzenstein et al. 1998). Presenting such poor outcome data, adults might be expected to more commonly express classic biological risk factors such as MYCN amplification, loss of chromosome 1p, or DNA ploidy, however these markers of disease severity are rarely encountered (Moody et al. 1996, Kushner et al. 2003). Regarding gender, several studies (Spix et al. 2006; Park et al. 2008; Wiangnon et al. 2003) have demonstrated a slight male preponderance for disease however this discrepancy is tenuous and most likely insignificant.

In the USA, neuroblastoma is the most common solid tumour of childhood excepting those occurring within the central nervous system (Reis et al. 1999). Asian / Pacific Islanders have also been identified as the groups most “at risk,” with 35% increased mortality (Johnson et al. 2011). A Children’s Oncology Group study found inconsistencies in survival between African-American and White populations (Henderson et al. 2011) however later studies suggest this could be due to inequalities regarding access to health care (Pui et al. 2012). Internationally it is generally regarded that no appreciable difference exists concerning race.

Among Europeans disease incidence is increasing. During the period 1978-82 disease occurred in 8.4 / 1,000,000 children whilst 1993-97 saw this figure increase to 11.6 (Spix et al. 2006). Across European regions, the UK and Ireland experience the lowest incidence (9.1) and also achieve some of the worst survival rates (49% Confidence Interval: 45-52). However the overall trend shows increased survival in Western Europe compared to the East which is worse-off by 20% (Spix et al. 2006). Regardless, overall 5-year survival has almost doubled within the last 30 years. This is most likely due to changes in treatment regimens following the identification of biological indicators of disease severity.

Screening

High incidences of neuroblastoma have been observed in Japan due to the presence of a National Screening Program running from the 1970’s aimed at identifying cases in children \leq 6 months old. Domestic and international evidence (Yamamoto et al. 2002, Woods et al. 2002, Schilling et al. 2002) halted all neuroblastoma screening programs by 2004 having demonstrated screening increases incidence but failed to significantly decrease disease mortality. It was found that the high incidences were due to an increase in low risk cases whilst the number of intermediate / high risk cases remained unchanged. In the past these low risk cases might have been asymptomatic undergoing spontaneous regression without the need for intervention.

1.1.2. Clinical Presentation

Anatomic location

Well known for its unpredictable nature, neuroblastoma may present with any number of highly variable symptoms. This is most likely due to its ability to develop throughout the sympathetic nervous system making tumour formation possible in most anatomic regions, see Figure 1.

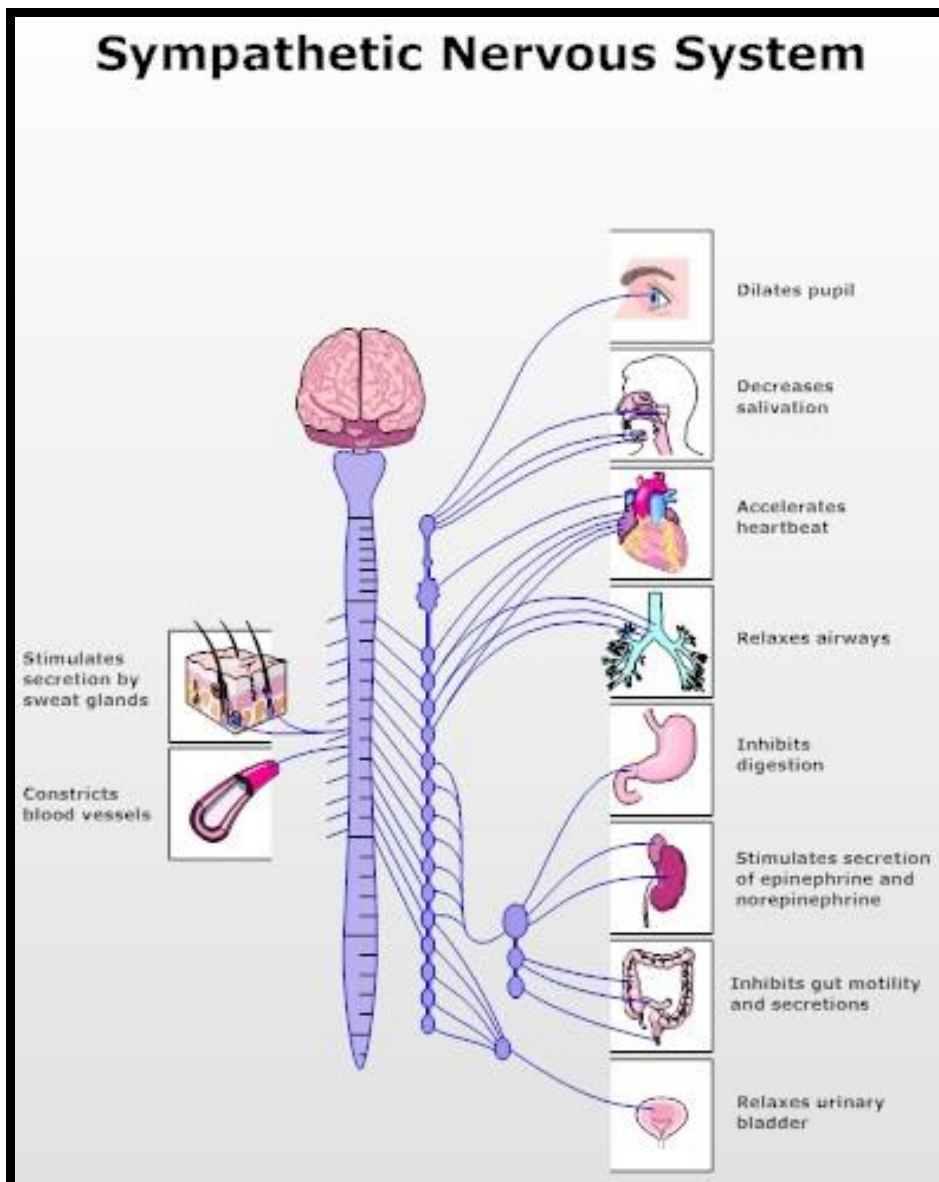


Figure 1. The sympathetic nervous system is present throughout the entire body and neuroblastoma can form at any location. This lends to the enigmatic nature of the tumour as any number of vital organs may be affected producing a host of confusing symptoms. Image reproduced from Web Reference 2.

Signs and Symptoms

The diagnosis of patients with low risk disease can quite commonly be made as a result of an incidental discovery due to the asymptomatic patient undergoing investigation for an unrelated problem. In the past however these patients were more frequently encountered following identification by screening programs which have now become redundant (Woods et al., Schilling et al. 2002).

Patients presenting with active symptoms commonly complain of pain and malaise. Primary tumours develop chiefly upon the adrenal glands (Park et al. 2008) resulting in abdominal bloating and constipation with severe cases developing liver metastases resulting in abdominal compartment syndrome and subsequent respiratory distress or anuria. Quantification of common anatomical regions is shown in Figure 2.

Regular sites for disease dissemination are liver, bone and bone marrow which are investigated when staging the tumour (Carlsen et al. 1985). Children presenting with metastasis are often very ill and may demonstrate “blueberry muffin” skin lesions, proptosis, and “raccoon eyes” known as periorbital ecchymosis. These classic pathologies of the eye were historically believed to be due to a propensity for orbital dissemination (Hutchison 1907) however this claim is yet to be tested in more recent times.

Rare Presentations

Rare presentations include associated; “VIPoma,” a Vasoactive Intestinal Peptide secreting tumour causing diarrhoea; or catecholamine secreting neoplasms such as phaeochromocytoma resulting in facial flushing and excessive sweating. Tumour formation in the thorax, head or neck can lead to complex problems such as spinal cord compression or Horner’s Syndrome, a triad of unilateral anhidrosis, miosis and ptosis. Occurring in around 2% of neuroblastoma cases, an immune-mediated paraneoplastic disease, opsoclonus-myoclonus ataxia, is a cerebellar pathology known to give patient’s “dancing eyes” (Rudnick et al. 2001, Mitchell et al. 2002). However, of all recorded opsoclonus-myoclonus, up to 50% have been observed to develop co-existing neuroblastoma (Pohl et al. 1996).

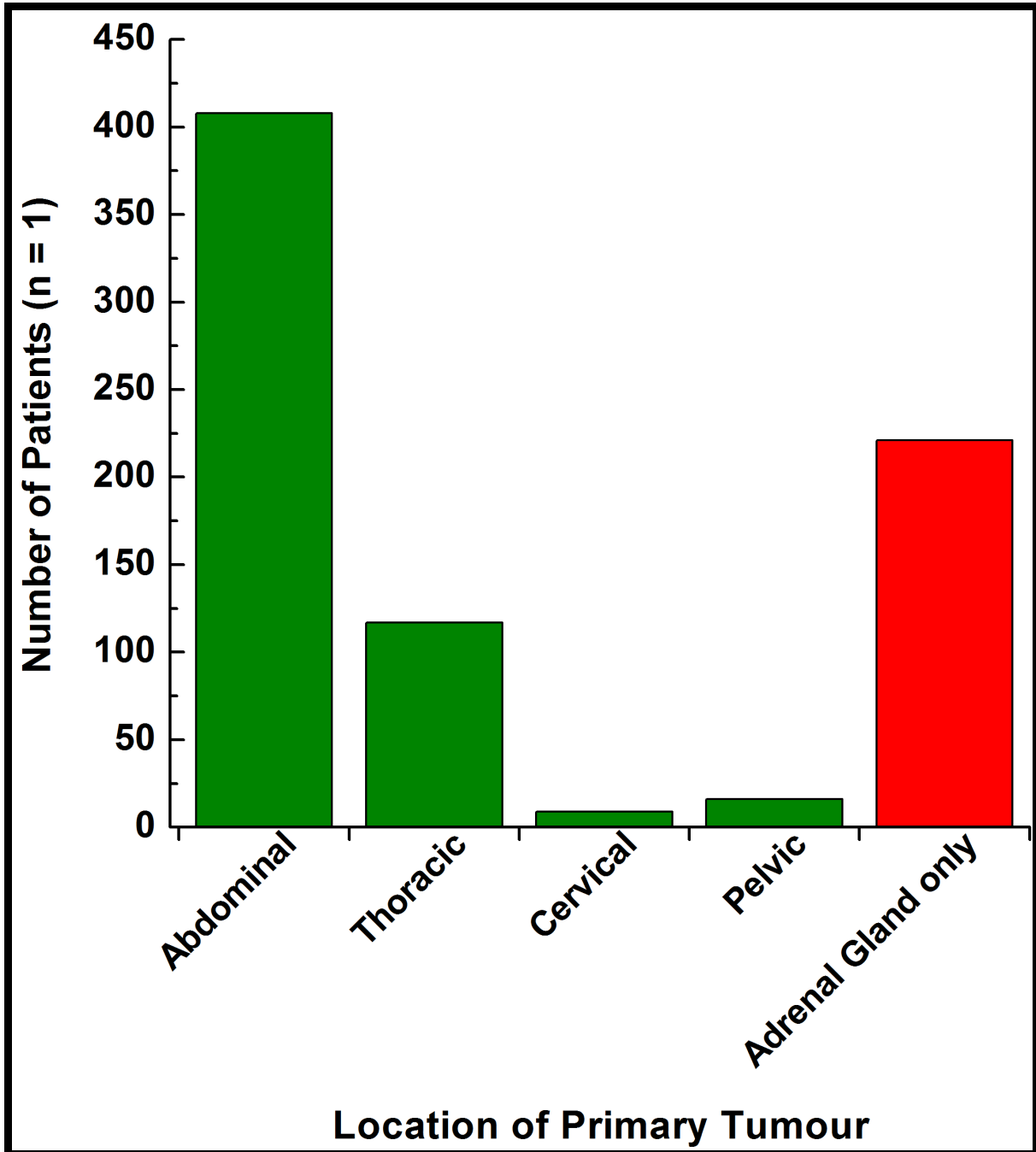


Figure 2. Primary Neuroblastoma Formation at various anatomic regions. This bar chart represents the number of primary neuroblastoma found forming within common territories at initial presentation. Total number of tumours, n=550; Abdomen n=408 (74%); Thorax n=117 (21%); Cervical n=9 (2%); and Pelvis n=16 (3%). Of 408 Abdominal tumours, 221 (54%) occurred in the Adrenal Glands suggesting they are the most likely site for primary tumour formation. This bar chart was created independent of data collection which was undertaken by Coldman et al. 1980.

1.1.3. Staging, Risk Classification and Treatment

Staging

As of the early 1990's neuroblastoma were staged according to the International Neuroblastoma Staging System (INSS) (Brodeur et al. 1993) shown in Table 1.

Table 1 The International Neuroblastoma Staging System (Brodeur et al. 1993).

Stage	Definition
1	Localised tumour with complete gross excision, with or without microscopic residual disease; representative ipsilateral lymph nodes negative for tumour microscopically (nodes attached to and removed with primary tumour may be positive)
2A	Localised tumour with incomplete gross excision; representative ipsilateral nonadherent lymph nodes negative for tumour microscopically
2B	Localised tumour with or without complete gross excision, with ipsilateral nonadherent lymph nodes positive for tumour. Enlarged contralateral lymph nodes must be negative microscopically.
3	Unresectable unilateral tumour infiltrating across the midline*, with or without regional lymph node involvement; or localized unilateral tumour with contralateral regional lymph node involvement; or midline tumour with bilateral extension by infiltration (unresectable) or by lymph node involvement.
4	Any primary tumour with dissemination to distant lymph nodes, bone, bone marrow, liver, skin and/or other organs (except as defined for stage 4S)
4S	Localised primary tumour (as defined for stage 1, 2A or 2B), with dissemination limited to skin, liver and/or bone marrow** (limited to infants < 1 year of age)

* The midline is defined as the vertebral column. Tumours originating on one side and crossing the midline must infiltrate to or beyond the opposite side of the vertebral column.

** Marrow involvement in stage 4S should be minimal, ie, < 10% of total nucleated cells identified as malignant on bone marrow biopsy or on marrow aspirate. More extensive marrow involvement would be considered to be stage 4. The MIBG scan (if performed) should be negative in the marrow.

Much of the literature refers to tumours according to this system however it has recently been replaced by the International Neuroblastoma Risk Group Staging System (INRGSS) shown in Table 2 below (Monclair et al. 2009). This is due to several practical issues such as the requirement to obtain tumour tissue which is no longer necessary in the treatment of some patients with low risk disease.

Table 2. The International Neuroblastoma Risk Group Staging System is the current system replacing the INSS however most published literature quotes the older system. Patients with multifocal primary tumours should be staged according to the greatest extent of disease (Monclair et al. 2009).

Stage	Definition
L1	Localised tumour not involving vital structures as defined by the list of image-defined risk factors and confined to one body compartment.
L2	Locoregional tumour with presence of one or more image-defined risk factors.
M	Distant metastatic disease (except stage MS)
MS	Metastatic disease in children younger than 18 months with metastases confined to skin, liver, and/or bone marrow.

Risk Classification

It is necessary to classify neuroblastoma in terms of prognosis in order to utilise the most appropriate methods of treatment. Originally the Shimada system quantified; level of stromal development; neuroblastic differentiation; mitosis-karyorrhexis index (MKI); and patient age in order to distinguish favourable from unfavourable cases (Shimada et al. 1984). However the International Neuroblastoma Pathology Criteria (INPC) later modified this system further subdividing disease subgroups, as shown in Table 3.

Table 3. International Neuroblastoma Pathology Criteria (Shimada et al. 2001). FH: favorable histology; UH: unfavorable histology; MKI: mitosis-karyorrhexis index.

Category and Subtype	Prognostic group
Neuroblastoma (Schwannian stroma-poor) Undifferentiated Poorly differentiated Differentiating	FH or UH based upon: Age Grade of Differentiation MKI class
Ganglioneuroblastoma (Schwannian stroma-rich)	FH
Ganglioneuroblastoma, nodular (Schwannian stroma rich/dominant and poor)	UH
Ganglioneuroma (Schwannian stroma dominant) Maturing Mature	FH

Treatment

Treatment can be extensive or simple depending upon the biological features unique to each tumour. Staging, tumour classification and the anatomic location of tumour development are also important factors to consider before administering therapy.

Low risk cases such as asymptomatic Stage 4s disease may be left to undergo spontaneous regression without the need for active management. However intermediate to high risk patients often require an array of therapies such as: chemotherapy, radiotherapy or extensive surgery, laparotomy, depending upon the severity of their condition.

Research efforts are continuing to develop novel therapies for the treatment of neuroblastoma patients. For instance, clinical trials are currently underway assessing the therapeutic benefits of anti-GD2, an antibody which is known to react with neuroblastoma cells (Mueller et al. 1990; Yu et al. 2010). Work is also continuing to discern the role of antiangiogenesis in solid tumour therapy (Chen et al. 2011; Huang et al. 2012). However, significantly more work must be undertaken if survival rates are to be improved in severe disease.

1.1.4. Metastasis and Classification in Neuroblastoma

Known as one of the most common malignancies identified in children, disseminated neuroblastoma are classified as either Stage 4 (INSS) / Stage M (INRGSS) or Stage 4S (INSS) / Stage MS (INRGSS). Metastatic sites are widely variable and this leads to difficulties in diagnosis as patients may be asymptomatic or present with a range of life threatening symptoms. A large number of patients suffering this disease are categorised as Stage 4 / M with some studies demonstrating up to 60% of neuroblastoma present in this category (Juárez-Ocaña et al. 2009; Palma-Padilla et al. 2010). Treatment protocols for this group are extremely severe and survival is truly dismal, recorded at 20 - 25% (Philip et al. 1991; Li et al. 2012).

Stage 4S disease is widely different with metastasis limited to bone marrow, liver and skin and overall survival rates approaching 90% (Katzenstein et al. 1998; Nickerson et al. 2000). However this classification encompasses only a small subsection of overall disease and the frequency of presentation decreases with age with the majority of cases occurring in neonates (Iehara et al. 2012). The significant difference between Stages 4 and 4S is the ability of the latter to undergo spontaneous regression resulting in a surprising recovery often without relapse. As such, some patients may receive no active treatment and instead are monitored until all signs of the disease have been absent for a continuous period of time, usually up to 10 years. This phenomenon is unique and distinguishes neuroblastoma as a particularly interesting tumour among other cancers.

Although Stage 4S has a drastically improved survival rate compared to Stage 4, patients still die. This is because they must remain alive for long enough for the metastatic secondary tumours to regress and in this time the normal function of their vital organs may be compromised as previously mentioned. MYCN status also has a role, as non-amplified infants with Stage 4 and 4S disease have excellent survival, with minimal or no treatment (De Bernardi et al. 2009). Finally a major problem facing clinicians occurs when patients with disseminated neuroblastoma are initially assessed. Here, there is a lack adequate tools to differentiate Stage 4S from Stage 4 disease, hence some patients may be subjected to severe and life-threatening treatments when a lesser approach would have been sufficient.

1.1.5. Embryology

Embryology

At the beginning of gestational week 3 human embryos initiate the process of neurulation whereby the nervous system forms from embryonic ectoderm (Figure 3A). This process encompasses neural fold specification and delamination with latter differentiation-migration-proliferation, which occur simultaneously. The first step is neural plate formation, resulting in a three layer structure constituting neural ectoderm, mesoderm and endoderm. Within days, plate edges thicken cranially resulting in the creation of neural folds which grow toward each other and eventually fuse to form the neural tube (Figure 3C). Inside this tube neuroepithelial cells are modified becoming neuroblasts which later differentiate to form mature neurons. Preceding fusion, neural crest cells become detached from neural folds, these cells are versatile and undifferentiated. Crest cells migrate throughout the body whilst simultaneously proliferating and differentiating in order to form mature adult structures such as, the autonomic nervous system, catecholamine producing adrenal medulla “chromaffin” cells, melanocytes, and thyroid “C” cells (Le Douarin et al. 1974; Le Douarin, Teillet. 1974; Dorsky et al. 1998).

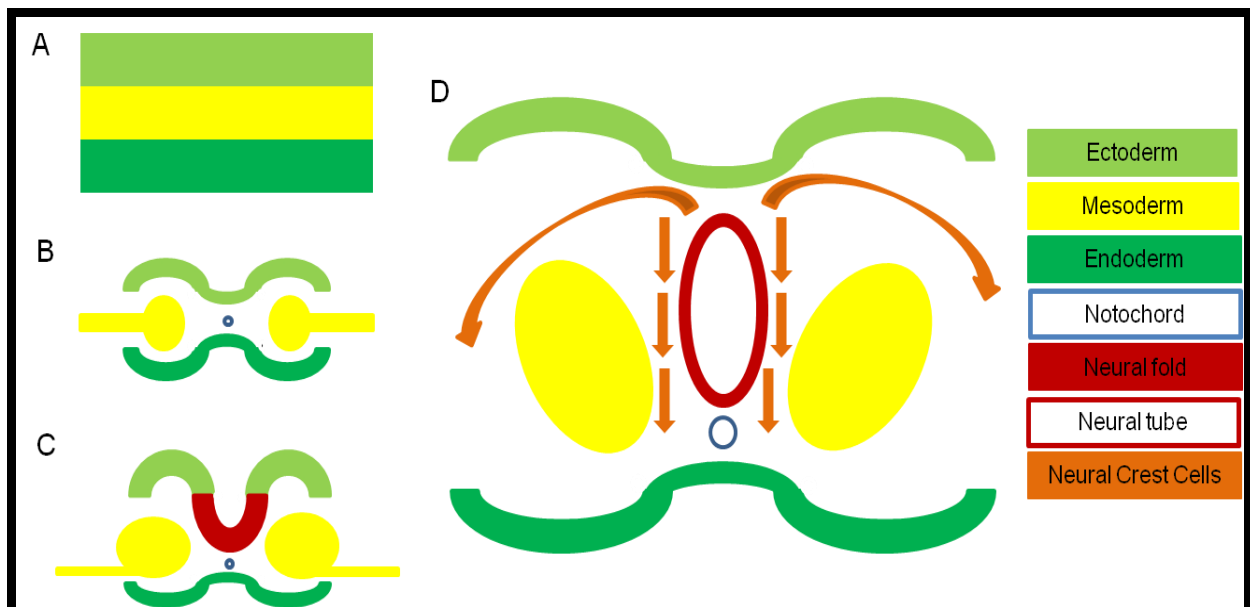


Figure 3. Neurulation begins in week 3 of human gestation. As neural folds form and eventually fuse, neural crest cells delaminate from the intended fusion zone. These cells are undifferentiated and may migrate throughout the body however many genes influence the transition by expressing coordinators of this process.

Specification & Delamination

Synthesis and migration of neural crest cells begins with strategic specification of the neural fold, as displayed in Figure 3C above. Key to this process are neural crest specifier genes such as; C-MYC (C-Myelocytomatosis Viral Oncogene Homolog – Aoki et al. 2003); Snail (Snail Homolog 1 {Drosophila} – Essex et al. 1993); and Slug (Zinc Homolog 2 {Drosophila} – Mayor et al. 1995) which are present prior to and throughout migration (Meulemans et al. 2004). However activation of these genes is reliant upon previous expression of PAX3 (Paired Box Homeotic Gene 3), PAX7 (Paired Box Homeotic Gene 7), DLX3 (Distal-less homeobox 3), DLX5 (Distal-less homeobox 5), MSX1 (msh homeobox 1) and MSX2 (msh homeobox 2) alongside many other neural plate border specifier genes (Bang et al. 1997; Luo et al. 2001; Tribulo et al. 2003).

On completion of specification, former neural fold cells must detach (delamination) to be made available for migration. Transcription factor ID3 (Inhibitor Of DNA Binding 3, Dominant Negative Helix-Loop-Helix Protein) performs the role of stabilising crest cells and may also aid segregation from the neural fold (Kee et al. 2005). Under the influence of Slug, cells undergo epithelial to mesenchymal transition (EMT), incidentally an established mechanism for cancer cell invasion (Thierry 2002). Mitosis is halted throughout this process via the action of Snail, permitting expression of Rho GTPases and cadherins which enable alterations in morphology and adhesion quality (Fukata et al. 2001).

Differentiation-Migration-Proliferation

Once free of the neural fold, crest cells migrate according to signalling pathways whilst constantly proliferating. Early in migration an important distinction is made, future melanocytes are forced to traverse dorsolaterally whilst future chromaffin / sympathetic nervous system cells journey ventrally (Thiery et al. 1982). Key to both dorsolateral and ventral pathway movement are ephrins which increase melanocytic crest cell affinity for dorsolateral pathway fibronectin (Meulemans et al. 2004, Santiago et al, 2002) whilst directing other crest cells ventrally (Krull et al. 1997, McLennan et al. 2002).

Eventually extracellular interactions commence via integrin binding with extracellular matrix (ECM), thus crest cells become available to migrate throughout the body (Humphries et al. 2006).

In a normal foetus, crest cell differentiation requires a level of environmental versatility (plasticity) provided by the strategic expression of specific genes. For example, transition from neural crest cell to sympathetic neuron relies upon a number of important transcription factors, notable key coordinators include: MYCN, Phox2A, Phox2B, HIF-1 α and p73 (Nakagawara 2004). Overall the process of differentiation is triggered by the presence of bone morphogenetic proteins (BMPs) (Huber et al. 2002) however it is postulated that BMPs may also serve to inhibit later phases of maturation. This complements independent findings that differentiation potential is progressively inhibited in postnatal adrenal medullary cells implying that there could be an overall restriction upon differentiation following initial triggers (Mascorro et al. 1989). Finally it has also been observed that individual crest cell diversifications may be reliant upon specific transcription factors, for instance it has been suggested that chromaffin cell maturation is largely dependent upon MASH-1 expression (Huber et al. 2002).

1.1.6. Pathology & Pathogenesis of Neuroblastoma

Pathology

Described as a small, round, blue-cell tumour of childhood, neuroblastoma appear histologically as a clutch of closely organised cells enclosed in neurofibrillary stroma and partitioned by fibrovascular septa. They are believed to be neural crest cell derivatives with a sympathoadrenal lineage classically defined histologically as forming a pattern known as Homer-Wright rosettes (Figure 4). Each rosette consists of a core resembling central nervous system neuropil (network of cytoplasmic neuronal processes between cell bodies at synaptic connections) regarded as neurofibrillary matrix, surrounded by small clustered rings of tumour cells (Owens, Irwin 2012). Though regarded as the classic pattern of tumour formation, undifferentiated neuroblastoma may demonstrate a complete absence of neurofibrillary matrix presenting diagnostic problems (Lack 2007).

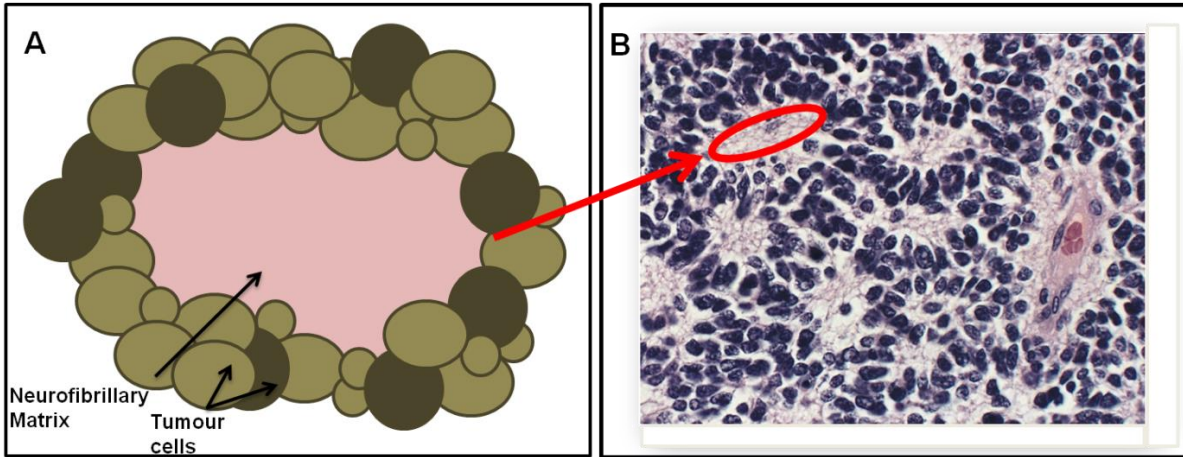


Figure 4. This figure displays a diagram (A) and a histological picture (B) demonstrating neuroblastoma cell formation as characteristic Homer-Wright rosettes. Diagram A displays cells of different shapes, sizes and shading (pleomorphic hyperchromasia), representing microscopic findings suggestive of malignancy. The red circle in B highlights a core of neurofibrillary matrix at the centre of a rosette. This is an image produced by the US Armed Forces Institute of Pathology, it has been released into the public domain, see Web Reference 3.

Macroscopically, tumours tend to appear either as voluminous multinodular masses or discrete spheroids and from time to time cystic neuroblastoma are reported however they are often misdiagnosed as adrenal cyst or haematoma (Lack 1997; Kozakewich et al 1998). Upon cross-section, chalky white calcification may be witnessed however regions of necrosis and haemorrhage among coarse nodular tissues are commonly observed (Lack 1997).

Pathogenesis

Solid tumours are regarded differently when they develop in children. An occurrence unique to this cohort of patients is the formation of embryonal tumours which most commonly appear as a remnant of foetal development, histologically resembling immature tissues. As neuroblastoma emanate from neural crest cells they are a prime example of an embryonal tumour and like all cancers, are believed to develop as a consequence of genetic alteration or abnormality. Supporting claims linking neuroblastoma to crest cells, expression profiling of favourable and unfavourable tumours has shown that many possess the genes required to permit normal neural crest cell differentiation (Ohira et al. 2003). From this it is sensible to suggest that tumour cells appear during differentiation-migration-proliferation, see Figure 5, because within this phase a key strategic advantage can be gained as a result of environmental plasticity which encourages propagation of normal crest cells within the foetus (Scotting et al. 2005).

Related to neuroblastoma are two disease subtypes which exist in a more differentiated state. Ganglioneuroblastoma and ganglioneuroma are more advanced tumours identified histologically following recognition of spindle cell Schwannian stroma (neuronal support network) and ganglion cells or their immediate precursors. The International Neuroblastoma Pathology Classification (INPC) demarcated these subtypes as follows; neuroblastoma – Schwannian stroma poor; ganglioneuroblastoma – Schwannian stroma rich; ganglioneuroma – Schwannian stroma dominant (Shimada et al. 2001). Further evidence of differentiation is determined by assessing for neurotrophin receptors such as; synaptophysin; TrkC; and TrkA with the latter inferring a favourable prognosis when highly expressed (Nakagawara et al. 1998, Brodeur et al. 2009).

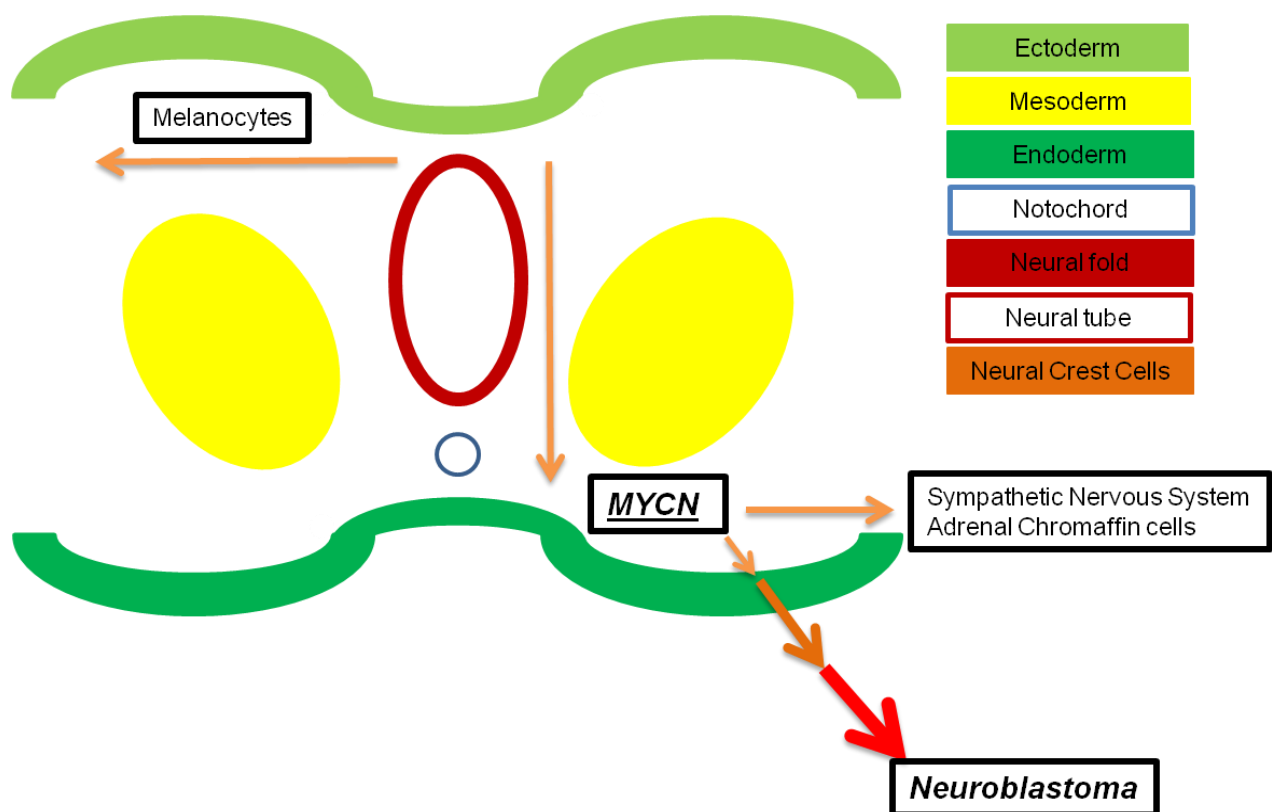


Figure 5. Tumourigenesis of Neuroblastoma during the differentiation-migration-proliferation stage of Neurulation. Cells set to become future melanocytes migrate dorsolaterally as ventrolateral migration is preferred by sympathetic nervous system and future adrenal crest cells. MYCN is expressed and later downregulated during neural crest cell migration. In some neuroblastoma with poorer outcome, MYCN expression remains amplified long after completion of neural crest cell migration. It has therefore been identified as a poor prognostic indicator.

1.1.7. Genetic Features

Genetic Features

Neuroblastoma derived Myc proteins (MYCN) are important neural crest cell transcription factors controlling cell maintenance and proliferation, Figure 5 (Pelengaris et al. 2002). Located at chromosome 2p24, gene amplification of >10 copies indicates rapid disease progression and poor prognosis. This can be identified using: FISH - fluorescence in-situ hybridization, or more recently using CISH - chromogenic in-situ hybridization (Squire et al. 1996; Bhargava et al. 2005). The INRG Classification System (Cohn et al. 2009) encourages investigation of MYCN status in all patients and further advises confirmation of DNA ploidy and chromosome 11q status. Fortunately amplification occurs in a minority of cases; 5-10% in infants (Kaneko et al. 2006); 20-30% in childhood (Conte et al. 2006). Survival is significantly improved in the absence of MYCN most notably in stage 4 disease where mortality rate of <10% has been demonstrated (Schmidt et al. 2000).

DNA-ploidy is investigated using flow cytometry with hyperdiploidy linked to TrkA over-expression (Brodeur et al. 2009), a receptor found in favourable outcome neuroblastoma (Nakagawara et al. 1993). However diploid tumours are associated with segmental chromosomal changes indicating an unstable genome and therapeutic resistance. Important segmental changes include deletions at 1p36 (30% of cases) and 11q23 (40%), whilst 50% of cases express gains at 17q (Caron et al. 1993; Attiyeh et al. 2005; Brown et al. 1999). Commonly deleted regions encode tumour suppressor genes, Eg. 1p36; chromatin helicase-binding domain 5 (CHD5); KIF1 β and p73, this may explain increased tumour aggression in patients with regional deletion. The most common chromosomal change, gain at 17q, is believed to impart oncogenic tools for tumour survival however loss at 11q is more useful clinically, indicating poor event-free survival (Attiyeh et al. 2005). Incidentally, increased expression of TrkB has been noted in 11q deficient tumours, signifying improbable spontaneous regression (Light et al. 2011).

1.2 Hypoxia

Introduction

Oxygen (O₂) is the vital component required to sustain mammalian life. It is such a crucial molecule that must be supplied continuously throughout the course of an individual's life. Appropriate oxygenation is crucial to maintain normal tissue function however some tissues (bone marrow) may endure fluctuating oxygenation with greater ease than others (brain parenchyma). In order to ensure adequate oxygenation of all tissues, humans employ a series of mechanisms which constantly monitor tissue oxygen tension and carry out adjustments according to supply and demand. E.g. baro / chemo – receptors exist close to O₂ sensitive organs, constantly testing the blood for potential changes in O₂. These efforts ensure high level O₂ is decreased whilst low level O₂ is boosted keeping tissue oxygen tension tightly controlled within strict parameters.

Normal atmospheric oxygen constitutes 21% of air inhaled by humans however levels decrease inside the body and what is more, different viscera are maintained at a range of various oxygen concentrations. Upon inhalation, O₂ concentrations are significantly lower (14%) when measured at the terminal alveoli. Levels are further reduced when molecules are exchanged into the blood and temporarily bound to haemoglobin. Newly formed oxyhaemoglobin complexes traverse the body via the vascular network and deliver fresh O₂ to nearby tissues through the process of diffusion. As a result, end-organ perfusion is variable but also much lower than atmospheric conditions. An example of this can be appreciated in the brain which is an extremely oxygen-sensitive collection of tissues. Overall, the mean cerebral concentration of O₂ is recorded at 3.2% however concentrations are widely altered throughout different territories of the brain (Dings et al. 1998).

Given expected variance in oxygenation across different viscera, normal physiological parameters are usually set between 2 – 9% O₂, also known as 'normoxia' (Simon, Keith. 2008). Excluding several special exceptions, pathologically decreased O₂, 'hypoxia,' is regarded as less than 2% O₂. Finally, extreme hypoxia (0.01%) and the complete absence of oxygen, 0% O₂, is known as 'anoxia.'

1.2.1. Hypoxia-inducible factor (HIF)

When studying erythropoietin gene expression in hypoxia a single DNA – protein complex was found to bind the gene (Semenza and Wang, 1992). A resultant increase in erythropoietin expression was observed expanding the vascular potential for O₂ carriage and directly linking hypoxia to erythropoiesis. The hypoxia dependent transcription factor, hypoxia-inducible factor (HIF), was later described as a heterodimer consisting of two PAS family basic helix-loop-helix proteins (bHLH-PAS) (Wang et al. 1995). The complex constitutes two subunits existing as isoforms, alpha and beta; HIF-1 α , 2 α ; and the latter (ARNT) aryl hydrocarbon receptor nuclear translocators 1, 2, 3 (Brahimi-Horn et al. 2009).

HIF-1 α and 2 α are constitutively expressed in the cell however they are vulnerable to hydroxylation by Prolyl Hydroxylases (PHDs) and Factor Inhibiting HIF (FIH) in the presence of sufficient O₂ levels. Normoxia predisposes alpha subunits to proteasomal degradation by ubiquitination. This process requires hydroxylation of two proline residues residing within HIF- α subunits by PHD's, principally PHD2 (Berra et al. 2003). Thereafter binding of tumour suppressor von Hippel-Lindau protein (pVHL) linked to elongin C in an E3 ubiquitin-ligase complex (Maxwell et al 1999) facilitates bonding to ubiquitin leading to degradation of HIF- α , see Figure 6 (Jaakkola et al. 2001).

While PHDs hydroxylate HIF at proline residues, FIH hydroxylates asparagine residue 803 in the carboxy-terminal transcriptional activation domain (C-TAD) of HIF-1 α (Dayan et al. 2006). This interaction is important as it inhibits later coupling with transcription coactivator p300, disrupting future expression of hypoxia associated target genes (Lando et al. 2002). Incidentally this coactivator is also required during activation of the tumour suppressor, p53 (Lill et al. 1997).

In hypoxia these mechanisms are negated and as a consequence, HIF- α activity is no longer suppressed. At low levels of oxygenation, PHD's are deactivated prior to FIH, as both components avail of O₂ during hydroxylation (Epstein et al. 2001; Lando et al. 2002). PHD activity is the first to decrease, stabilising a large proportion of α -subunits, the surplus avoid deactivation until O₂ levels are further reduced. At which point FIH activity is impaired (Koivunen et al. 2004). Consequently, non-ubiquitinated HIF- α translocates to within the nucleus via C-terminal interactions with nuclear pore proteins.

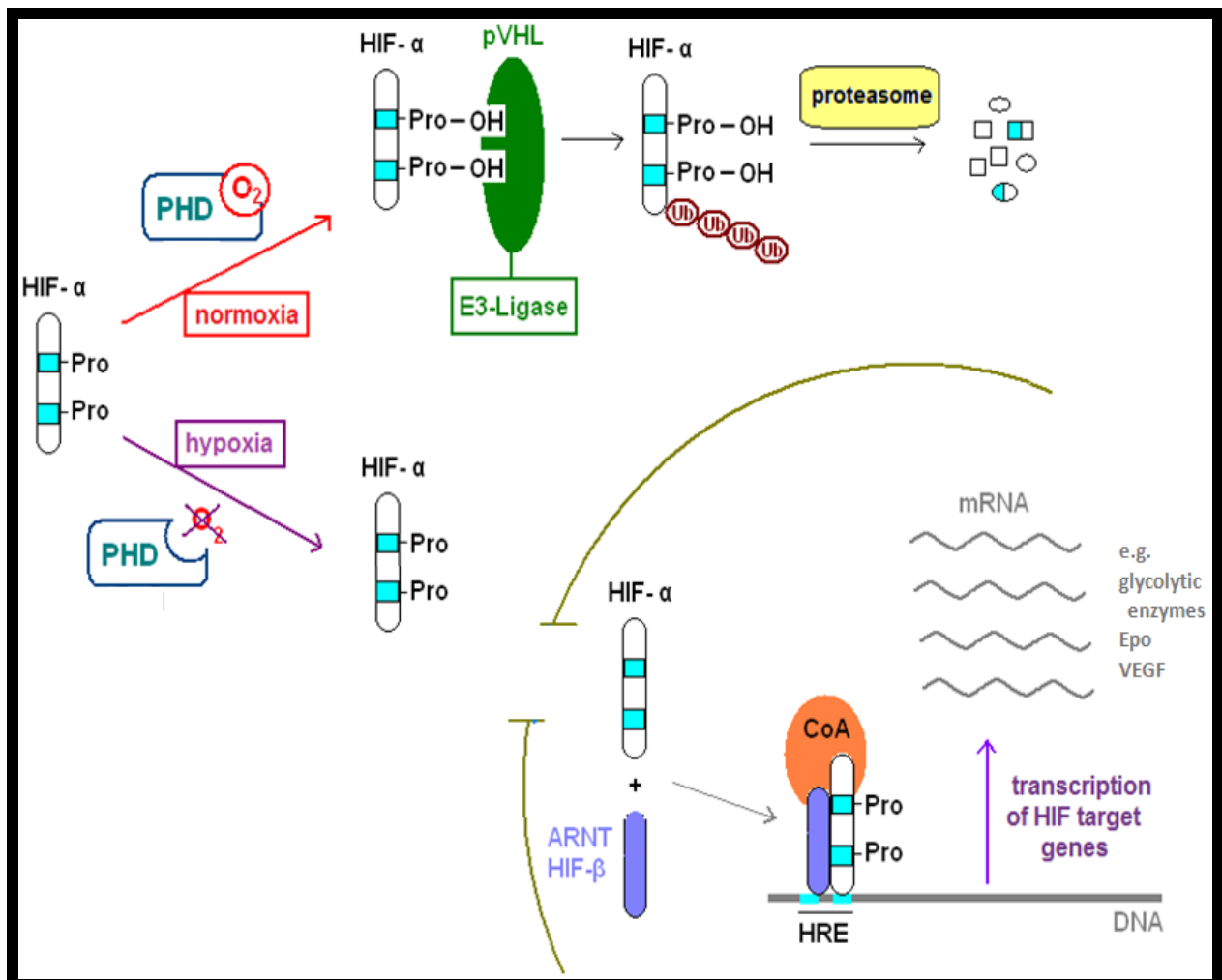


Figure 6. The contrasting role of HIF- α under normoxic and hypoxic conditions. In normoxia, PHD activity results in proteasomal destruction via ubiquitination. In hypoxia, hydroxylation of prolyl residues (labelled Pro) no longer occurs due to the absence of hydroxylation substrates (O₂). This permits translocation with latter transcription of hypoxia response elements following β subunit dimerisation. Diagram kindly provided by Amelie Schober.

Dimerisation of α to β subunits takes place within the nucleus prior to gene transcription. Autonomous to O_2 , HIF- β isoform expression is regarded as constitutive with ample supplies located within cell nuclei. Throughout the dimerisation process, subunits strategically bind to ensure transcription activation domains are impeded as they must remain available to bind with specific target gene sequences, known as hypoxia response elements (HRE) (Wenger et al. 2005). HRE's are domains of DNA stimulated by HIF to modify gene expression which in turn stimulates proteins that promote cell survival and suppress factors inhibiting adaptation. When initiating transcription, HIF targets necessitate the presence of a coactivator such as SRC-1 or p300 (Ema et al. 1999; Carrero et al. 2000), these have become therapeutic targets for tumour shrinkage (Kung et al. 2000).

Enabling HIF activity alters expression in hundreds of genes (Mole et al. 2011). This indicates the grandeur of cellular adaptive responses associated with hypoxia. As shown in Table 4, these genes are varied affecting a number of major physiological pathways.

Table 4. List of key pathways affected by HIF. Hypoxia results in the transcription of a wide range of genes across a broad spectrum of processes which occur throughout the body affecting the organism as a whole. This list of pathways is not exhaustive, rather it is meant to serve as an indicator of the extensive reach of the HIF transcription factor. References have been added to demonstrate some of the evidence currently available in the literature.

HIF Effected Process	Evidence
Angiogenesis	<i>Shweiki et al., 1992; Carmeliet et al., 1998; Ryan et al., 1998</i>
Apoptosis	<i>Bruick, 2000; Sowter et al., 2001; Leuenroth et al., 2000</i>
Cell Proliferation	<i>Carmeliet et al., 1998</i>
Erythropoiesis	<i>Semenza et al., 1991; Wang and Semenza 1993</i>
Extracellular matrix synthesis	<i>Pfander et al., 2003; Bruick and McKnight, 2001</i>
Glucose metabolism	<i>Kim et al., 2006; Papandreou et al., 2006; Fukuda et al., 2007</i>
Growth-factor signaling	<i>Zelzer et al., 1998; Caniggia et al., 2000</i>
Iron transport	<i>Rolfs et al., 1997; Lee et al., 1997; Mukhopadhyay et al., 2000</i>
Metastasis	<i>Graeber et al., 1994; An et al., 1998; Blouw et al., 2003</i>
pH regulation	<i>Ullah et al., 2006; Shimoda et al., 2006</i>

1.2.2. Physiology and Pathophysiology of Hypoxia

Table 4 demonstrates the important role of hypoxia in human physiology. This is most notable in foetal development whereby regions of hypoxia have been observed in rat embryos with negative morphological connotations precipitated by altering levels of oxygenation (Chen et al. 1999). Subsequent, mouse and chick studies also identified hypoxia as essential to cardiogenesis with imposed oxygenation impeding development of the heart and hindering the chances of survival to birth (Wikenheiser et al. 2006; Krishnan et al. 2008). In the early phases of foetal development human embryos grow rapidly in hypoxia. Not only does this ensure adequate protection from O₂ free-radicals, it also promotes cell proliferation and placentation (Genbacev et al. 1996). Therefore early hypoxic states are vital in the development process, however hypoxia also occurs in normal healthy children and adults, moreover it can occur as a cause or the result of pathology.

In health, hypoxic regions exist in areas where adult stem cells reside such as the bone marrow and subventricular hippocampus (Mohyeldin et al. 2010). In disease states the story is more complex. For example, children born with congenital defect of the aorta / heart regularly demonstrate formation of accessory vasculature, developed in order to ease tissue hypoxia due to obstructed throughput; follow-up of adults surviving myocardial infarction or presenting with peripheral vascular disease also highlight accessory development, easing the hypoxic burden upon otherwise ostracised tissues. Further examples include, anaemia, which reduces vascular O₂ carriage, leading to end-organ hypoxia; pulmonary disease, resulting in decreased arterial pick-up of O₂ with overall hypoxia as a consequence; or obstructive sleep apnoea, a known indicator of cardiovascular disease (Khayat et al. 2009), emanating in chronic hypoxia following regular interruptions in O₂ supply.

For some time, angiogenesis - the formation of new blood vessels - has been an area of intense interest, both independently and in association with hypoxia. Vascular development is a highly regulated process which may cease almost as instantly as it begins. It is integral to natural development and regarded as the basis for wound healing. However, angiogenesis often occurs in the wake of pathological change, such as neovascularisation in age related macular degeneration (wet subtype), whereby the retina becomes detached from vascular diffusion fields. The

retinal layer must be reperfused immediately as starving these cells of O₂ results in apoptosis within a matter of hours.

The 'angiogenic switch' is understood to require among other things, vascular endothelial growth factor (VEGF), one of the main HIF-1 α target genes (Shweiki et al. 1992; Forsythe et al. 1996). Not only does HIF-1 α directly induce elements essential for vascularisation (nitric oxide synthases, matrix metabolism regulators etc.), it also regulates most other angiogenic instruments indirectly (Ryan et al. 1998). Nonetheless, VEGF alone has been seen to cause hypervascularity in mice with upregulated gene expression (Thurston et al. 1999). However the same study also found radical VEGF amplification responsible for the formation of hyperpermeable / 'leaky' vasculature. This fits evidence indicating that duration and level of hypoxia have a vital influence upon HIF target gene expression, e.g. mild hypoxia results in expression of HIF targets, while healthy cell functions are maintained. However, severe hypoxia can lead to cellular impairment with associated modifications to processes such as angiogenesis.

1.2.3. Hypoxia and Solid Tumours

Multiple genes regulated by HIF transcription code for products which are highly expressed in tumours. For instance up-regulation of metabolic enzymes and transporters (GLUT 1, etc.) are now identified as HIF targets (Yamamoto et al. 1990; Ebert et al. 1996; Airley et al. 2001). Other HIF targets such as angiogenic growth factors or genes enabling anti-apoptosis (Leuenroth et al. 2000), are linked to tumourigenesis. Indeed 53-54% (Zhong et al. 1999; Talks et al. 2000) of malignant tumours stain positive with HIF-1 α and HIF-2 α antibodies while most normal tissues appear negative. Groups have attempted to link HIF status with prognosis uncovering a mixed message. Lung cancer studies concluded tumour aggression decreased with HIF expression (Volm and Koomagi, 2000), the opposite was observed in cervical cancer with the presence of HIF-1 α indicating poor prognosis (Birner et al. 2000). This has been further complicated by demonstrations of hypoxia increasing resistance to treatments such as radiotherapy and chemotherapy (Flamant et al. 2012; Sermeus et al. 2012).

As solid tumours proliferate, they reach a critical mass whereby tumour size becomes a threat to survival (Figure 7). At this juncture neoplasms become dependent upon angiogenesis. Cells often proliferate rapidly and outstrip previous metabolic requirements which were once satisfied by simple diffusion from local vasculature (Folkman. 1990). Failed O₂ supply initiates tumour hypoxia in territories furthest from the blood vessel network, i.e. the tumour core. This drives the HIF pathway, triggering angiogenesis, however tumour cells also die in anoxia as newly constructed vasculature is inefficient and semi-permeable. It is thought that inhibition of angiogenesis in solid tumours will boost anoxia or even HIF induced apoptosis. However that is not necessarily the case. In fact some tumour cells accelerate the rate of metastasis when angiogenesis is deterred (Ebos et al. 2009; Pàez-Ribes et al. 2009).

Nonetheless, the role of anti-angiogenic therapy is currently under revision with the aim of enhancing tumour specific immunotherapy (Huang et al. 2012) and antiproliferative treatment (Chen et al. 2011).

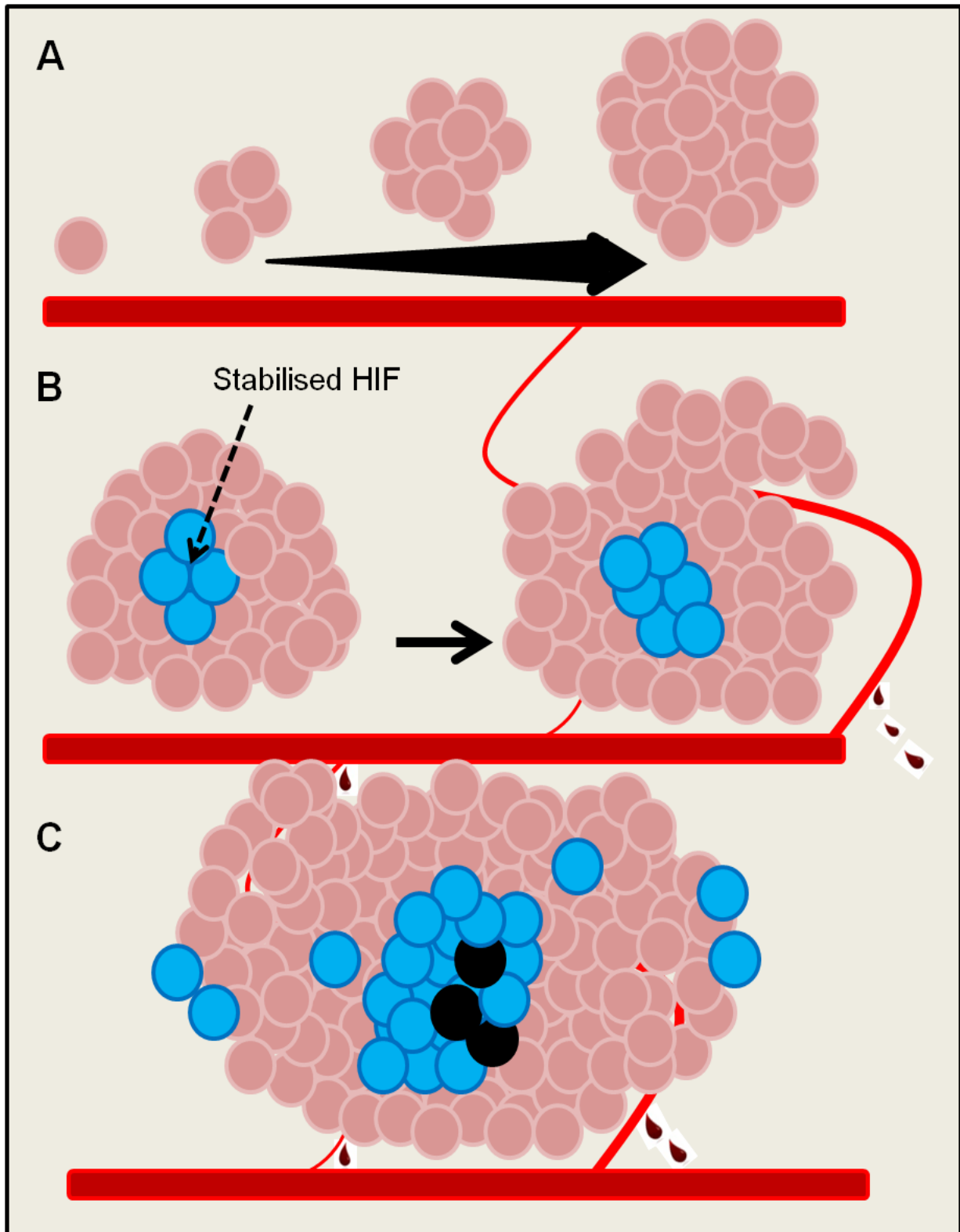


Figure 7. Tumour Cell Survival and Proliferation. Initial survival is dependent upon diffusion from nearby vasculature (A). Hypoxic cells (blue) appear due to increased tumour size, previous inhibition of HIF has been suppressed and tumour-derived 'leaky' blood vessels develop (B). With increased tumour size there is evidence of tumour cell death (black cells) caused by extreme hypoxia / anoxia (C).

Studies of apoptosis in hypoxia have revealed stabilisation of the tumour suppresser protein, p53 (Graeber et al. 1994). This protein, once coined 'guardian of the genome,' targets multiple tumour suppressor genes in response to cellular stressors. p53 target gene, WAF1, encodes p21, a protein regulating cell cycle arrest and apoptosis (Waldman et al. 1995; Asada et al. 1999; Jin et al. 2000). Other genes further regulate DNA repair, cellular senescence (Chen et al. 2005) and pluripotent stem cell reprogramming (Marión et al. 2009). Non-mutant p53 is responsible for maintaining a non-neoplastic phenotype, loss of p53 via TP53 mutation or protein deactivation can have a devastating effect upon abolition of tumour cells (Petitjean et al. 2007). Early investigation of p53 demonstrated autoregulation by murine double minute 2 (MDM2), which is in turn downregulated by p53 (Wu et al. 1993). Hypoxic stability of p53 is dependent upon HIF1- α subunits (An et al. 1998), inferred by direct and indirect interactions. MDM2 – p53 complexes bind and destroy HIF-1 α (Ravi et al. 2000), while concurrently, local p53 and HIF-1 α compete to interact with common coactivator p300 (Blagosklonny et al. 1998). Reduced HIF transcription ensues whilst p53 expression increases (Carmeliet et al. 1998), resulting in apoptosis.

1.2.4. Hypoxia and Neuroblastoma

In early foetal development HIF-2 α is essential for formation of the sympathetic nervous system (SNS) (Tian et al. 1998). At this point, the SNS is composed of cellular subtypes, neurons and neuroendocrine cells, which have been found within hypoxic regions of neuroblastoma. Here cells switch from one lineage to the other (Gestblom et al. 1997), a differentiation which has been investigated *in vitro* and *in vivo* showing hypoxic neuroblastoma loose SNS markers such as ID2 (inhibitor of differentiation 2), HASH-1 (human achaete-scute homolog-1) and dHAND (heart- and neural crest derivatives-expressed protein). They also up-regulate markers characteristic of neural crest cells, c-kit and Notch-1, indicating cellular regression to an earlier phenotype (Jögi et al 2002). Furthermore, previously expressed MYCN is no-longer present 72 hours post-hypoxia. In consolidation of these findings, quantitative polymerase chain reaction confirmed dedifferentiation with cellular regression to stem-cell like states, enhanced survival, proliferation and induction of differentiation inhibitors (Jögi et al. 2004). Linking to earlier discussion regarding neuroblastoma,

(see Neuroblastoma, Pathology and Pathogenesis, section 1.1.5.), differentiated tumours (e.g. ganglioneuroma) are perceived as lesser disease states and therefore induced differentiation has been trialled clinically with reasonable success. Dedifferentiation inhibitor, 13-cis-retinoic acid, improves overall survival in stage 3 neuroblastoma when administered after myeloablative therapy alongside bone marrow transplant (Matthay et al. 2009).

Segments of neuroblastoma surrounded by vasculature, strongly express HIF-2 α on immunohistochemical staining in contrast to HIF-1 α which is rapidly accrued at the onset of hypoxia but decreases significantly within 72 hours (Holmquist-Mengelbier et al. 2006). In addition to altered subunit expression, different neuroblastoma cell lines show widely varied transcription when cultured in hypoxia, even among cells with similar biology e.g. MYCN status (Fredlund et al. 2008). Moreover, both HIF-1 α and HIF-2 α stimulate VEGF transcription although each subunit maintains a degree of subtlety in genetic expression.

For instance, HIF-2 α does not exhibit the negative correlation with angiogenesis seen for HIF-1 α (Noguera et al. 2009). Uniquely, normoxic neuroblastoma display inhibition of HIF-2 α targets via microRNA-145 binding, which stifles tumour cell dissemination and proliferation (Zhang et al. 2012).

The presence of HIF-2 α is thought to infer poor prognosis, as opposed to HIF-1 α , which has been independently linked with improved survival and low tumour stages (Holmquist-Mengelbier et al. 2006; Noguera et al. 2009). Controversially, other studies challenge the positive outlook for HIF-1 α expression finding that the disease presented at more advanced age with poor tumour biology and higher clinical staging when HIF-1 α was expressed (Birner et al. 2000; Dungwa et al. 2012). This implies HIF-1 and 2 α stabilisation is dissimilar in neuroblastoma however their association with prognosis may be similar although this remains elusive.

Neuroblastoma is a life-threatening disease and chemotherapy is used extensively in treating all disease stages. The link between hypoxia and resistance to chemotherapy has been discussed, as has the predisposition of solid tumours, neuroblastoma, to hypoxia. However, hypoxia induced chemoresistance is extremely important in neuroblastoma, as cells become resistant to commonly used drugs such as etoposide and vincristine in a process driven by HIF-1 α over 1 to 7 days at

reduced levels of O₂ (Hussein et al. 2006). This is in contrast to resistance in acute hypoxia (< 23 hours) observed in colorectal cancer.

Finally, the issue of chemoresistance in neuroblastoma and other solid tumours remains unresolved. In order to address the situation it is necessary to understand the molecular mechanisms triggered by hypoxia in solid tumour formation. By doing this, it should become possible to develop novel treatments inhibiting the proliferation and migration of solid tumour cells. Furthermore this will also improve current clinical practice by identifying therapeutic agents which are not suitable for specific patients.

1.3 The Chorioallantoic Membrane and Tumour Cell Invasion

Introducing the Chick Chorioallantoic Membrane

The molecular mechanisms underpinning cancer and cancer cell aggression remain elusive. As such, all study models should be evaluated and modified in order to develop a more robust investigative tool which can be used to uncover the key aspects of tumour growth and migration. Promising results *in vitro* lay foundations for focused *in vivo* experiments providing an understanding of tumour cell behaviour in an environment similar to the human body. For years, murine models have been the most commonly used species *in vivo*, however they present many disadvantages such as interaction of the host immune system and imaging limitations. Species from zebra fish to chimpanzee inclusive have been examined and utilised in studies, for example, to trial therapeutic interventions before beginning human testing.

Chick embryos are an extremely useful candidate for *in vivo* studies as chicken reproduction is associated with low husbandry, high throughput, straight forward animal care in comparison with other *in vivo* models, non-invasive real-time and time-lapse imaging may be undertaken allowing short-term follow-up, interactions do not occur between the embryonic immune system and tumour cells in early gestational phases, and finally the CAM is intimately united with the embryo by a common blood supply, therefore interventions may be examined both upon the CAM and within the embryo avoiding insult to the foetus (Fuchs, Lindenbaum. 1988; Cimpean, Ribatti. 2008).

Developing chicks exhibit characteristics ideal for the study of angiogenesis, antiangiogenesis, tumourigenesis, tumour dissemination and metastasis (Chambers et al. 1982; MacDonald et al. 1992; Auerbach et al. 2003). A key experimental feature characteristic of the chick embryo model is the chorioallantoic membrane – CAM – a thin, transparent, easily accessible film which surrounds the embryo. Once formed this surface is cohesive with the porous eggshell, acting as a placenta presenting a large, heavily vascularised surface area for the provision of embryonic respiration (Deryugina, Quigley. 2008).

Despite wide applicability and several advantages, the chick model has also some disadvantages including, non-specific inflammatory reactions may occur, techniques require practice, chick survival can be limited depending upon duration of intervention, embryos are susceptible to infection, imaging potentially dries the embryo resulting in chick death before the experiment is concluded, and lastly, events witnessed in this model may not be of relevance to humans, although this is the common risk associated with all *in vivo* study.

1.3.1. Anatomy and Development of the CAM

The chorioallantoic membrane, CAM, is a womb-like structure engulfing the chick embryo and providing a boundary for gas exchange across the porous eggshell. The structure constitutes three layers, ectoderm – mesoderm – endoderm, sandwiched together to form a transparent collagenous matrix approximately 100 micrometers thick. CAMs develop as an amalgamation of two embryonic structures, allantois and chorion, which fuse on embryonic day E5 – 6 surrounding the embryo completely 6 – 7 days later at E12 – 13 (Tufan and Satiroglu-Tufan. 2005).

In the chick embryo, chorionic ectoderm facilitates gas exchange, becoming adhesive to porous eggshell at E10 whilst also forming a fine capillary plexus. Within this plexus the vessel lumen can be minuscule allowing passage of erythrocytes in single file. The inner chorionic mesoderm fuses with the allantoic mesoderm at E5 – 6 forming a segment which will later become heavily vascularised by a host of different calibre blood vessels (Fuchs and Lindenbaum. 1988). The allantois is derived from embryonic hindgut which herniates into the extra-embryonic coelom, before fusing with chorionic mesoderm to fulfill the CAM mesoderm and endoderm, a border to the allantoic cavity (Romanoff. 1960). Figure 8 depicts a cross-section of the CAM.

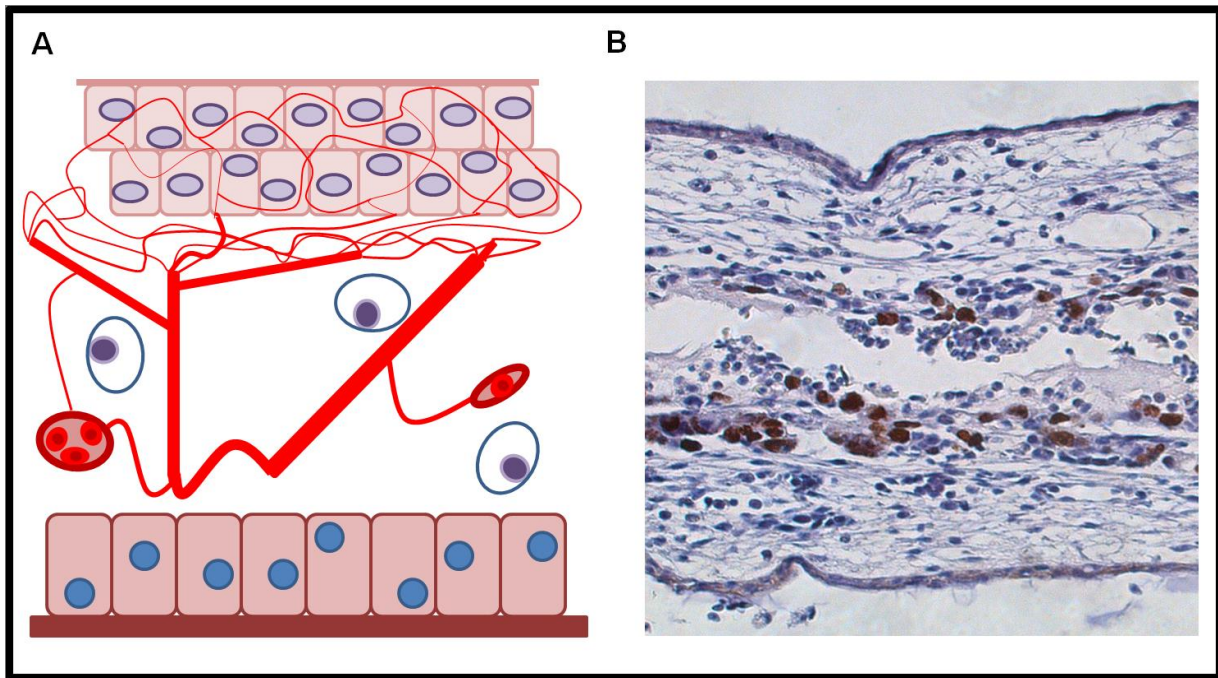


Figure 8. Cross-section of chick CAM. A is a diagram depicting a cross-section of the CAM and B is a microscopic photograph through the CAM, following immunohistochemical staining. Beginning superiorly, the initial layer – Ectoderm – constitutes 2 rows of epithelia and a fine capillary network. This surface sticks to the porous egg shell (E12-13). This gas exchange surface promotes rapid vascularisation and is ideal to support implanted cells. The middle layer – Mesoderm – is heavily vascularised and consists of collagen. Blood vessels run longitudinally and vertically as demonstrated by sectioned vessels containing erythrocytes in A. Finally, embryonic – Endoderm – borders the allantoic cavity. Brown cells (B) are neuroblastoma stained with a human specific antibody Ki-67, which indicates cellular proliferation.

CAM mesoderm contains extensive vasculature supporting arterioles and venules which communicate within the ectodermal capillary plexus. Links with the embryo itself are supplied by an umbilical artery which dichotomises into a pair of chorioallantoic arteries and a single chorioallantoic vein (Fuchs and Lindenbaum, 1988). Early vessel walls span one single, undifferentiated endothelium in width however by E8 they become embedded in mesenchymal cells sheathed in a basal lamina (Ausprunk et al. 1974). Later cellular differentiation to smooth-muscle cells has been observed as has expression of VEGFR-2 (Wilting et al. 1996) and lymphatic formation in regions common to venous drainage.

Chick lymphatic formation occurs after initial angiogenesis is well underway. Thus, embryonic immunity lags behind that observed in early gestation murine models. Evidence of differentiated immune cells indicates heterophil and monocyte formation detected around E10 – 15. The former, a major source of matrix-metalloproteinase 9, act as early neutrophils (Zijlstra et al. 2006), whilst the latter express the angiogenic promoter matrix-metalloproteinase 13 (Zijlstra et al. 2004). Late establishment of lymph and mature immune cells is thought to explain why the chick embryo is immunodeficient, making it an excellent model to study tumour cell proliferation and metastasis.

1.3.2. Chick embryo and CAM model in Cancer studies

Initially shown to support murine sarcoma xenografts, the chick embryo has been exploited for more than 100 years (Rous and Murphy, 1911). Further experiments investigated compatibility with human tumour cells confirming proliferation of: adenocarcinoma, bronchial carcinoma, embryonal rhabdomyosarcoma, Hodgkin's lymphoma, melanoma and squamous-cell carcinoma (Karnofsky et al. 1952; Korngold and Lipari. 1955; Harris. 1958). Tumour aggression and metastasis has been evaluated by embryonic dissection and the effects of chemotherapy have also been assessed.

Overall the chick embryo model is utilised according to three methods, each focused on highlighting specific steps in tumour formation and the metastatic cascade. First, the spontaneous metastasis model is used to demonstrate different features concerning tumour growth and intravasation by implanting tumour cells upon the CAM. Many different tumour cells are supported and proliferate to establish primary tumours, although some cell lines have been identified as unsuitable for this model (Deryugina, Quigley. 2008). Following survival and proliferation of a successful cell line, individual cells segregate themselves from the tumour body and commit to invasion of the CAM and local vasculature, a process known as intravasation. An additional benefit of using the spontaneous model is that one may witness the overall metastatic process providing cells proliferate – intravasate – migrate – extravasate – metastasise within experimental time constraints. In this sense the chick model permits the observation of true metastasis.

The experimental metastasis model involves introduction of tumour cells into the embryonic environment, often via injection into the extra-embryonic vasculature which is embedded within the CAM. This is undertaken in order to understand exactly how cells exit blood vessels, 'extravasation,' to later establish metastatic secondaries. Tumour metastasis theory suggests disseminated cells traverse the vascular tree and extravasate into tissues or organs, where they form secondary tumours. It was once thought tumour cells with increased metastatic capabilities, extravasate more effectively than cells with lower metastatic potential however imaging of fluorescently-labelled tumour cells contradicted this theory (Koop et al. 1996). Indeed more recent mouse and human studies suggest normal and pre-neoplastic cells may intravasate, migrate and extravasate to exist at locations other than their origin (Podsypanina et al. 2008; Pantel et al. 2012).

Finally the on-plant model provides an opportunity to observe and extrapolate the mechanisms behind angiogenesis stimulated by tumour cells. One group carried out this model by lacerating the CAM before introducing a plastic ring containing 3 – 5 million human glioma cells (Hagedorn et al. 2005). Similarly, osteosarcoma cells have been implanted upon the CAM via Thermanox™ plastic discs (Balke et al. 2010) whilst matrigel grafts have also been utilised to insert ovarian cancer cells (Lokman et al. 2012). These methods are important as neovascularisation is crucial to both primary and metastatic solid tumour survival and dissemination (see Hypoxia, Physiology and Pathophysiology of Hypoxia, section 1.2.2). Similar to the study of tumour proliferation and metastasis, independent study of angiogenesis has made great use of the avian model (Rabatti et al. 2000 and 2001; Tufan, Satiroglu-Tufan. 2005).

Consolidating the chick assay as a method used to study metastasis, human epidermoid carcinoma cells were implanted upon the CAM with resultant formation of metastatic foci in the heart and lung (Ossowski and Reich. 1980). Foci were confirmed as implant disseminations by identifying the highly specific human plasminogen activator. Another study verified the experimental metastasis model by injecting melanoma cells into CAM vasculature demonstrating extravasation and the foundation of secondary micrometastasis (MacDonald et al. 1992). Lastly, a range of materials have been verified for use in the onplant model such as collagen gel and

gelatin sponges containing angiogenic stimulators / inhibitors which provoke a response upon the CAM with 72 – 96 hours (Ribatti et al. 2006).

Importantly, in common with murine metastasis models the chick completely reproduces each step of the metastatic cascade. Moreover, human tumour cells are easily detected among chick tissues on a morphological basis, with appreciable differences in nuclear size. Furthermore, immunohistochemical staining of tumour samples may be used to discriminate chick tissues from tumour cells as was observed using fibrosarcoma of variable differentiation (Deryugina et al. 2005). This group also used fluorescently-labelled tumour cells to carry out live-cell imaging and quantification of angiogenesis / intravasation, demonstrating an advantage unique to the chick embryo above other *in vivo* models.

1.3.3. The Chick Embryo and Neuroblastoma

In recent years the chick embryo has enabled significant findings through the study of malignant melanoma, an invasive tumour stemming from melanocytes. These studies concluded that malignant cells (melanoma C8161) can be reprogrammed to adopt normal crest cell-like behaviour when introduced to a specific embryonic microenvironment such as the developing neural tube of chick embryos. Tumour cell 'normalisation' was characterised by identifying expression of neural crest cell markers and witnessing cell conformity to normal migration along crest cell pathways (Kulesa et al. 2006). Introduction of B16 mouse melanoma cells outside of the neural tube, e.g. the eye, demonstrated tumour cell proliferation and formation of focal structures, confirming the importance of cellular microenvironments (Oppitz et al. 2007). Melanocytes are neural crest derivatives which undergo differentiation and migration during the process of neurulation, (see Figure 3, Neuroblastoma, Embryology, section 1.1.4.). Similarly, neuroblastoma cells are also crest derivatives, thus it was believed they could be suitable for *in vivo* study via the chick model.

Currently we appreciate neuroblastoma as undifferentiated neural crest products, commonly exhibiting a host of genetic alterations, however we do not fully understand its aetiology. For this reason, it was necessary to identify a unique cellular feature in order to permit cellular lineage tracing. Utilising the chick model, a

transcriptome signature unique to neuroblastoma and neural crest cells was discovered, allowing researchers to isolate individual tumour cells for genome-wide expression screening of neural crest progenitors (Rabadán et al. 2013).

In total the expression of 27 genes were shown to be common to neural crest cells and neuroblastoma. More recently this has resulted in discovery of Lim domain only protein 4 (LMO4), a crucial cofactor in Snail2 mediated cadherin suppression expressed in disseminating neuroblastoma and delaminating crest cells (Ferronha et al. 2013).

When implanted upon the CAM, some neuroblastoma cell lines have been shown to survive and proliferate. Fewer have also demonstrated the ability to invade chick tissues to form metastatic deposits (Stupack et al. 2006). Variable invasion among cell lines may be due to features characteristic of specific neuroblastoma subtypes with some tumours categorised as more aggressive depending upon age of onset, clinical staging or poor prognostic indicators (see Table 3, Neuroblastoma, Risk Classification, section 1.1.3).

Aggressive neuroblastoma regularly exhibit genetic modifications such as MYCN amplification or loss of caspase-8 expression, an essential component in cellular apoptosis (Teitz et al. 2001). Using the experimental metastasis model, MYCN amplified Kelly cells have been shown to form tumours in several different chick tissues and organs. It had been expected that tumour cells would congregate within the sympathetic nervous system, however no tumours developed. Instead, cells extravasating in these areas started to conform to crest cell characteristics, mirroring prior melanoma studies. The most impressive cellular modification was the loss of previously expressed MYCN amplification (Carter et al. 2012). This finding could have profound implications given MYCN's reputation regarding neuroblastoma aggression (see Neuroblastoma, Genetic features, section 1.1.6.).

In another study the spontaneous metastasis model was used to compare tumourigenesis and metastasis in several neuroblastoma cell lines demonstrating various expression of the pro-apoptotic enzyme, caspase-8. The study findings concluded loss of caspase-8 permitted construction of metastatic deposits which were absent in the presence of the enzyme (Stupack et al. 2006). They further added that enzymatic expression results in the apoptosis of invasive cells

disseminating from the margin of the primary tumour and leaving the primary structure unaffected.

Lastly, the on-plant metastasis model has been used to show that current chemotherapy treatments can activate endothelial cells and upregulate angiogenic signalling in neuroblastoma (Michaelis et al. 2011).

1.3.4. Tumour cell Migration

Understanding the metastatic pathway is important as patients presenting with secondary tumours are less likely to survive. Treating these patients is difficult and often unsuccessful, hence today's clinicians are heavily reliant upon early identification of disease using tools such as population screening. Although rigorously challenged, the theory behind metastatic focal formation is more than a century old. The hypothesis was initially put forward in 1889 by the surgeon, Mr. S. Paget who proposed the now famous 'Seed and Soil' theory. In his metaphor, seeds represent select cells which disembark from the primary tumour and invade interstitial tissues to later enter the circulatory system. Once cells begin to journey around the body, 'seeds identify fertile soil,' a tumour cell extravasates into an organ / tissue and depending upon the microenvironment, it forms metastatic deposits (Paget S. 1889). This implies that tumour invasion is organ specific, as visceral microenvironments differ widely with each tumour cell requiring a specific microenvironment in order to establish metastasis.

Many lines of evidence verify the legitimacy of 'Seed and Soil' theory. For example, murine B16 melanoma cell clones were injected into a mouse model and followed up identifying widespread disparities in the ability of individual cells to form local tumours (Fidler and Kripke, 1977). On intramuscular administration, some cells neglected invasion altogether, although most formed secondary tumours in the ovary and lung, regions such as the kidney were unaffected, indicating tumour cell affinity for specific microenvironments. Further evidence was provided following induced melanoma formation, whereby invasive lesions were found to express remarkable contrast between each other and the primary tumour (Fidler et al. 1981).

Finally, a range of human tumours were injected into the vasculature supply of the murine brain. Tumour cells were removed from the circulation establishing metastatic deposits however different tumours demonstrated unique growing patterns with some developing in the cerebrum and cerebellum only, whilst others formed in meningeal territories (Schackert and Fidler, 1988).

Opponents of Paget's hypothesis postulated tumour cells may simply succumb to random mechanical arrest within the capillaries of nearby organs rather than expressing a preference for specific organ microenvironments. This idea gained momentum from experimental evidence demonstrating tumour cell arrest via fusion to capillary wall endothelium. Cancer cells were therefore suggested to invade tissue in a manner similar to that observed when studying lymphocytes during inflammation (Greene and Harvey. 1964). Further experiments concluded different cancers bind to different endothelium with varying affinity (Auerbach et al. 1987).

Overall mechanical arrest has been observed showing tumour cells which become lodged within capillary networks (Hart and Fidler. 1980), however the same study concluded lesion formation was influenced by specific organ cells. Additionally migration based solely upon the theory of mechanical arrest does not explain why metastasis identified in the spleen was consistently greater than that recorded in the kidney when retinaculum cell sarcoma were administered in equal quantities (Pilgrim. 1969). Moreover, this theory does not sufficiently address the various metastatic patterns observed clinically, eg. colorectal carcinoma regularly migrate to liver and lung and rarely affect bone or brain.

In summary, metastasis has been the subject of intense study for more than a century and modest progress has been made, however the specific mechanisms utilised in cancer cell invasion remain poorly understood. This is especially relevant in highly erratic cancers such as neuroblastoma and therefore a greater insight into the metastatic behaviour of this truly unique tumour remains highly valuable.

1.4. Study Aims

Neuroblastoma is a uniquely enigmatic, common, solid tumour of childhood. Although some disease states demonstrate spontaneous regression, the overall survival is dismal. Hypoxia is known to have profound effects upon tumour cells, stimulating angiogenesis and promoting aggression in cancer cells. It is also a condition which occurs naturally within solid tumours such as neuroblastoma.

We hypothesised that hypoxia might play a key role in neuroblastoma metastasis, and aimed to test this hypothesis using the chick embryo model.

The chick embryo model is a tried and tested method used to study the metastatic pathway. It provides strategic benefits above other *in vivo* models which enable better comprehension of the morphological and molecular changes occurring during tumour formation and invasion. Furthermore it is a quick, efficient and safe method of investigating metastasis, free of tumour cell interactions with the developing immune system.

This study aims to establish the role of hypoxia and hypoxia signalling pathway in neuroblastoma metastasis. Specific objectives of the project were:

1. To identify whether different neuroblastoma cell lines survive, proliferate and later establish primary tumours upon the chick chorioallantoic membrane.
2. Dissect and analyse chick tissues in order to observe and record examples of neuroblastoma cell migration and invasion from the outer CAM layer to organs and tissues located within the chick embryo.
3. Identify the influence of hypoxia upon the metastatic potential of neuroblastoma cells.
4. Elucidate the molecular mechanisms underpinning cellular alterations due to hypoxia.

Conclusions drawn from this study are expected to be beneficial for the study of neuroblastoma. It is also hoped that these findings may be useful in the future regarding development of novel drug therapies.

2. Materials and Methods

2.1.1. Overview of Cell lines

This study required four different neuroblastoma cell lines (Table 5). Each cell line was cultivated from primary tumours or metastatic deposits which were surgically removed from patients. Therefore the cell lines exhibit a range of different characteristics.

Table 5. Neuroblastoma cell lines used in this thesis. Additional details have been provided such as medium required to nourish the cells in culture and special features specific to each cell line. Minimum Essential Medium (MEM), Dulbecco's MEM and RPMI (Roswell Park Memorial Institute Medium) were purchased from Life Technologies; fetal calf serum (FCS) was purchased from PAA; and non-essential amino acids (NEAA) from Invitrogen, L-Glutamine from Life Technologies. Original location of tumour sample is preceded by an asterix (*).

Cell Line	Culture Medium	Features
Sk-N-AS	MEM 10% FCS 1% NEAA	Primary – unknown *Metastasis – Bone Marrow non-amplified MYCN Chromosome 1p deletion
Sk-N-BE(2)C	DMEM F12 : MEM (1:1) 10% FCS	Primary – unknown *Metastasis – Bone Marrow MYCN amplified Chromosome 1p deletion Chromosome 17 translocation Resistant to Chemotherapy
IMR-32	RPMI + L-Glutamine 10% FCS 1% NEAA	*Primary – abdomen Metastasis – unknown MYCN amplified Chromosome 1p deletion
Kelly	RPMI + L-Glutamine 10% FCS	MYCN amplified

Cell lines: Thiele CT. Neuroblastoma Cell Lines. In (Ed.) Masters, J. Human Cell Culture. Lancaster, UK: Kluwer Academic Publishers. 1998, Vol 1, p 21-53.

2.1.2. Tissue Culture Protocol

In order to identify NB cells in the chick embryo, cell lines were transduced with lentiviral particles containing eGFP or dTomato which provided individual cells with a stable fluorescent label (carried out by Dr. Anne Herrmann at the University of Liverpool). Cells were cultured in T75cm² tissue culture flasks (Corning, UK) containing 20mL of culture medium. Flasks were incubated in a humidified environment using a Sanyo CO₂ incubator (MCO175) set at 37°C, 5% (v/v) CO₂. In order to replace culture media nourishing NB cell lines, previous medium was discarded and replaced by 20mL of fresh, pre-warmed medium. Cells were passaged when culture dishes reached 80 – 90% confluency. During passaging, old medium was discarded, cells were washed once with 5mL of DPBS (Dulbecco's Phosphate Buffered Saline, Life Technologies) and 1mL of 0.05% Trypsin EDTA 1x Solution (Sigma Aldrich) was added, followed by an incubation step for 1min at 37°C. Detached cells were transferred to a Falcon tube and centrifuged (5min, 101×g). The pellet was resuspended in 8mL pre-warmed medium and counted with a Z₂ Coulter Particle Count and Size Analyzer (Beckman Coulter). 2×10⁶ viable cells were resuspended in 20mL pre-warmed medium and transferred to a tissue culture flask. Mycoplasma testing was carried out regularly using MycoAlert™ Mycoplasma Detection Kit (Lonza) according to manufacturer's instruction.

2.1.3. Culture and treatment of cells prior to CAM implantation

Cells subjected to CAM implantation were precultured either in normoxia, hypoxia or treated with DMOG. For normoxic preculture, fluorescently labelled NB cells were incubated for 3d prior to CAM implantation using a Sanyo CO₂ incubator (MCO175) which was humidified and set at 37°C, 5% (v/v) CO₂.

In order to preculture in hypoxia, fluorescently labelled NB cells were incubated 3d prior to CAM implantation in an oxygen controlled chamber (Don Whitley Scientific – Hypoxystation H₃₅). CO₂ was set at 5% and O₂ at 1%.

When administering treatment with DMOG (Dimethyloxalyl Glycine), fluorescently labelled NB cells were incubated in a humidified environment using a Sanyo CO₂ incubator (MCO175) set at 37°C, 5% (v/v) CO₂. DMOG (Enzo Life Sciences) was added to the culture medium 1d prior to CAM implantation at a final concentration of 0.5mM.

2.2. Incubation and Fenestration of Chick embryos

All chick embryo experiments were performed according to the guidelines set by the Home Office of the United Kingdom.

This study used fertilised white leghorn chicken eggs obtained from Lees Lane Poultry, Wirral, UK. The eggs were placed into an automatic incubator (Multihatch Mark II) and maintained at a temperature and humidity similar to normal physiological conditions. Eggs were not rolled as they would be in normal physiological settings, in order to ensure easy access to the embryo at later stages in development. Within 72 hours the eggs were removed from incubation, gently cleaned with 70% (w/v) alcohol, and punctured at the base with a needle (Figure 9). Next, a needle (19G Terumo) and syringe (5mL Terumo) were introduced into the embryonic environment and 3mL of albumin was removed carefully avoiding disruption to the embryonic yolk sac. As a result, the embryo dropped lower within the egg, freeing space between the shell and vital embryonic structures: the embryo and associated extraembryonic blood vessels. The needle hole was later sealed preventing leakage. At this stage a circular drill was used to cut a small rectangular segment in the eggshell. Communication was maintained between the window and the rest of the egg shell, a scalpel was used to sever this connection. Finally, Scotch Magic adhesive tape was attached to the loosened shell segment permitting complete removal of the window which was reattached to reduce the risk of infection (Figure 9). Lastly, eggs were stored in a temperature and humidity controlled incubator (Brinsea) until E7.

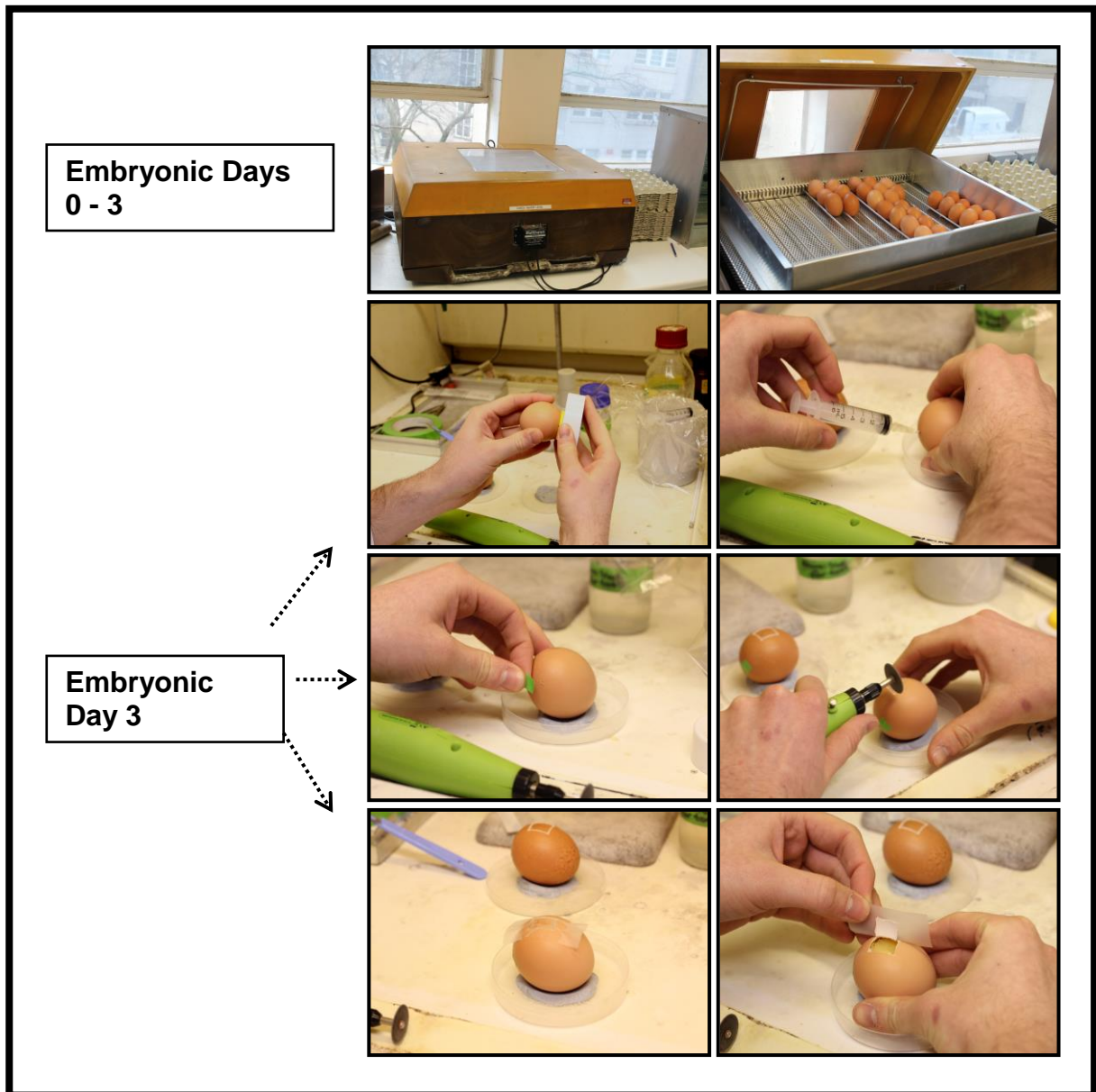


Figure 9. Between E0 – 3 eggs are incubated under controlled conditions. Fenestration concerned cleaning, removal of albumin, drilling and resealing the windowed shell. Eggs were further stored under incubation until E7.

2.3. Implantation of Tumour cells upon the “CAM”

When eggs reach E7 the CAM has started to become established. Accordingly, tumour cells were prepared for implantation on this day in order to provide enough time for tumourigenesis and subsequent metastatic invasion.

Preparation of tumour cells followed a process similar to passaging. Firstly, tumour cell morphology was assessed, ensuring that the cells were healthy. Next, old medium was removed; cells were washed in DPBS; detached using trypsin and refluxed from flask walls. Samples were centrifuged (5min, 101×g), counted and resuspended in serum free medium at a density of 1×10^6 cells / μL . Between $1.5 - 2 \times 10^6$ cells were implanted per egg.

At this time unfertilised eggs or those that had not survived were removed from the study and survivors were re-opened in preparation of implantation. Filter paper was cut into ribbons and sterilised in 100% ethanol which was allowed to evaporate before the paper was used to disrupt vasculature upon the CAM surface, creating an area appropriate for cell implantation, see Figure 10. Cells were carefully introduced to this area and shell windows were then replaced. Eggs were again stored in a temperature / humidity controlled environment until E14.

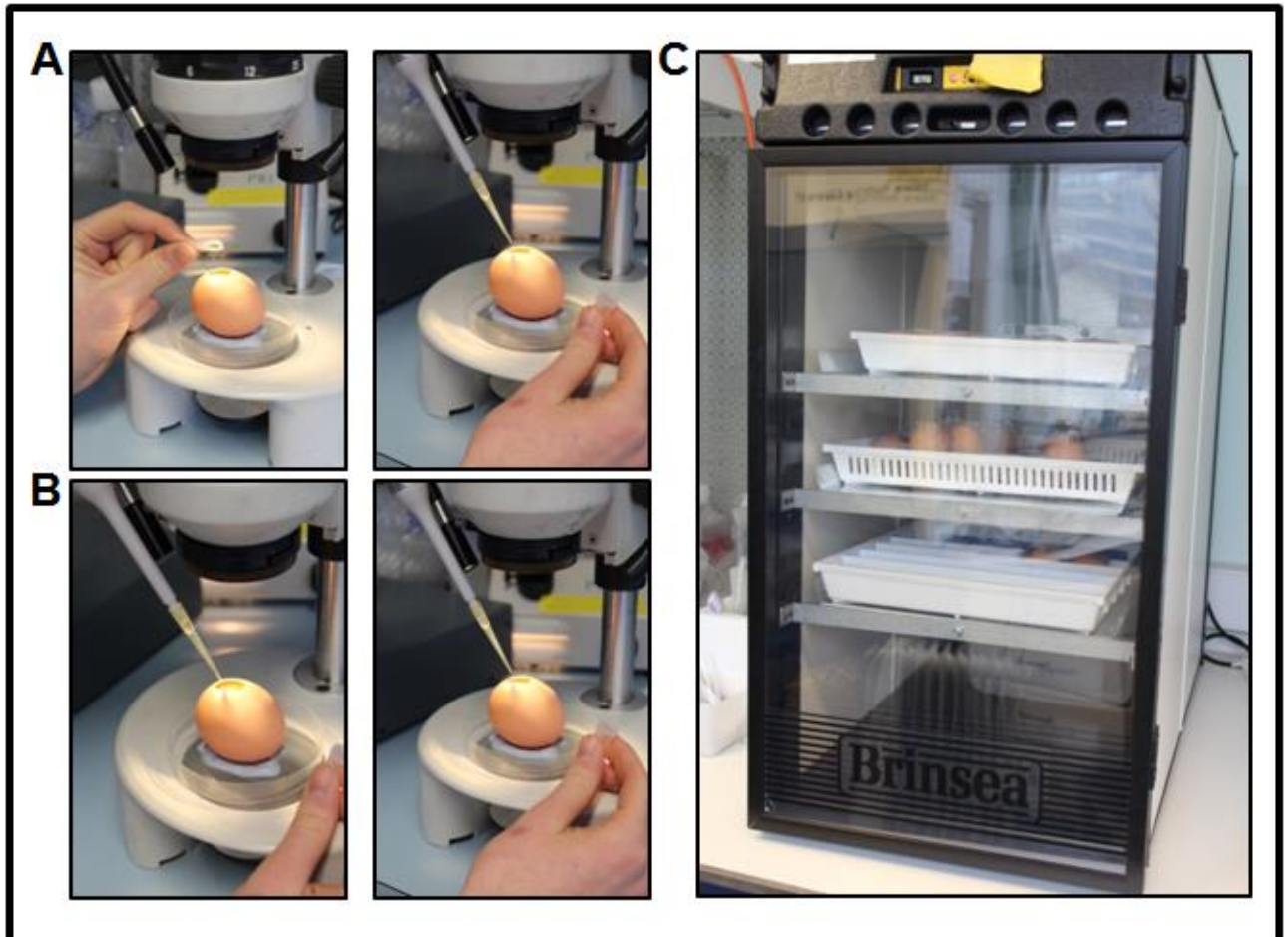


Figure 10. At E7 surviving embryos are implanted with fluorescently labelled NB cells. The method favoured in this study, CAM traumatisation (A), is undertaken by disrupting the surface with sterilised filter paper followed by implanting cells upon the freshly disrupted region. Also attempted was laceration of the CAM (B), whereby the embryonic membrane was scored with a pipette tip and cells were implanted in the disturbed area. All eggs undergoing implantation were stored in a controlled environment (C) until dissection at E14.

2.3.1. Dissection of Mature Embryos

At the end of the experimental period, E14, dead embryos were removed and survivors were reopened. Using forceps, surrounding shell was discarded to improve the visual field permitting close inspection of the CAM and identification of fluorescently labelled cells or tumours. Analysis of the CAM was performed under a Leica M165 FC fully apochromatic corrected stereo microscope with 16.5:1 zoom optics. Fluorescence was GFP and dsRed and images were captured using a Leica DFC425 C microscope camera alongside the computer software package, Leica V4.0.

Tumours grown upon the CAM were removed using size 5 dissection tweezers and dissection scissors. All tumours were imaged from three different perspectives, the investigators view from above the CAM, the “chick’s view” from below the CAM, and a cross-sectional view demonstrating depth of tumour growth. Tumour volume was calculated by taking measurements from these specially orientated images using the computer software, ImageJ. Samples were fixed for up to 12h in either 10% (w/v) Formalin or 4% (w/v) Paraformaldehyde (Sigma Aldrich) depending upon whether the sample was to be embedded in paraffin or frozen.

Following removal of primary tumours from the CAM, embryos were removed from their shells and dissected. Organs were removed with care and each tissue was assessed under fluorescent fields in order to identify tumour cells / metastatic deposits.

2.4. Paraffin embedding, Sectioning & Staining

Embedding samples in paraffin wax is an excellent method used to preserve tissues, providing safe storage of samples and the option of imaging tumour cores.

Firstly samples were fixed in 10% Formalin for no longer than 12 hours and taken to the University of Liverpool, Department of Cellular & Molecular Physiology. They were then dehydrated for 48 hours in a plastic cassette. Later samples were aligned appropriately within a metal mould which rested upon a cold surface while hot paraffin wax was poured in using a Thermo SHANDON HISTOCENTRE 3. Once the sample was fully covered in wax it was left to cool down and set over 24 hours. Samples were stored at room temperature until sectioning got underway.

On the day of sectioning, samples were cooled on a block of ice with a thin film of surface water to prevent adhesion. After approximately 40mins, samples were fitted onto a microtome (SHANDON) equipped with S35 Feather microtome blade (JDA-0100-00A). Sections were trimmed at 20 μ m until the sample was uncovered at which point 4 μ m sections were cut in continuous 'ribbons' consisting of 5 – 8 sections. Ribbons were floated upon the surface of a waterbath (Fisher Scientific) preheated at 35 – 40 $^{\circ}$ C and individual sections were separated using 125mm fine point curved forceps. Subsequently sections were 'caught' upon microscope slides (APES coated slides, Leica) which were stored upright in wooden racks and placed in a small oven to dry for at least 24 hours.

Staining was carried out upon an Autostainer (Dako) and required the following reagents, De-ionized water, Primary antibodies, Antibody Diluent (DAKO K8006), 5% (w/v) Bovine Serum Albumin in Tris Buffered Saline (TBS) (5% BSA/TBS), DAKO EnvisionTM FLEX/HRP Detection System (DAKO, K8012), EnvisionTM FLEX Wash Buffer (20x) (DAKO, K8007), AEC, Xylene, Industrial Methylated Spirits (IMS), Haematoxylin solution, Scott's Tap Water Substitute, DPX resinous mountant, and Aquatex aqueous mountant.

Up to 10 litres of FLEX Wash Buffer was required per staining session. This was prepared in the laboratory constituting: 50 μ M Tris, 150 μ M sodium chloride, 0.05% Tween (purchased from BDH). It was imperative that the pH was exactly 7.6.

2.5. Freezing samples, Sectioning & Staining

Rather than embedding in paraffin the majority of samples were preserved as frozen sections following removal from the CAM. Tumours were initially suspended in DPBS removing excess blood before fixation in 4% (w/v) Paraformaldehyde at 4°C for 12h.

Following fixation samples were removed and began sucrose infiltration for cryoprotection using a solution of 6% (w/v) sucrose (Fisher Scientific, UK) in deionised water. According to size, samples were maintained at this step for up to 16hours. Next they spent 24hours in 12% (w/v) sucrose followed by a further 24hours in 20% (w/v) sucrose. Peel-a-Way disposable embedding moulds with a truncated 22mm square top tapered to 12mm bottom (T-12) acted as the final receptacle for samples after cryoprotection. The sample was correctly orientated and covered in Shandon Cryomatrix embedding solution (Thermo Scientific), and a cork or plastic top was added to the mould acting as a cover. Finally moulds were placed upon dry ice and left to set for 10mins before long term storage at -80°C in a Sanyo Ultra Low freezer.

Sectioning of frozen samples required a Leica CM1950 cryostat set to -20°C. Samples were cut at 10µm and collected using Superfrost PLUS glass slides (Thermo SCIENTIFIC). Frozen samples retain fluorescence therefore slides were assessed for the presence of tumour cells before being stored in a freezer at -20°C.

In order to stain samples slides were thawed at room temperature and sections were circumscribed using a hydrophobic pen (SUPERPAP by Invitrogen) to create a containment area for solutions. Samples were then rehydrated for 10mins in DPBS before this was replaced by Ammonium Chloride (NH₄Cl) for 20mins. Next a blocking buffer was made constituting; 1% (w/v) Bovine Serum Albumin in DPBS (by Gibco), 0.1% Triton X-100 (Sigma Aldrich), and 0.4% (v/v) Tween 20 (Sigma Aldrich). This was applied to samples for 30mins following removal of NH₄Cl.

Primary antibody dilutions were prepared in blocking buffer and applied at 4°C overnight, in accordance with Table 6.

Table 6. Primary Antibodies used in this study. (h) human; (chk) chick; ms (mouse); (IHC-F) or (F) Immunohistochemical staining if Frozen sections; (IHC-P) or (P) Immunohistochemical staining if Paraffin sections. All antibodies were calibrated prior to staining tumour samples.

Antigen	Reactive Species	Host Species	Application	Dilution	Manufacturer
SMA-α	h, chk, cow, dog, ms, rat	rabbit	IHC-F	1 : 200	Abcam
Ca9	H	rabbit	IHC-F IHC-P	(F) 1 : 500 (P) 1 : 1000	Abcam
CD56	H	mouse	IHC-F	1 : 50	Leica Novocastra
CD133	H	mouse	IHC-F	1 : 50	Miltenyi
GFAP	h, cat, cow dog, ms, rat, sheep	rabbit	IHC-F	1 : 500	Dako
GLUT 1	h, ms, rat	rabbit	IHC-F IHC-P	(F) 1 : 500 (P) 1 : 250	Abcam
HIF-1α	h, ms, monkey, rabbit, sheep	mouse	IHC-F IHC-P	(F) 1 : 100 (P) 1 : 100	Novus Bio
HIF-2α	h, ms	rabbit	IHC-F IHC-P	(F) 1 : 100 (P) 1 : 1000	Abcam
Ki-67	H	mouse	IHC-F IHC-P	(F) 1 : 100 (P) 1 : 100	Novocastra
Nestin	H	mouse	IHC-F	1 : 1000	Millipore
NB84	H	mouse	IHC-F	1 : 100	Leica Novocastra
Vimentin	avian, h, pig, rat	mouse	IHC-F	1 : 200	Santa Cruz
β-III-Tubulin	Mammalian	rabbit	IHC-F	1 : 1000	Covance

Following removal of the primary antibody, three consecutive washes in blocking buffer were undertaken, each lasting 10 – 15mins. Later, secondary antibodies were added, 100µL per sample, to slides in solution with blocking buffer. Antibodies were left to stain for 1hour at room temperature with details listed in Table 7 below;

Table 7. Secondary antibodies used in this study. All secondary antibodies were used upon IHC frozen sections and were subjected to extensive calibration prior to tumour staining.

Antigen	Reactive Species	Host Species	Application	Dilution	Manufacturer
Cy 3	Anti-mouse IgG	Sheep	IHC-F	1 : 500	Sigma-Aldrich
Alexa Fluor 555	Anti-rabbit IgG	Goat	IHC-F	1 : 500	Invitrogen
Cy 5	Anti-rabbit IgG	Goat	IHC-F	1 : 200	Abcam
Alexa Fluor 488	Anti-rabbit IgG	Goat	IHC-F	1 : 500	Invitrogen
Alexa Fluor 647	Anti-mouse IgG	Goat	IHC-F	1 : 200	Invitrogen

A further three wash steps were undertaken using blocking buffer and finally an appropriate nuclear stain was applied for 10mins in solution with DPBS, see Table 8. Finally, slides were washed twice for 10mins in DPBS and rinsed in deionised water, dried then mounted with Anti-fade Medium (Dako). Slides were sealed with 25x60mm cover slips (VWR International). They were dried overnight in a cool dark place and finally stored at 4°C.

Table 8. Cell nuclei stains used in this study. TO-PRO®-3 Iodine is excited at 642 nm resulting in emission at 661nm in the invisible spectrum. Hoechst 33342 trihydrochloride is excited at 350nm and emits at 461nm, therefore it is viewed in the visible spectrum as the colour blue. For simplicity, Topro-3 iodine stained nuclei are assigned the colour blue in this study.

Antigen	Application	Dilution	Manufacturer
Topro-3 iodine	IHC-F	1 : 1000	Invitrogen
Hoechst 33342	IHC-F	1 : 1000	Invitrogen

2.6. Imaging

In this study, paraffin embedded sections were imaged via stereo microscopy using a Leica DFC425 C camera. All slides bearing frozen sections were imaged and photographed by confocal microscopy using a Zeiss LSM 710 confocal microscope with associated computer software (Zen 2010 B SP1).

3. Results

3.1. Introduction

In order to investigate the role of hypoxia in neuroblastoma cell migration and invasion it was essential to first establish the chick embryo as an appropriate model for the study of metastasis *in vivo*. The chick chorioallantoic membrane has previously been shown to support other implanted tumour cells permitting survival, proliferation, tumourigenesis and metastasis, however it was crucial to ensure that chosen cell lines – Sk-N-AS, IMR-32, Kelly, Sk-N-BE (2)C – were compatible upon the CAM.

Fluorescently labelled cell lines were incubated in normoxia, implanted upon the CAM and stored under temperature and humidity controlled conditions for 7 days. Subsequently the membrane was scrutinised and imaged to identify tumour formation. Chicks were then dissected in search of cells which may have migrated, invaded viscera or established metastatic deposits.

3.1.1. Pilot study investigating cell line survival upon the CAM

An initial pilot study found three out of four tumour cell lines remained upon the CAM seven days post-implantation, see Figure 11. Interestingly tumours expressing MYCN amplification did not produce positive results when compared to Sk-N-AS cells despite the theoretical increase in tumour aggression linked to positive MYCN status. Moreover the chemotherapy resistant Sk-N-BE(2)C cells could not be identified upon the membrane during imaging. Kelly cells were observed developing a 2D mosaic-like pattern, however IMR-32 cells gathered as a sphere of small cellular satellites surrounding a hollow, bubble-like, core. This led to larger scale repeat experiments whereby Sk-N-AS cells were studied first, due to the 3D tumour structures produced.

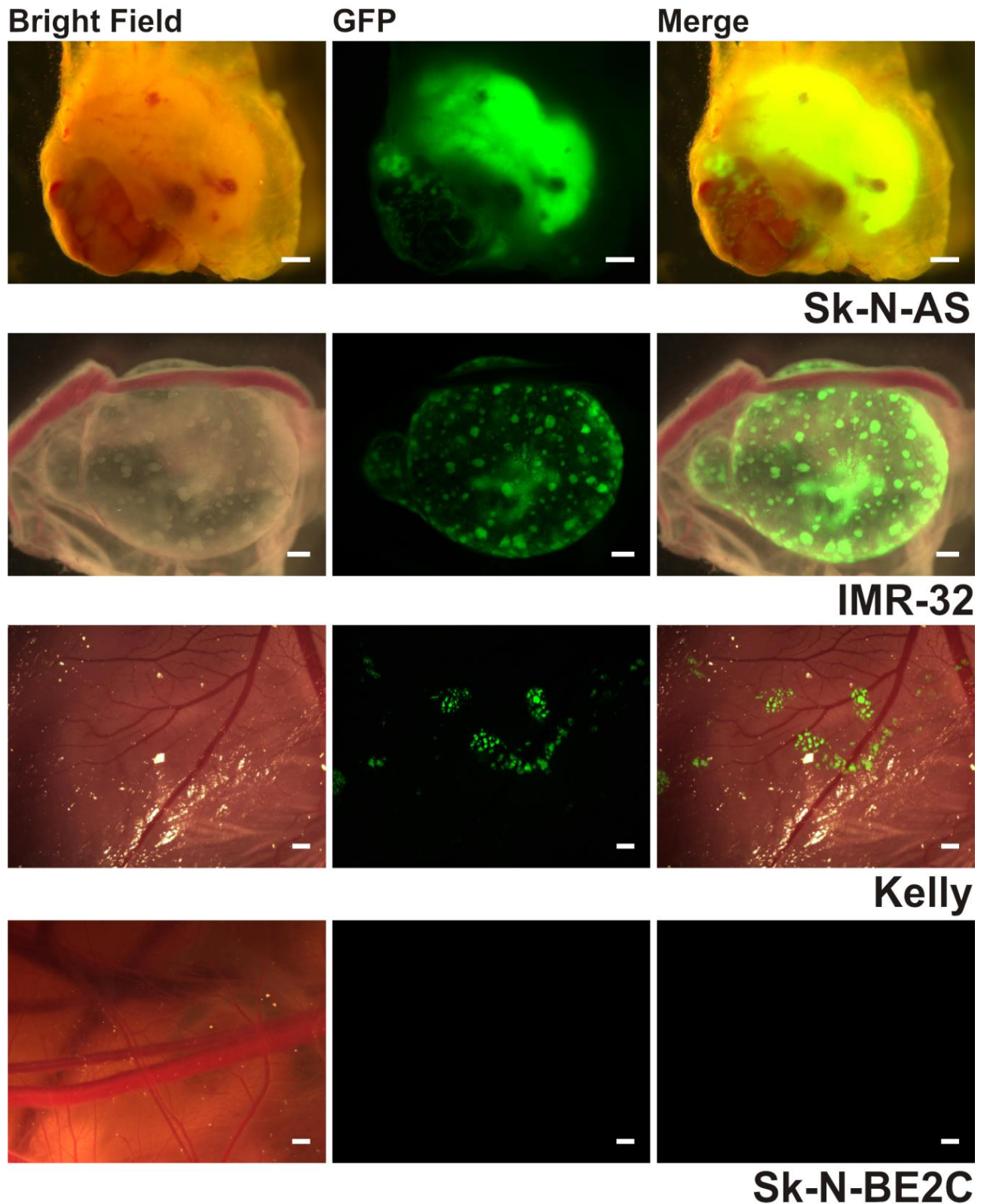


Figure 11. A summary of initial cell line implants screening. GFP labelled tumour cells were precultured at 21% O₂, 5% CO₂ and 37°C. Images on the left were taken in the bright field, middle images were captured under fluorescence, those on the right represent an overlay of bright field and fluorescence. Scale bar - 500µm.

3.1.2. Implantation of Normoxic Sk-N-AS

When undertaking in-depth study of Sk-N-AS cell tumourigenesis upon the CAM the pilot study methods of preculture (37°C, 5% CO₂, 21% O₂ - normoxia) and implantation (1.5 - 2 x 10⁶ cells per egg), remained unchanged.

More than 3 independent experiments were undertaken implanting Sk-N-AS cells upon the CAM. Large, heavily vascularised tumours developed regularly in several chicks during each experiment, overall n= 17, see Figure 12A. In order to exclude the possibility that the fluorescent GFP label influenced tumour cell behaviour, additional experiments were carried out using dTomato labelled cells, Figure 12B. dTomato labelled SK-N-AS cells survived and proliferated to form solid tumour structures on the CAM with no difference in cell behavior, morphology or tumour growth observed.

Although tumours formed regularly following Sk-N-AS implantation, tumour morphology was widely variable, see Figure 13. Some implanted cells congregated together forming large, lone, spheres while others developed in irregular shapes as smaller, multiple satellite tumours. Regardless, one also observed similarities between structures, for instance tumours demonstrated a relatively smooth surface area and were bordered by an intense network of intricate blood vessels.

Additionally some tumours were found entirely engulfed in blood cells giving them a much darker complexion when viewed in the bright field. The identification and aetiology of such structures remains unclear, however this phenomenon was not an anomaly as it occurred repeatedly throughout many independent experiments.

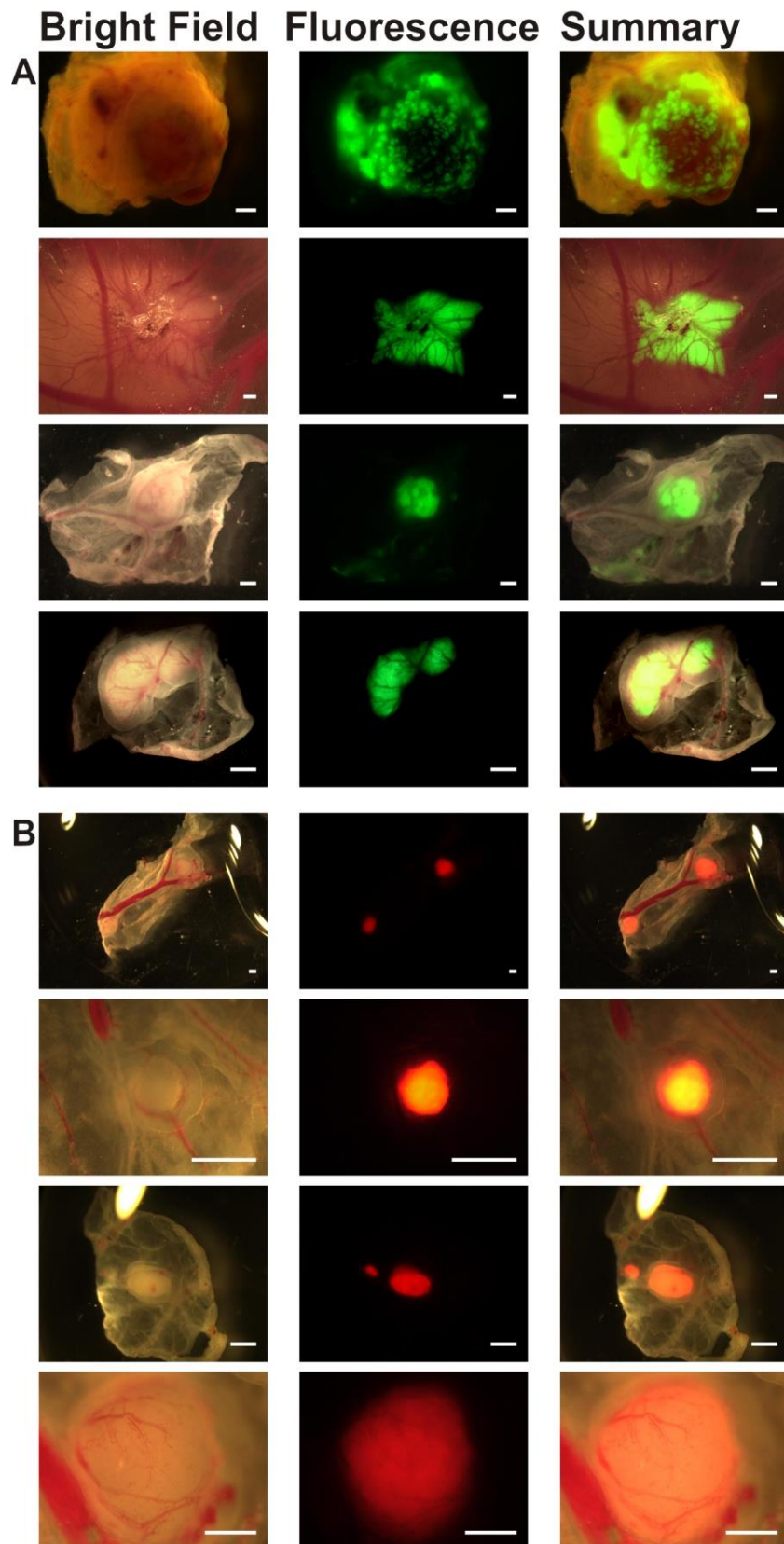


Figure 12. Sk-N-AS tumour formation. Cells were precultured at 37°C, 5% CO₂ and 21% O₂. Tumour cells were labelled with GFP (A) or dTomato (B) and tumours were established regardless of lentiviral labelling. Bright field images (left column) show tumours as they appeared upon the CAM, fluorescent images depict cohorts of individual tumour cells, the right column is an overlay of both images. Scale bar - 500µm.

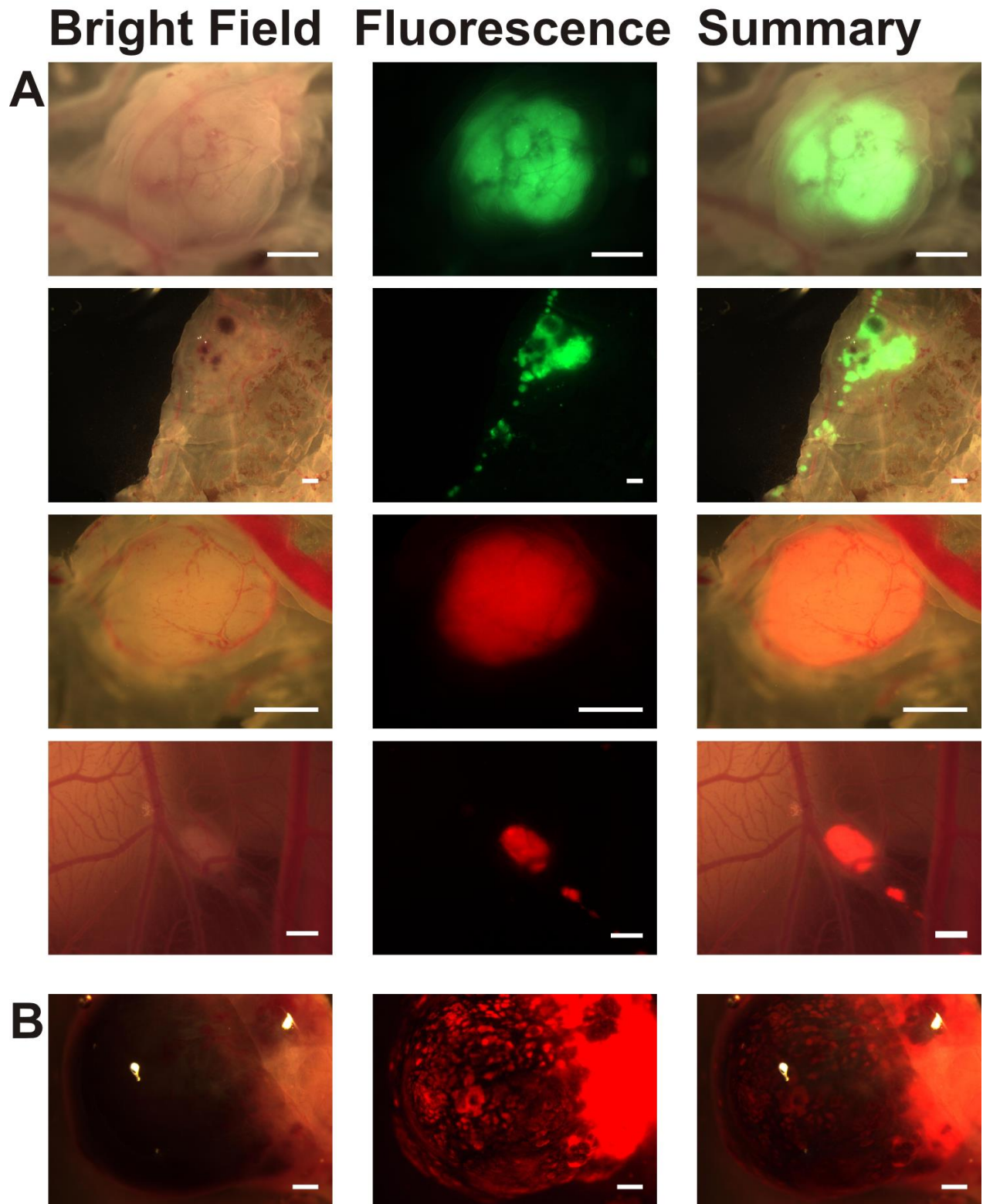


Figure 13. Different patterns of Sk-N-AS tumour formation. Tumours formed as single solid structures or multiple small satellites (A). They regularly presented as/within structures heavily laden with blood cells (B). Left column - bright field images, middle - fluorescent images, right - overlay. Scale bar - 500 μ m.

3.1.3. Normoxic Sk-N-AS Migration & Invasion

Following identification of tumours or tumour cells surviving upon the CAM, samples were imaged and removed. They were washed, imaged again in different planes determining tumour size, and stored appropriately for later sectioning and staining. At this point the chick was systematically dissected with each organ carefully removed and analysed for the presence of migrated / invading tumour cells and more importantly, to identify metastatic secondary tumours.

Rigorous examination of all chick tissues / organs was unsuccessful in identifying metastatic Sk-N-AS cells precultured in normoxia. Therefore, although the CAM was proven to be an excellent supporter of normoxic Sk-N-AS tumourigenesis, formation of metastatic secondary tumours did not occur within the chick over 7 days post-implantation. Figure 14 shows representative organs of the chick embryo. Invasion could not be found in any organ or tissue of the chick embryo upon implantation of normoxic precultured Sk-N-AS cells.

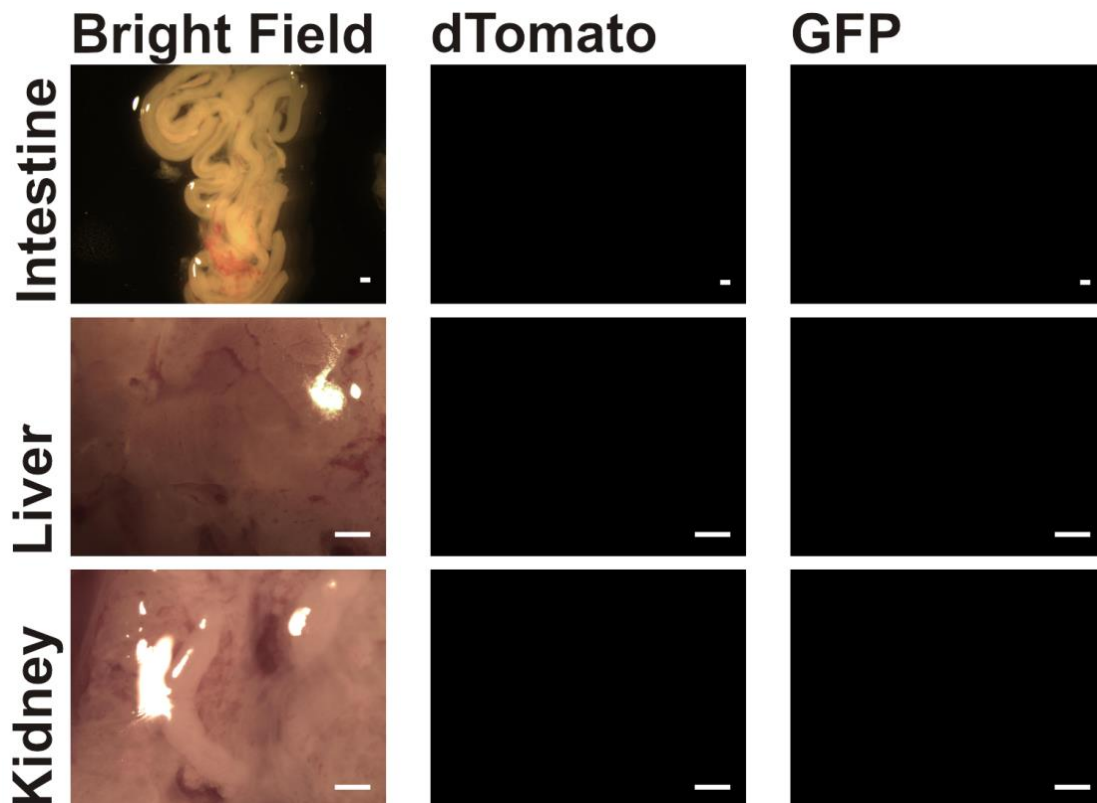


Figure 14. Normoxia and Tumour cell Invasion in representative organs. Top row indicates chick intestine which was free from fluorescent tumour cells labelled dTomato or GFP. In the middle row one can see chick liver, no tumour cells were present. Bottom row demonstrates no secondary tumours formed in the kidneys or adrenal glands. Scale bar - 100µm.

3.1.4. MYCN amplified cell lines

Having observed the results produced using Sk-N-AS cells, attentions were shifted to the MYCN amplified cell lines also investigated in the pilot study. Before beginning this study, it was postulated that MYCN amplified cells would survive upon the CAM and more importantly, they may be more likely to invade the chick embryo to form metastasis. This hypothesis of increased metastatic potential was based on the increased tumour aggression and reduced overall survival linked to neuroblastoma patients overexpressing MYCN proteins (see Introduction, Neuroblastoma, Genetics 1.1.6).

IMR-32 cells, a commercial line derived from an abdominal primary tumour, were precultured in normoxia as previously mentioned. They were then tested extensively upon the CAM however tumourigenesis did not occur in a fashion similar to Sk-N-AS cells. Many eggs did not display tumour cells at all when imaging after 7 days incubation however 3 independent experiments repeatedly resulted in chicks presenting a structure similar to that observed in the pilot study, see Figure 15A. Structures consisted of a hollow sphereoid seemingly containing multiple small tumour deposits, which were surrounded on the outside by a dense vascular network. Chick dissection again demonstrated the absence of tumour invasion and metastasis.

The Kelly cell line (Figure 15B) did not appear to form solid tumour structures. Instead they were observed either forming a mosaic-like pattern or a solid 2D layer of dried, flakey cells. Once again invasion of cells was unidentifiable using either fluorescent label.

The chemotherapy resistant, MYCN amplified, Sk-N-BE(2)C cell line is derived from a metastatic bone marrow sample, however these cells were also incapable of tumourigenesis upon the CAM following preculture in normoxia. Migration and invasion of tumour cells was also unsuccessful, metastatic foci were not established.

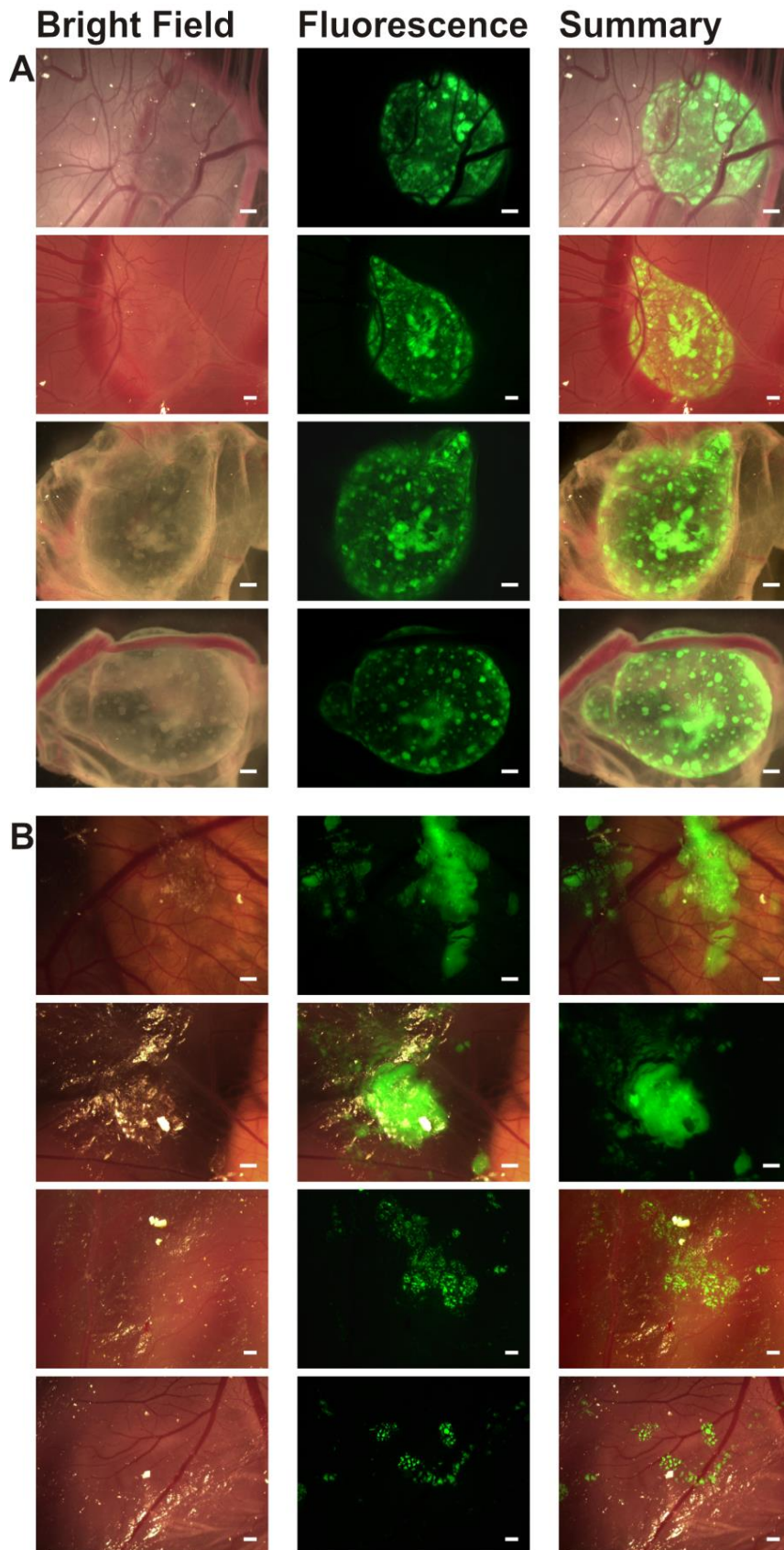


Figure 15. IMR-32 and Kelly cell tumourigenesis upon the CAM. IMR-32 cells (A) formed similar to the pilot study. Kelly cells (B) remained as a 2D structure. Images were acquired at day 14 over 4 independent experiments. Left column - bright field images, middle column - GFP labelled cells under fluorescence, right column - image overlay. Scale bar - 500µm.

3.2.0. Implantation of Hypoxic Sk-N-AS cells

In order to test the effects of hypoxia on tumour cell migration and invasion, cells were incubated for three days under hypoxic conditions (1% O₂), prior to implantation upon the CAM. Each experiment was carried out using GFP labelled cells and then repeated with dTomato labelled cells with no difference in result. Upon removal from the hypoxic chamber, cells were prepared as described previously in the Methods section, next they were implanted upon the chick CAM.

Given the success in tumourigenesis demonstrated by implanting Sk-N-AS cells upon the CAM it was decided this cell line was the ideal candidate to progress onto hypoxic preculture experiments. In keeping with previous methods at least three independent experiments were undertaken.

Both GFP and dTomato labelled tumours developed successfully upon the CAM as was previously observed using normoxic cells, see Figure 16. Further similarities with normoxic cells were drawn by assessing tumour morphology as a range of differing tumour formations were recorded, see Figure 17. Section A of this figure demonstrates how some chicks formed larger, singular, tumours while others developed multiple smaller tumours. Other morphologies are displayed in Figure 17B which exhibits the different chain-like tumour formations which stretched across the length of the CAM. Additionally Figure 17C highlights a reoccurrence of 'haematoma-like' tumours seen in normoxia.

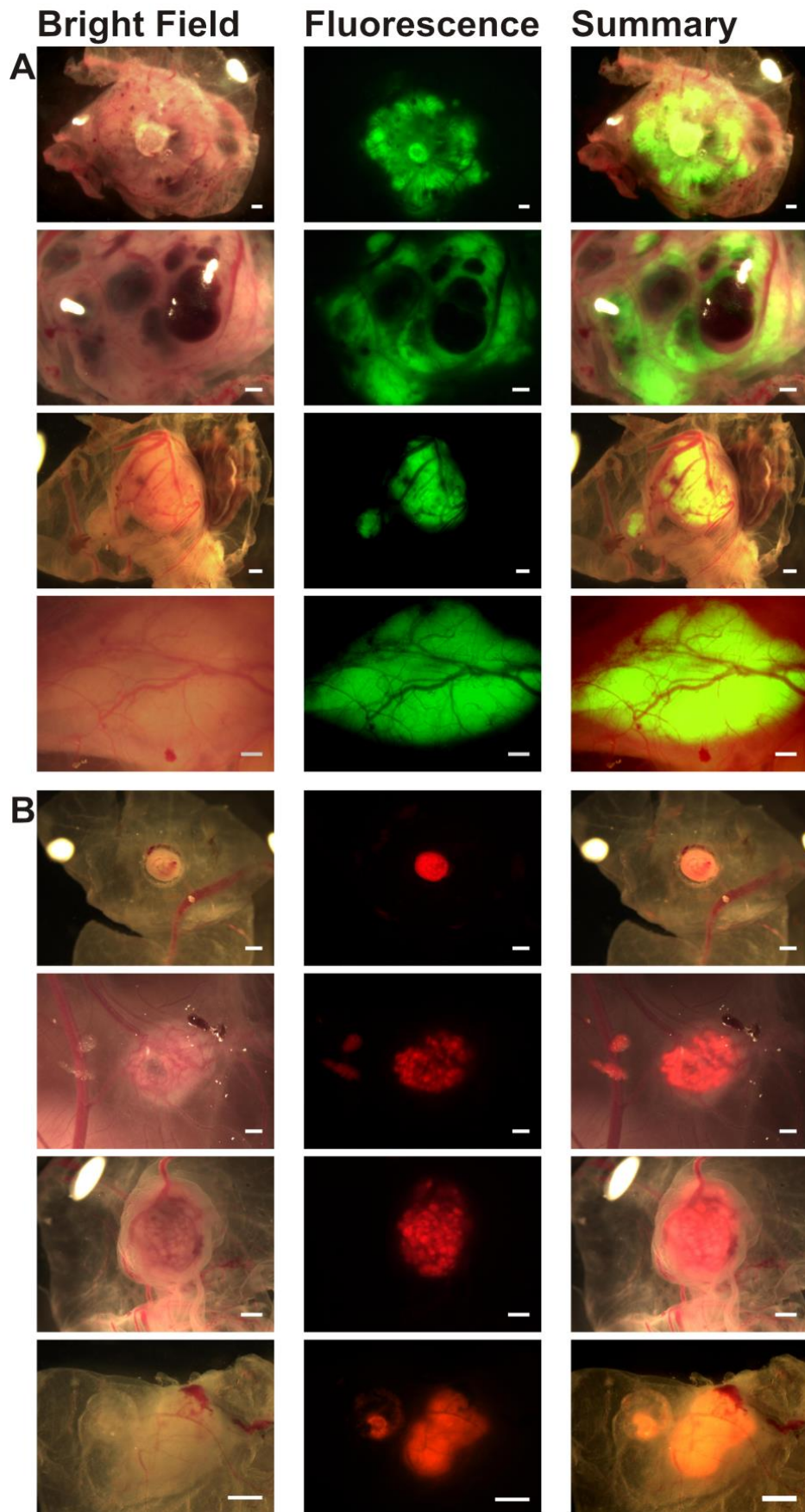


Figure 16. Sk-N-AS cells precultured in Hypoxia for 3 days. A and B depict tumour formation of GFP (A) and dTomato (B) labelled cells exposed to hypoxia prior to implantation. Scale bar - 500µm

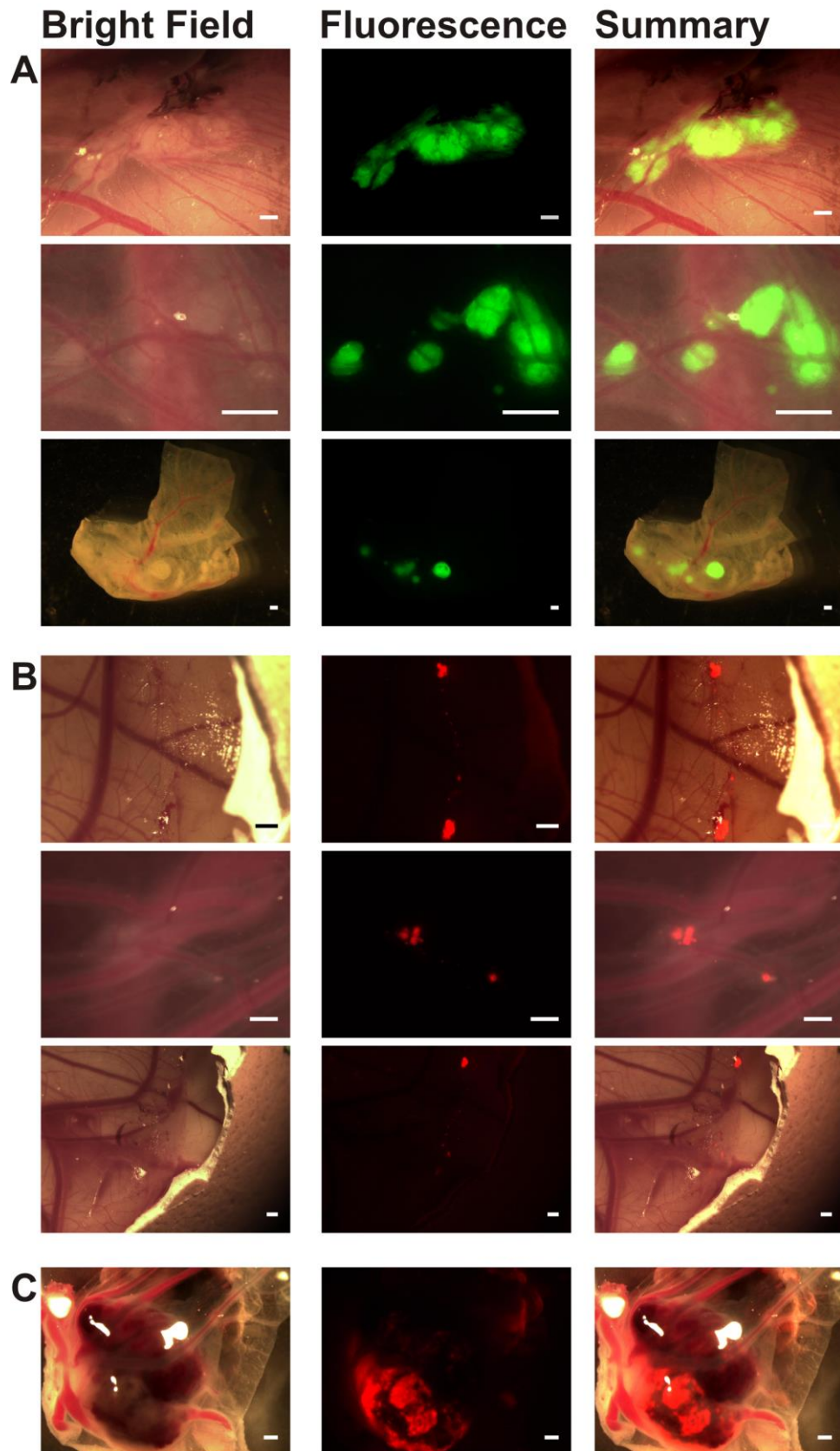


Figure 17. Sk-N-AS (3day hypoxia) - patterns of tumour formation. A range of different tumour formations were demonstrated by cells cultured at 37°C, 5% CO₂ and 1% O₂. All tumours were heavily vascularised. Section A exhibits tumours fluorescently labelled with GFP. Different patterns of dTomato labelled, chain-like tumourigenesis formed across the CAM in B. Haemorrhagic tumour / Haematoma formation was not uncommon, this is shown in section C. Scale bar - 500µm.

3.2.1. Tumour differences – Normoxic versus Hypoxic Preculture

SK-N-AS cells formed a range of morphologically different tumours upon the CAM when both normoxia and hypoxia preconditioned cells were introduced. Upon removal of tumours at E14 individual embryos were noted to produce tumours of different sizes for hypoxia compared to normoxic preculture condition. In order to quantify the difference in tumour size, a series of images were captured over 10 different hypoxic and normoxic experiments.

Each egg was implanted with $1.5 - 2 \times 10^6$ cells, however several tumours produced from hypoxia precultured cells were extremely large. Results from this comparison indicated hypoxic tumours had a larger median value (8mm^3 compared to 1.4mm^3) represented by middle horizontal lines in Figure 18. Hypoxic tumours also demonstrated a greater mean (54mm^3) and quartile values ($4.4 - 29.4 \text{mm}^3$) when compared to tumours formed by cells precultured in normoxia; mean - 11.7mm^3 ; and quartile values, $0.33 - 16.5 \text{mm}^3$. There was no significant difference in tumour size when comparing normoxic and hypoxic preculture (Mann-Whitney test $U = 68$, $p = 0.079$). Differences may be attributed to quantity of cells implanted ($1.5 - 2 \times 10^6$).

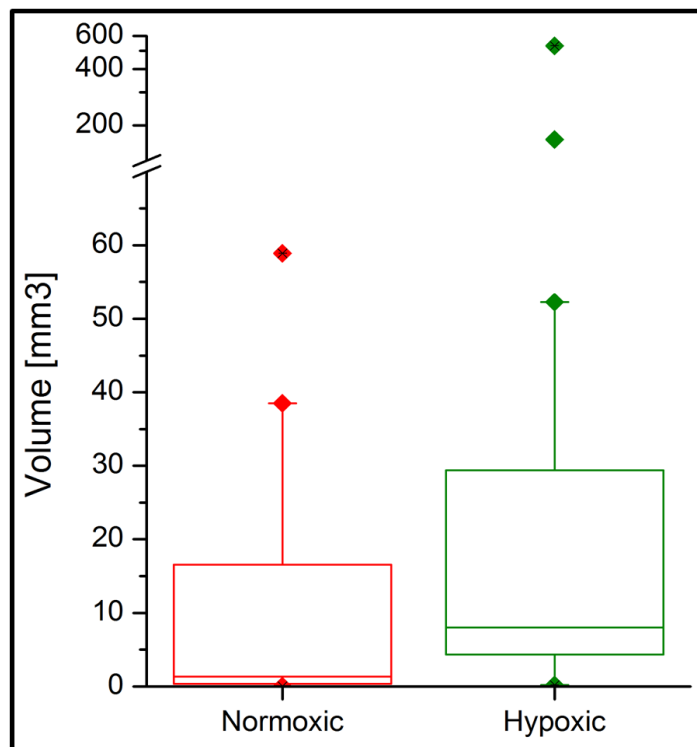


Figure 18. Sk-N-AS Tumour volume – Normoxia Vs Hypoxia. Quantification of tumour volume (mm^3) between tumours formed following implantation of cells precultured in normoxia (red) or hypoxia (green). Regarding egg number; normoxic preculture, $n=13$; hypoxia preculture, $n=17$.

The main difference between Sk-N-AS cells precultured in normoxia or hypoxia was the successful formation of tumour metastasis for the cells preconditioned in hypoxia (Figure 19). Cells which were precultured in 1% O₂ had the ability to migrate and invade embryonic tissues or organs. Subsequently this resulted in the formation of multiple metastatic foci.

Highly favoured locations for tumour cell invasion were the intestines, adjoining tissues (mesentery) and crucially, the liver which is a very common site for tumour metastasis in patients with neuroblastoma. Furthermore, extensive liver metastasis can often prove deadly in neuroblastoma, especially in children with stage 4S disease. Other less frequently affected regions of the embryo were the kidneys and meninges.

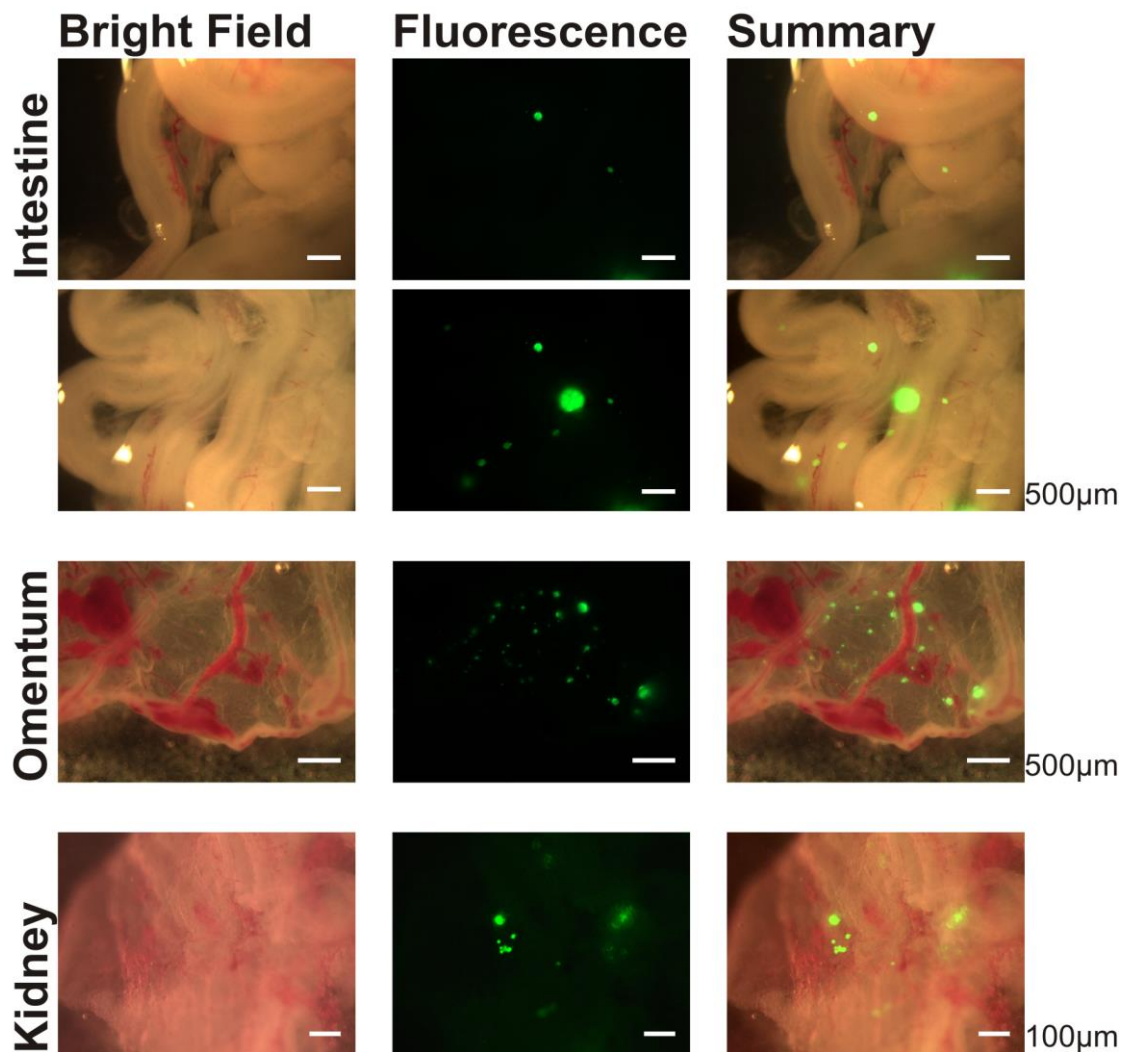


Figure 19. Invasion of Hypoxic Sk-N-AS cells. Fluorescently labelled cells precultured in 1% hypoxia for 3 days pre-implantation, formed primary tumours upon the CAM with metastatic secondaries inside the chick embryo. Shown are organs (intestine-kidney) and mesenteric tissue (omentum) with metastatic foci.

3.2.2. Effects of DMOG on Sk-N-AS tumourigenesis

As discussed previously (Introduction, Hypoxia, Physiology and Pathophysiology of Hypoxia 1.2.2.) the effects of hypoxia prompt many changes upon cells, some concerning cell survival, are more vital than others. Modifications are extensive ranging from altered glucose metabolism to stimulation of angiogenesis however most are controlled under the action of the hypoxia-inducible factor (HIF) pathway. When cells are incubated for 3 days at 1% O₂ the mechanisms in place during normoxia, PHD activated ubiquitinylation and FIH fail to degrade and inactivate HIF. This enables HIF accumulation and activation permitting the expression of specific hypoxia induced genes. In the absence of hypoxia, HIF may be stabilised by treating cells with DMOG for 1 day. DMOG is a PHD inhibitor hence its presence permits direct HIF activation without inducing other HIF independent effects caused by hypoxia.

In order to investigate the role of HIF in the observed cell invasion, cells were treated with DMOG for 1 day before implantation. Again Sk-N-AS cells with different fluorescent labels were utilised. On this occasion tumourigenesis was again accomplished and confirmed over 3 independent experiments, whereby tumour morphology was indiscriminant from that recorded under normoxic and hypoxic preculture conditions (Figure 20A). Equally comparable was tumour-haematoma formation which was identified regularly (Figure 20B). Tumour cell invasion was observed and was mainly present in the intestines and liver, however metastasis followed the same pattern as that observed in cells precultured in hypoxia (Figure 20C).

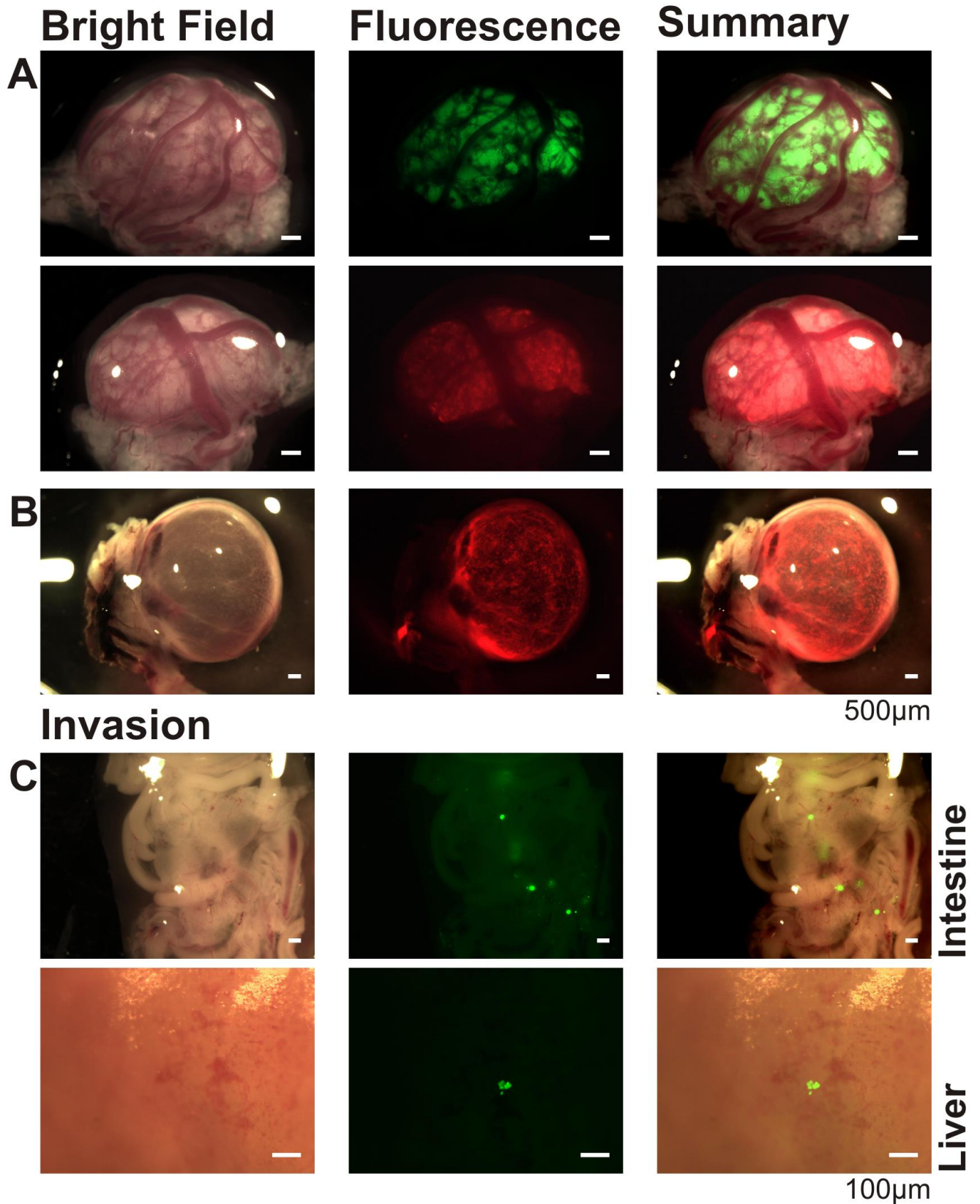


Figure 20. Sk-N-AS + DMOG - Tumours and Secondary Invasion. Section A presents tumours formed upon the CAM having been pretreated for 1day with DMOG. B demonstrates familiar tumour-haematoma formation while C displays significant invasion of viscera. Tumour cells labelled with GFP or dTomato.

3.3.0. Co-application of Normoxic and Hypoxic Sk-N-AS

So far the results of this study have shown that Sk-N-AS cells invade tissues and organs throughout the chick embryo when they have been precultured in hypoxia (1% O₂) for 3 days prior to implantation. This phenomenon was not observed when cells were precultured in normoxia (21% O₂). It was decided to study whether cells precultured in hypoxia were able to influence the invasion of other noninvasive cells. In order to achieve this, normoxia and hypoxia precultured cells were implanted upon chick embryos simultaneously.

In early experiments, GFP labelled cells were precultured under hypoxia and implanted upon the CAM while normoxic dTomato labelled cells were simultaneously introduced to the membrane at a different location (Figure 21). This made it possible to visualise interactions occurring between each preculture group while providing an excellent opportunity to understand subtle differences in tumour morphology.

Overall, tumour cells did not interact when placed apart upon the CAM. Tumour morphology was variable although this was independent of preculture conditions presenting as large masses or small, multiple tumour chains. As previously described hypoxic (green) cells invaded while normoxic (red) cells did not (result not shown).

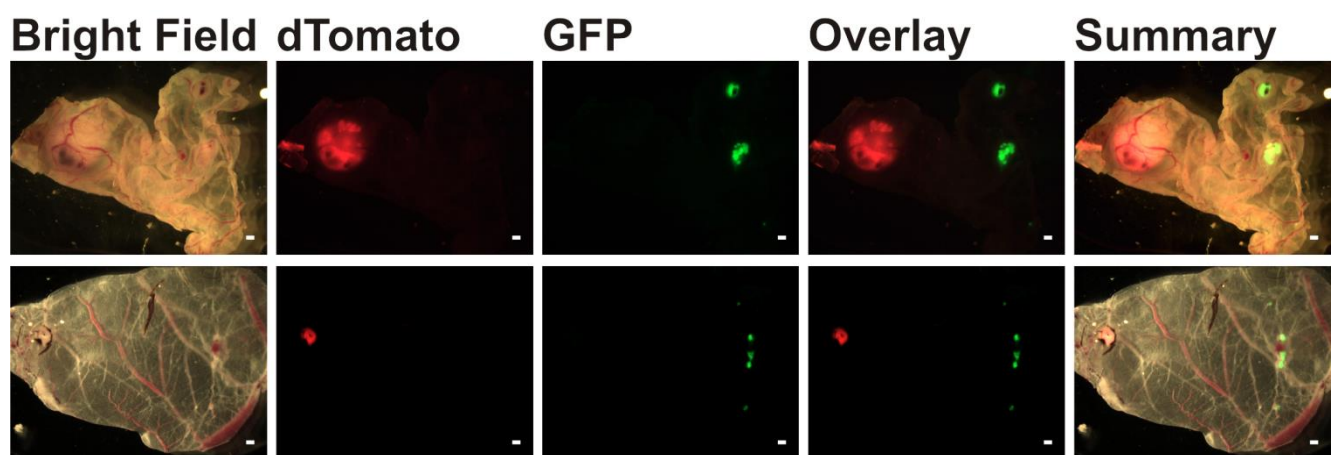


Figure 21. Differently precultured Sk-N-AS cell implanted in different locations. Cells precultured in normoxia (Red) and hypoxia (Green) were simultaneously implanted in different areas of the CAM. Tumour morphology was varied regardless of preculture condition. Scale bar - 500µm.

3.3.1. Implantation of Normoxic – Hypoxic Mixtures

As no interactions were observed between hypoxic and normoxic tumour cells placed on separate regions upon the CAM, an alternative method was devised whereby cells were mixed together prior to implantation. This removed the obstacle of travelling distances across the CAM in order to make contact with other tumour cells. Mixing took place during preparation for implantation and then cells were promptly introduced to the CAM.

In line with previous experiments cells were deposited at $1.5 - 2 \times 10^6$ cells per egg. Hypoxic cells were labelled green with GFP and normoxic, red with dTomato. Three independent experiments were undertaken.

When mixing cells before implantation the tumour formation was varied (Figure 22 and 23A). The presence of tumour-haematoma was again recorded (Figure 23B).

Not only did combined normoxic – hypoxic tumours develop, as identified by individual fluorescent images, mixed tumour invasion also occurred, (Figure 24). Hypoxic cells invaded in the usual pattern but unique to these experiments, normoxic cells were also identified undergoing secondary metastasis. Interestingly, cells existed as unique, separate entities. Metastatic tumour spheres were also identified within the intestines (Figure 24B).

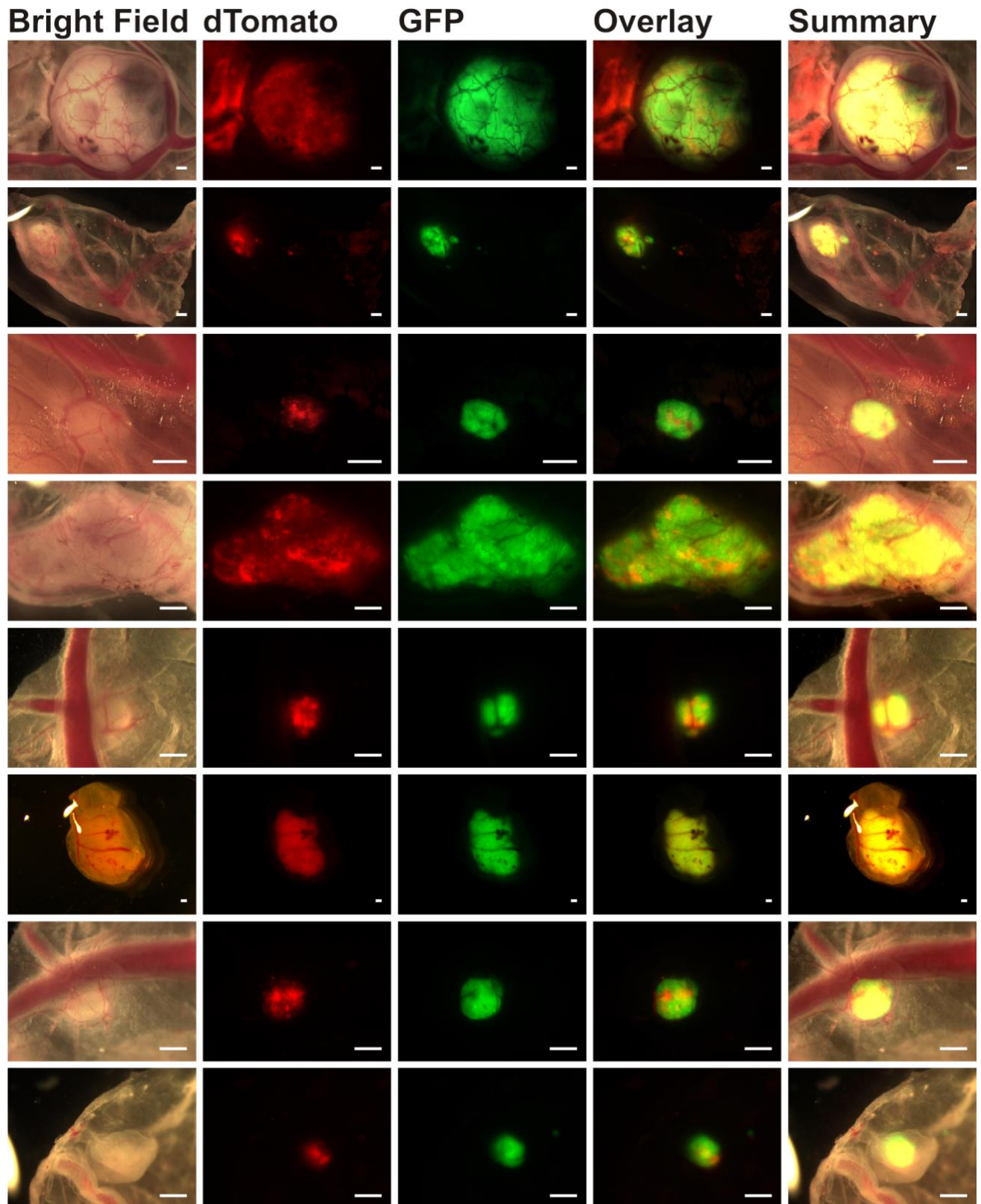


Figure 22. Normoxic-Hypoxic Sk-N-AS Mixture implanted at the same location. Tumours developed as a result of mixing hypoxic (green) and normoxic (red) Sk-N-AS cells immediately pre-implantation. Scale bar - 500µm.

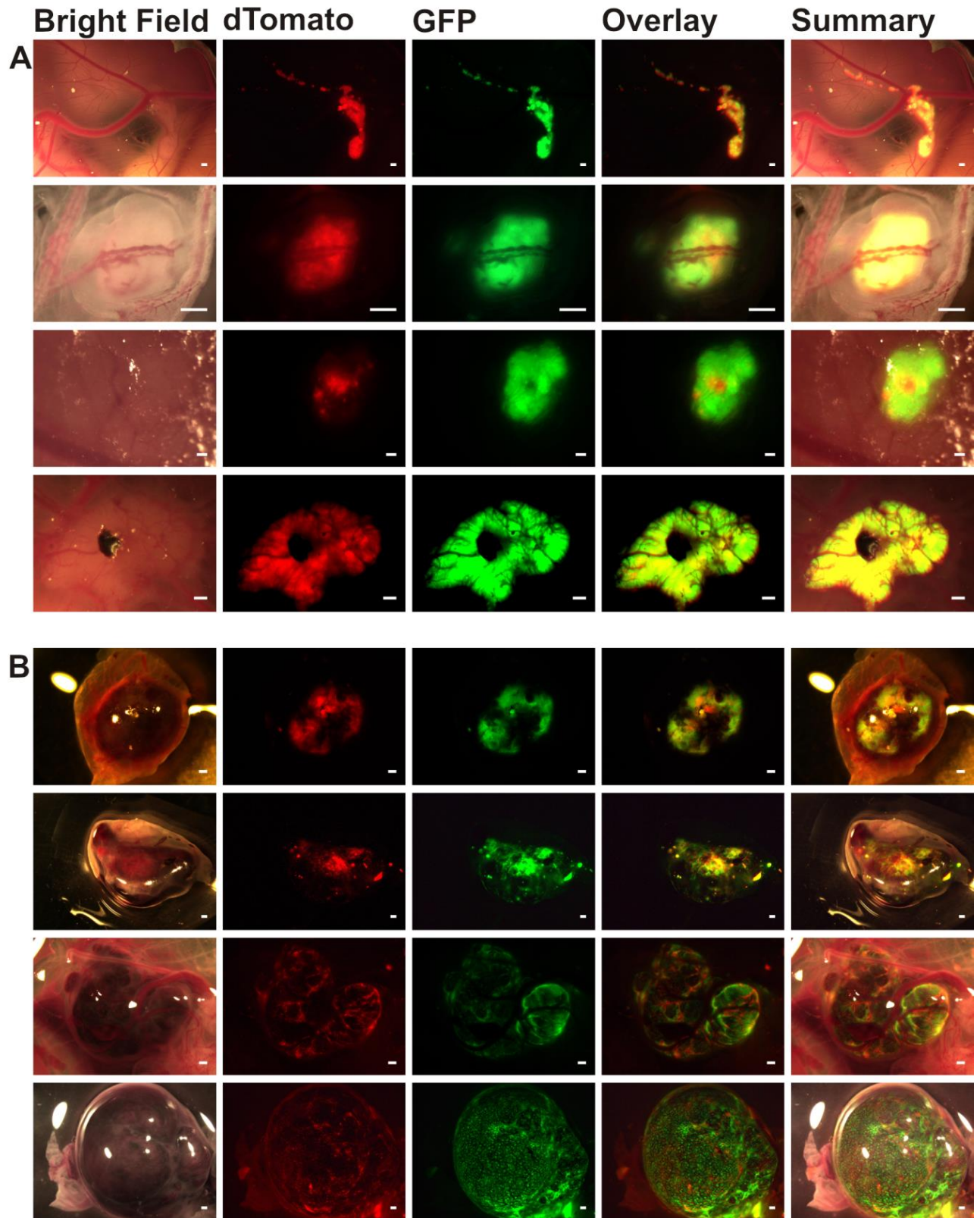


Figure 23. Patterns Tumour Formation in Mixed Sk-N-AS. Section A demonstrates differences in tumour morphology. Section B depicts haematoma / haemorrhagic neuroblastoma forming upon the CAM. Cells labelled red (dTomato) were precultured in normoxia, green (GFP) were precultured in hypoxia. Scale bar - 500µm.

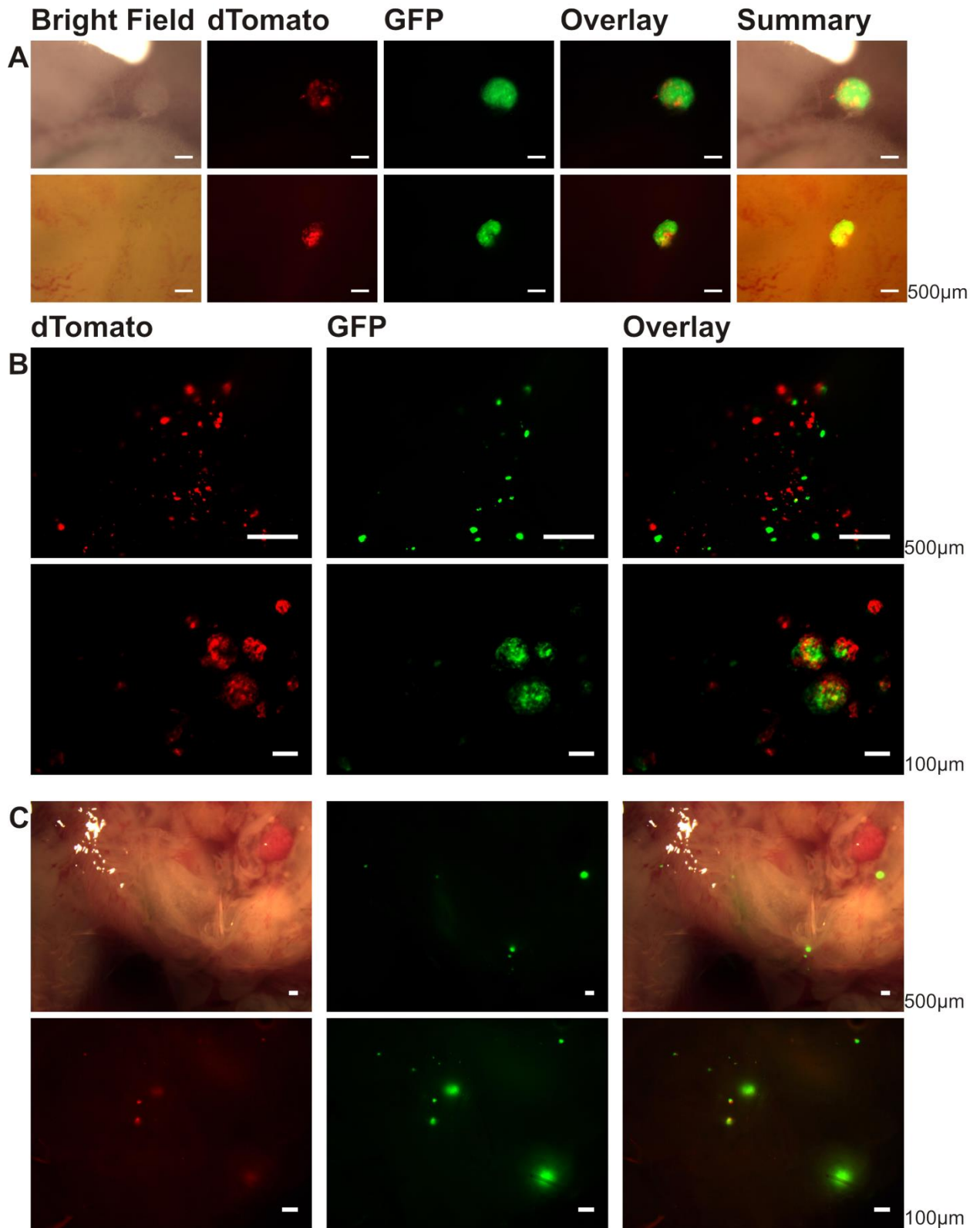


Figure 24. Invasion of organs/tissues following implantation of mixed Sk-N-AS. Section A exhibits large metastatic foci proliferating within chick intestines. B provides zoom images demonstrating metastatic spheroid formation, also highlighting normoxic invasion independent of hypoxic cells. In part C, invasion of the intestinal mesentery / omentum has occurred, metastasis is widespread.

3.3.2. Sk-N-AS Tumourigenesis and Invasion

In summary, multiple experiments were carried out testing the ability of Sk-N-AS cells to; 1) survive upon the CAM; 2) proliferate to form tumours; 3) migrate throughout the embryo and form metastatic foci. Regardless of various conditions applied to cells before introduction to the egg, tumourigenesis was repeatedly witnessed, as quantified (Figure 25). A chi-squared test demonstrated enhanced tumourigenesis in normoxic cells when compared to hypoxia ($X^2 = 4.49$, $p < 0.05$).

The key difference observed between normoxic (21% O₂) and other conditions is the ability to undergo metastatic invasion. Hypoxic or hypoxia-like effects of non-normoxic preculture regimens seemed to impact tumour cell ability to metastasise. Figure 25 and 26 provide a summary of tumourigenesis occurring in different preculture conditions and Table 9 demonstrates common locations for metastasis. While normoxic (21% O₂) preculture resulted in metastasis in 0% of chicks, preconditioning in hypoxia (1% O₂) resulted 33.3% of chicks demonstrating invasion. This was found to be HIF dependent as DMOG treated cells invaded in 20% of cases. Mixed tumour cells invaded in 44.4% of chicks surviving until E14.

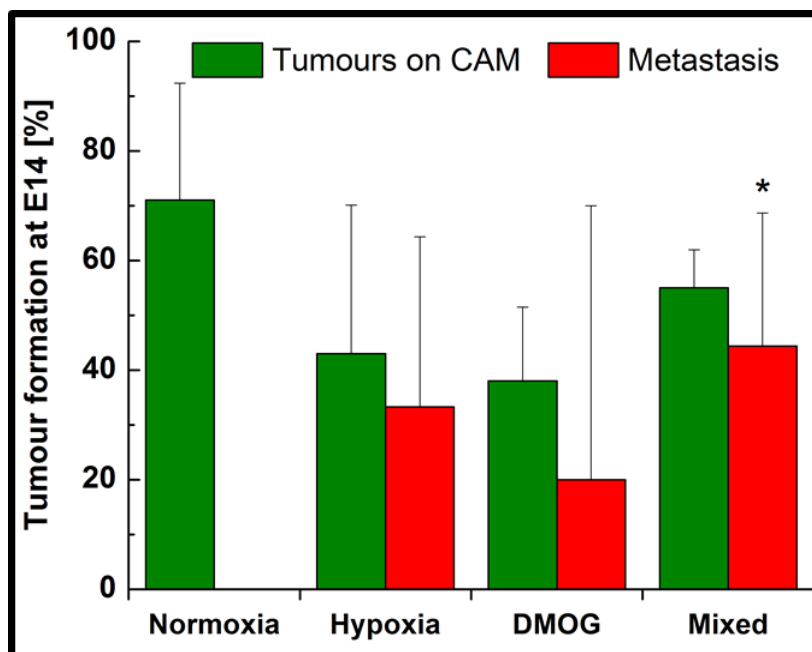


Figure 25. Sk-N-AS Tumourigenesis & Metastasis. Tumourigenesis (green), occurred regardless of preculture condition. Normoxia n=17 (SD-21.3, 95%CI \pm 33.9); Hypoxia n=15 (SD-27.1, 95%CI \pm 28.5); DMOG n=7 (SD-13.5, 95%CI \pm 33.5); Mixed n=18 (SD-6.96, 95%CI \pm 17.3). Invasion (red): Normoxia n=0; Hypoxia n=5 (SD-31, 95%CI \pm 32.6); DMOG n=2 (SD-50, 95%CI \pm 124.2); Mixed n=8 (SD-24.2, 95%CI \pm 60.2). Each condition was investigated over 3 independent experiments. Error bars express Standard Deviation (SD). y axis - tumour formation as percentage of chicks surviving to embryonic day. x axis - various preculture conditions. * denotes statistical significance.

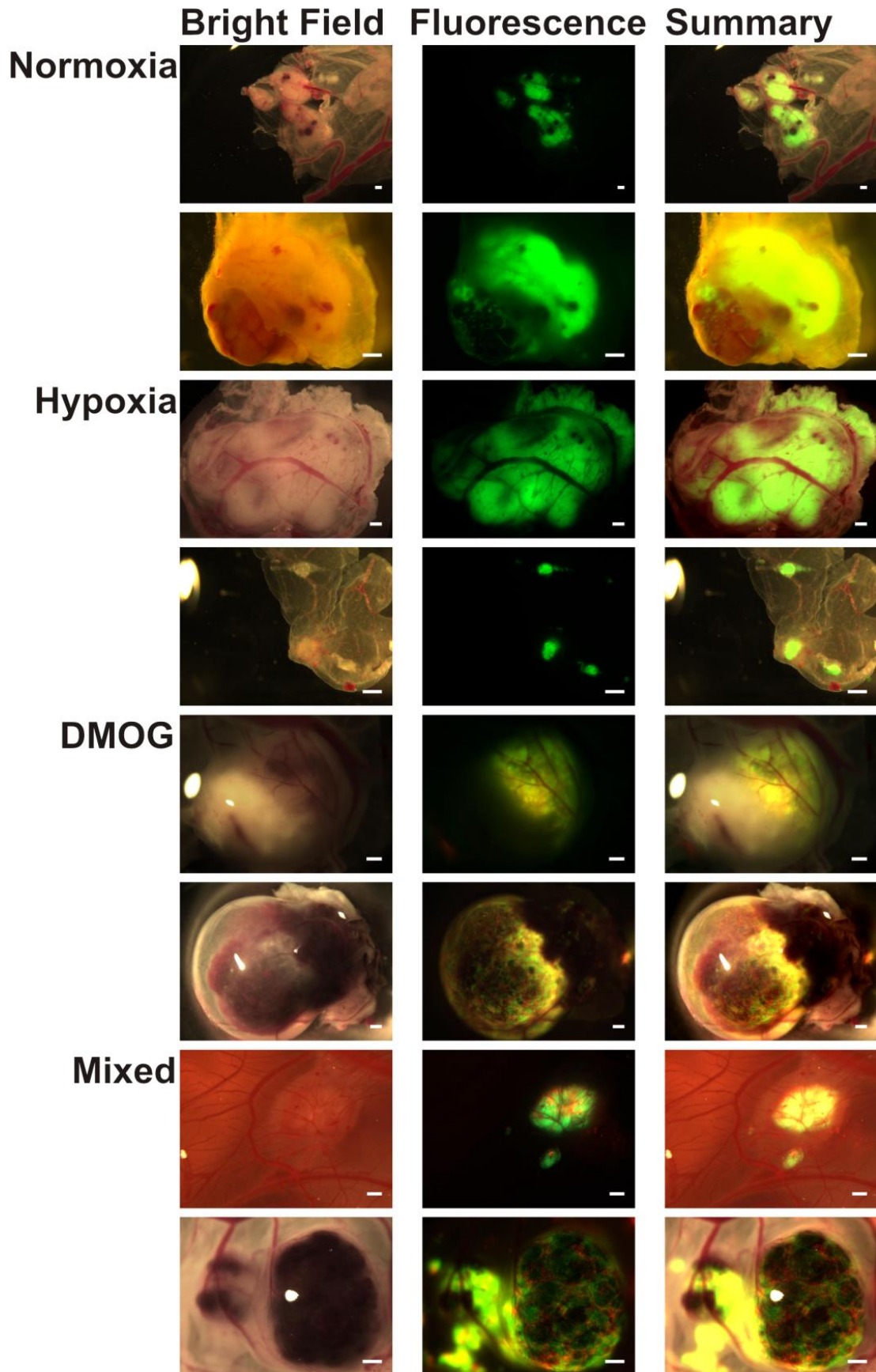


Figure 26. Summary Tumour Pictures. Sk-N-AS tumourigenesis following preculture in: Normoxia (21%O₂); Hypoxia (3days 1%O₂); DMOG (1day); Mix (Red, 21%O₂ – Green, 1%O₂). Scale bars - 500µm.

Table 9. Proportion of Metastases identified in different organs / tissues within the embryo. The most common site for development of metastatic foci was the liver (n=10), followed by the intestines (n=7), the Omentum (n=3), Kidneys (n=3), and Meninges (n=3).

Location of Metastatic Deposits	Frequency of Presentation
Liver	38.5%
Intestine	27%
Omentum	11.5%
Kidney	11.5%
Meninges	11.5%

3.3.3. Hypoxia unlocked tumourigenesis in MYCN amplified cell line

Results from the initial pilot experiment were used to supplement further in-depth study of chemotherapy resistant, MYCN amplified Sk-N-BE(2)C tumour cells. Analysis of findings recorded over three independent experiments indicated this cell line did not survive or proliferate to form solid tumours upon the chorioallantoic membrane following preculture in normoxia (21% O₂).

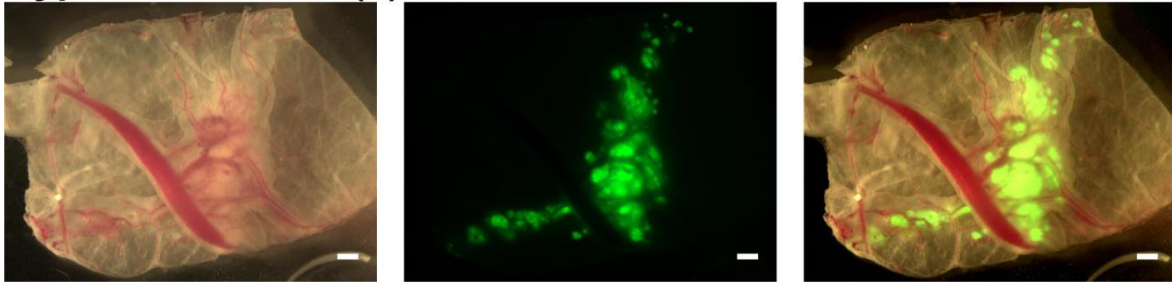
However, when cells were precultured under hypoxic conditions (1% O₂) tumourigenesis was accomplished, Figure 27. Tumours resembled those observed in the study of Sk-N-AS cells however they formed mostly as a cohort of small singular structures developing within close quarters. Large vasculature was regularly identified nearby and closer inspection revealed fine capillary structures which intricately communicated throughout the tumour colony. Consolidating this finding was the identification of successful tumourigenesis following cellular treatment with DMOG. Moreover, application of mixed preculture tumour cells resulted in tumourigenesis, again demonstrating chain-like morphology.

Excitingly, tumour cell migration and invasion was also observed (Figure 27), with Hypoxia, DMOG and mixed preculture tumour cells successfully invading chick tissues and organs to establish metastatic secondary tumours. Interestingly, the sites of tumour cell invasion remained similar to those occupied by Sk-N-AS cells.

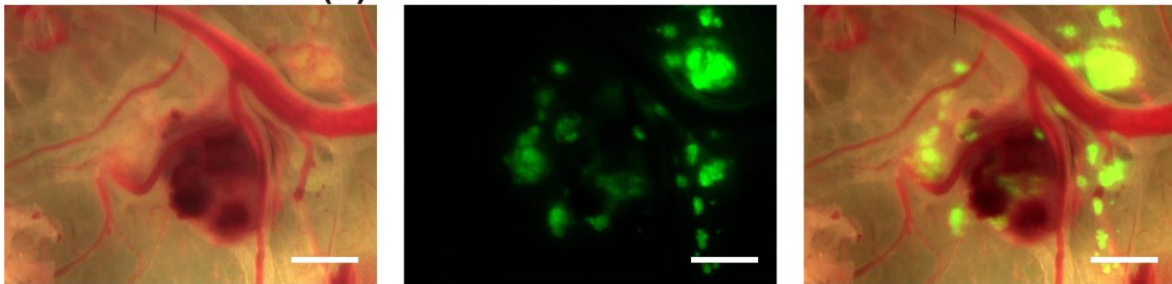
Normoxic Sk-N-BE (2)C



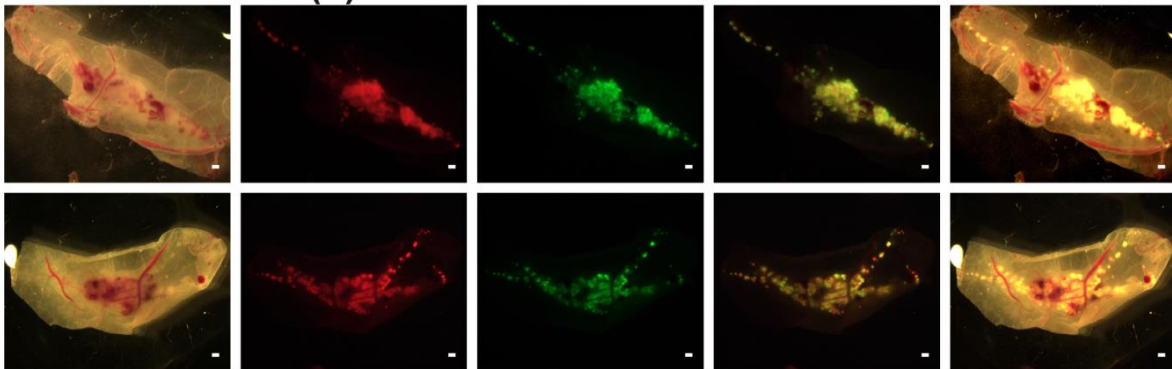
Hypoxic Sk-N-BE (2)C



DMOG Sk-N-BE (2)C



Mixed Sk-N-BE (2)C



Sk-N-BE (2)C Mixed Invasion

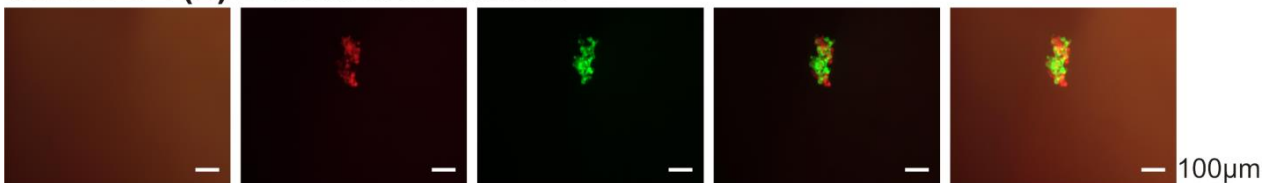


Figure 27. Sk-N-BE(2)C Tumour Formation following altered preculture conditions; Normoxia (21%O₂); Hypoxia (1%O₂ for 3days); DMOG (1day); Mixed (red – 21%O₂, green – 1%O₂). Normoxic BE(2)C cells did not flourish upon the CAM however hypoxic / DMOG preculture encouraged cells to form 3D tumour structures. Mixed implantation resulted in hypoxic and normoxic tumour proliferation and subsequent intestinal invasion. Scale bars - 500µm, except 'Sk-N-BE (2)C Mixed Invasion - 100µm.'

3.4.0. Paraffin staining of Sk-N-AS tumour samples

All tumours were stored either embedded in paraffin wax or as frozen sections. Each preculture condition produced multiple tumours forming in various individual chicks over several independent experiments. These were sectioned and stained accordingly.

Initially it was important to discriminate tumour cells from those of the chick membrane. This was performed by staining paraffin sections with Haematoxylin and Eosin (H&E), a method favoured by pathologists when identifying cancer cells histologically. With reference to Figure 28, one can observe tumour cells appeared to be tightly congregated in cohorts of larger, darker nuclei with respect to surrounding chick stroma. H&E stained DMOG and Mixed sections, Figure 28, exhibit tumour-haematoma which constituted tumour colonies surrounded by blood cells. A traditional neuroblastoma marker, CD56 (NCAM), positively stained cellular membranes confirming that the tumours were neuroblastoma.

Tumour cell proliferation was demonstrated in all preculture conditions using Ki-67, a marker expressed in proliferating neoplastic tissues. It has to be noted that cells precultured in hypoxia show a stronger staining for Ki-67, suggesting more proliferation in this condition.

The presence of HIF- α subunits was assessed by attempting to identify the expression of HIF-1 α / 2 α . Tumour sections were found to be uniformly positive for HIF-1 α protein expression. Surprisingly this included samples precultured in normoxia. HIF-2 α was uniformly unexpressed regardless of preculture.

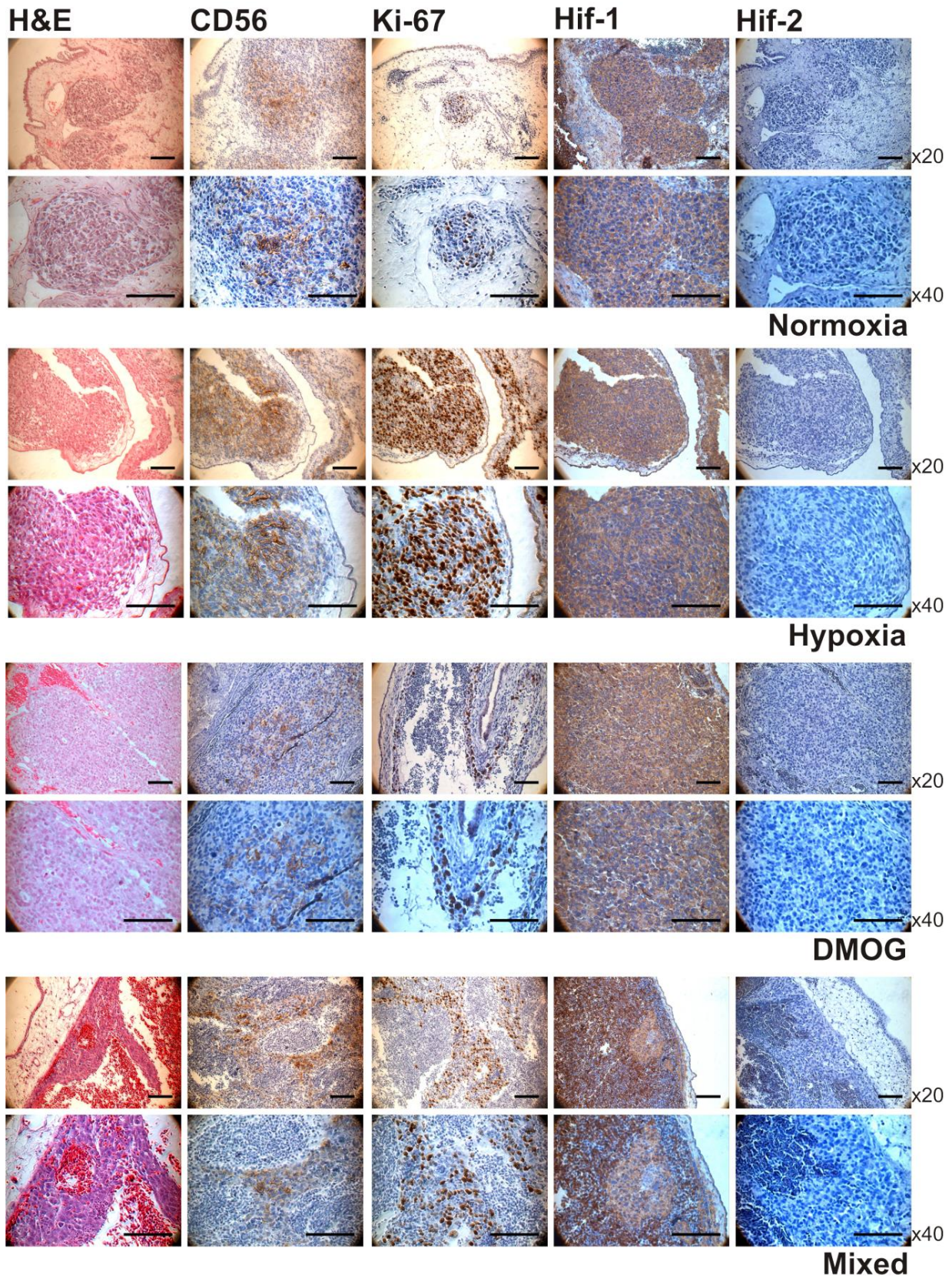


Figure 28. Staining of Sk-N-AS – Paraffin. Differently precultured Sk-N-AS tumours; Normoxia (21%O₂); Hypoxia (1%O₂ for 3days); DMOG (1day); Mixed (red – 21%O₂, green – 1%O₂); were removed from the CAM, sectioned and stained with: Haematoxylin & Eosin, CD56 (tumour identity), Ki-67 (tumour proliferation), Hypoxia inducible factor 1 α (Hif1), Hypoxia inducible factor 2 α (Hif2). Positive and negative controls were produced for each stain. Scale bar - 100 μ m.

3.4.1. Staining for markers downstream of HIF expression

Previous findings indicate that to ones surprise, tumour samples expressed HIF-1 α regardless of the variable preculture conditions. Building upon these results it was decided to stain tumours in order to identify downstream products of HIF activation, see Figure 29.

Anti-Glucose Transporter antibody stains cells which express the glucose transporter GLUT-1. This is an end product of HIF transcription expressed in a host of tissues such as metabolising cancer cells. It was found to positively stain all tumours regardless of preculture conditions. Anti-Carbonic Anhydrase IX antibody, Ca9, is human specific becoming expressed in cells responding to hypoxia. This stain was absent when cells were precultured in normoxia (21%O₂), and also in those pretreated with DMOG. It was expressed strongly in hypoxic cells and intermittently in mixed tumours.

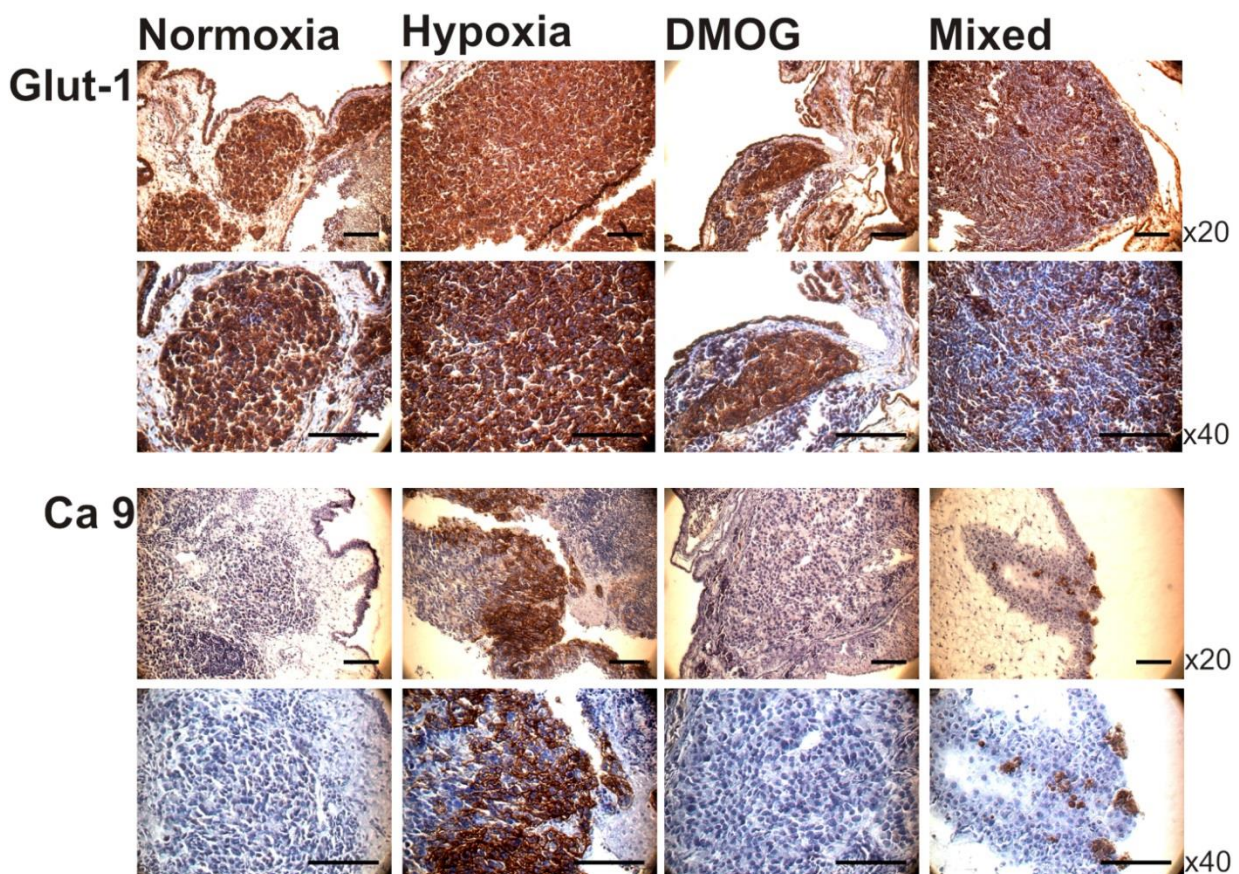


Figure 29. Downstream HIF targets. Sk-N-AS tumours precultured in; Normoxia (21%O₂); Hypoxia (1%O₂ for 3days); DMOG (1day); Mixed (red – 21%O₂, green – 1%O₂) were stained with GLUT-1 and Ca 9 antibodies. GLUT-1 was positive in all conditions. Ca9 was uniformly positive throughout hypoxic tumours, intermittent in mixed conditions, absent in normoxia and DMOG treated cells. Scale bar - 100 μ m.

3.5.0. Tumour cell Proliferation and Intravasation - Normoxia Vs Hypoxia

Ki-67 – tumour cell proliferation

Due to the previous observation that cells pre-cultured in hypoxia display a higher level of Ki-67 staining (Figure 28), frozen tumour sections were stained with the antibody for confirmation. In each preculture condition three independent experiments were carried out, tumours were removed from three different chicks per experiment and the results are displayed in Figure 30A and B. Tumour cells are GFP-labelled and proliferation marker (Ki-67) is shown in red. Nuclei were stained using TOPRO-3®, and then assigned the colour blue. Some proliferating cells appear pink / lilac due to overlap by nuclear staining. Chick cells were present in the sample however they appear with significantly smaller nuclei and were easily discounted. The number of Ki-67 positive cells was quantified as a percentage of the total number of tumour cells present. Figure 30A displays images of tumour cells stained with Ki-67 while Figure 30B provides quantification of tumour cell proliferation in normoxia and hypoxia precultured neuroblastoma cells.

In normoxia, 53.7% of tumour cells were shown to proliferate with SD 6.08%. In contrast, hypoxia precultured tumour cells were observed to proliferate at 90.0% with SD 13.7%. A student's t-test was performed showing a significant difference between preculture conditions (student's t-test – 0.0000000063). See graph below, Figure 30B.

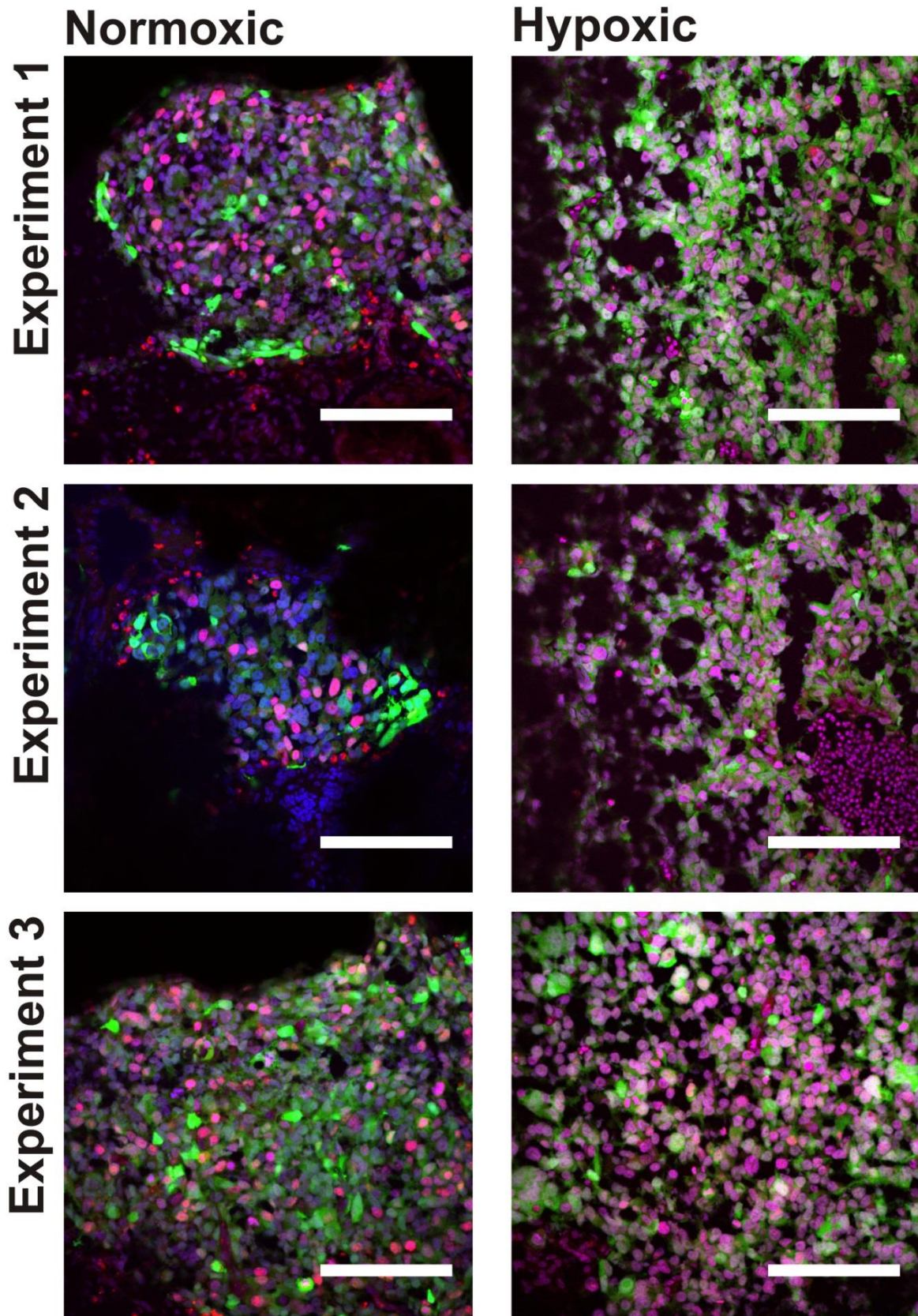


Figure 30A. Frozen Tumour samples Stained with Ki-67. Tumour samples demonstrated cellular proliferation regardless of preculture conditions. In each image tumours are labelled with GFP, Ki-67 appears red and cell nuclei blue. Cells positive for Ki-67 and nuclear stain appear a shade of lilac. Smaller nuclei are chick cells and were disregarded during quantification. Scale bar - 100µm.

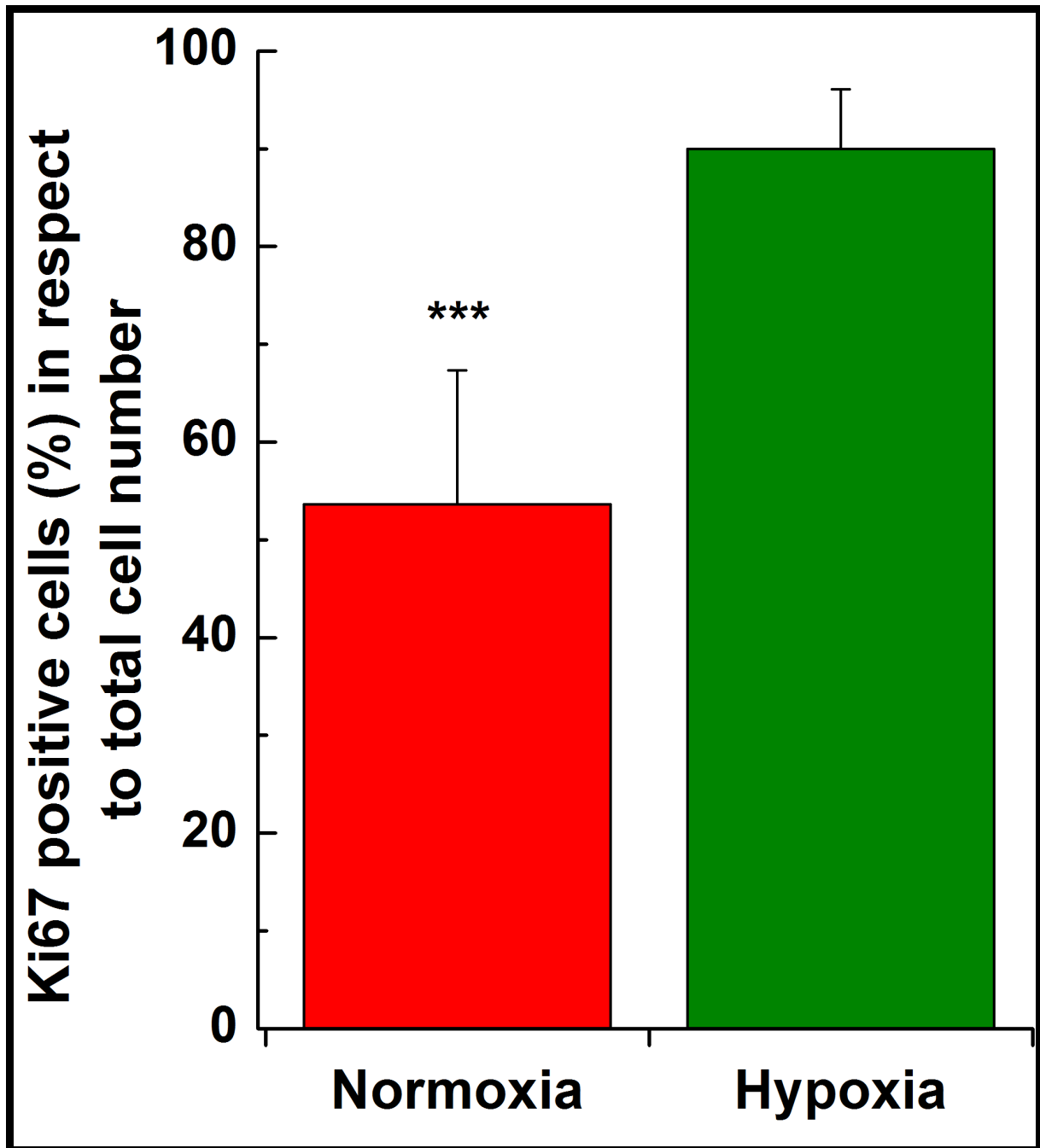


Figure 30B. Tumour cell Proliferation in Normoxia compared to Hypoxia. Here, Ki-67 positive cells are shown with respect to the total cell number (%) for tumours formed by cells precultured in normoxia (red) or hypoxia (green). In each preculture condition images were captured from 13 chicks at 3 images per chick. Normoxia = mean of 53.7% (n=251) cells stained positive for Ki-67. Hypoxia = mean of 90.0% (n=362) cells stained positive for Ki-67. 40x zoom, error bars represent Standard deviation.

*** denotes p value > 0.0001







Normoxic preculture - 37°C, 5% CO₂, 21% O₂; Hypoxic preculture - 37°C, 5% CO₂ and 1% O₂.

Anti Smooth Muscle Actin - α

This antibody binds to Smooth Muscle Actin - α which exists within cells lining the luminal walls of blood vessels. In this study it was used to stain vasculature situated within solid tumours in order to identify fluorescently labelled tumour cells entering the vasculature during the process of intravasation.

The results can be observed in Figure 31 A and B. Tumours can be identified in green (GFP) and blood vessels in red. Nuclei were again stained with TOPRO-3® and assigned the colour blue. In each preculture condition three independent experiments were carried out and tumours were removed from three different chicks per experiment. In hypoxia, cells were repeatedly observed migrating away from the body of the primary tumour and intravasated the vasculature. Normoxic cells were not observed to perform in this way.

Figure 31A. Normoxic – Hypoxic Tumours analysed for tumour cell intravasation. This table demonstrates with a tick or an x whether tumour cells precultured in Normoxia or Hypoxia, migrated and intravasated chick blood vessels. In association with Figure 20B it can be recognised that tumour cells cultured in Hypoxic condition were found to undergo intravasation whilst Normoxic cells were not. Normoxia - 37 °C, 5% CO₂, 21% O₂, Hypoxic – 37 °C, 5% CO₂ and 1% O₂.

Experiment	Normoxia	Hypoxia
1		
2		
3		

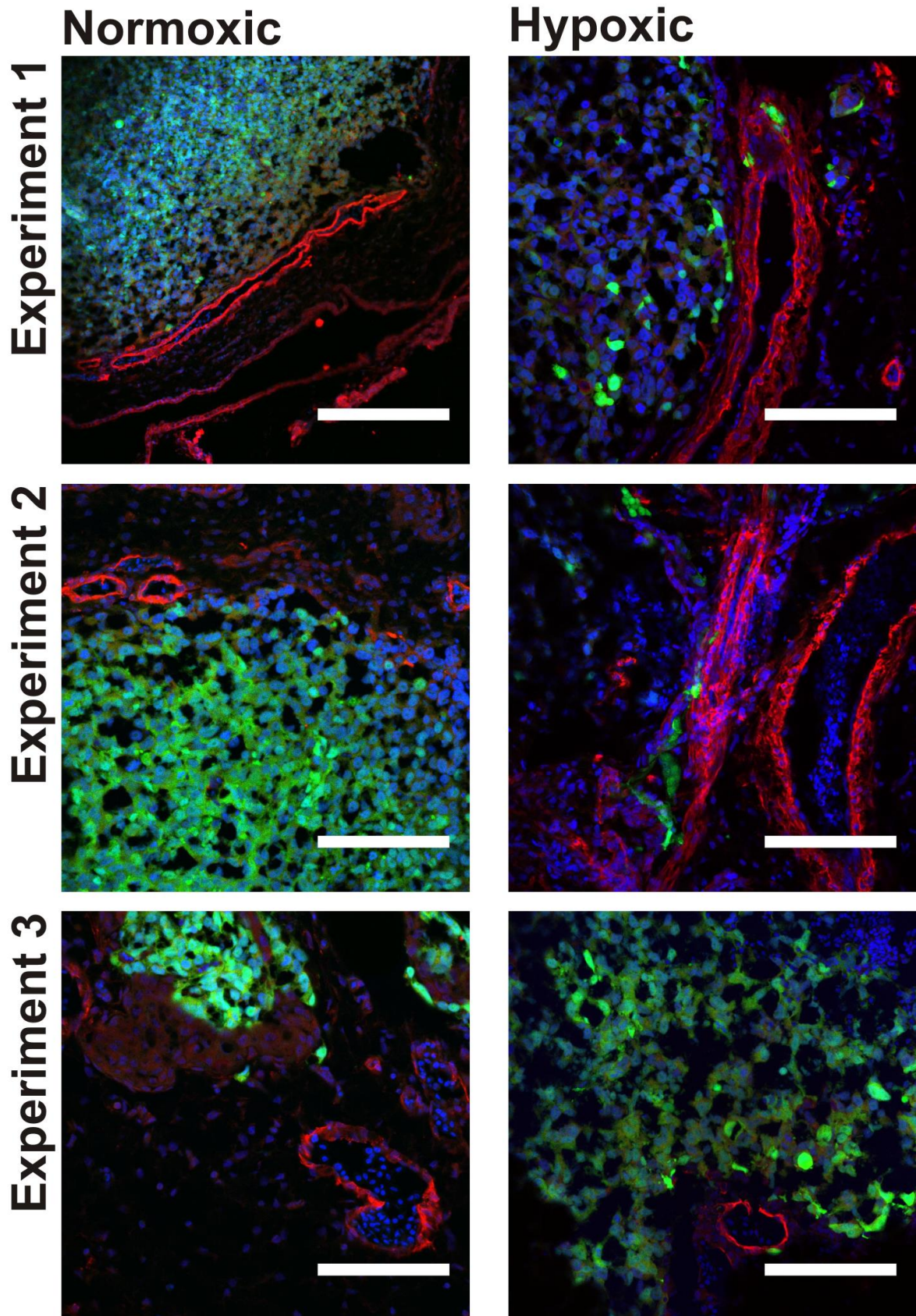


Figure 31B. Tumour cell Intravasation. All images depict GFP labelled tumour cells (green), blood vessels stained with Smooth Muscle Actin- α (red), and cellular nuclei stained blue. Migrating cells can be seen undergoing intravasation in images depicting hypoxia pretreated tumours whilst normoxic tumour cells were not observed crossing blood vessel walls. Scale bar - 100 μ m.

3.5.1. Frozen section tumour characterisation – Hypoxia Vs Normoxia

Tumour sections were collected from three chicks in each of three independent hypoxia and normoxia preculture experiments, (18 chicks in total). Following this a host of staining antibodies were applied in order to characterise differences existing between cells precultured in normoxia as opposed to hypoxia (Figure 32). Overall outcomes were based on evidence gathered from eighteen embryos.

Firstly, tumours were stained with anti-Glial Fibrillary Acidic Protein (GFAP) which constitutes the principle intermediate filament found forming part of the cytoskeleton in mature astrocytes of the nervous system. Tumours grown in both preculture conditions were positively stained, marked differences were not observed.

Next, neuronal stem cell markers Nestin and Vimentin were investigated. Anti-Nestin is a human specific antibody highlighting primitive neuroepithelium. Vimentin is a general marker for cells originating from mesenchymal tissue whilst also acting as a neural stem cell marker. Both antibodies are expressed in neoplastic cells such as melanoma, Vimentin is often used to identify the origins of metastatic tumours (De Amicis et al. 2013). Neuroblastoma sections tested equally expressed both of these markers regardless of preculture condition.

It was also decided to stain with a highly specific neuronal marker, Neuronal Class III β -Tubulin Polyclonal Antibody. Samples stained uniformly in both normoxia and hypoxia precultured tumours. Finally, Cd133, a marker of both neural progenitor cells and cancer stem cells was monitored in both tumour samples however this was positive in each preculture condition.

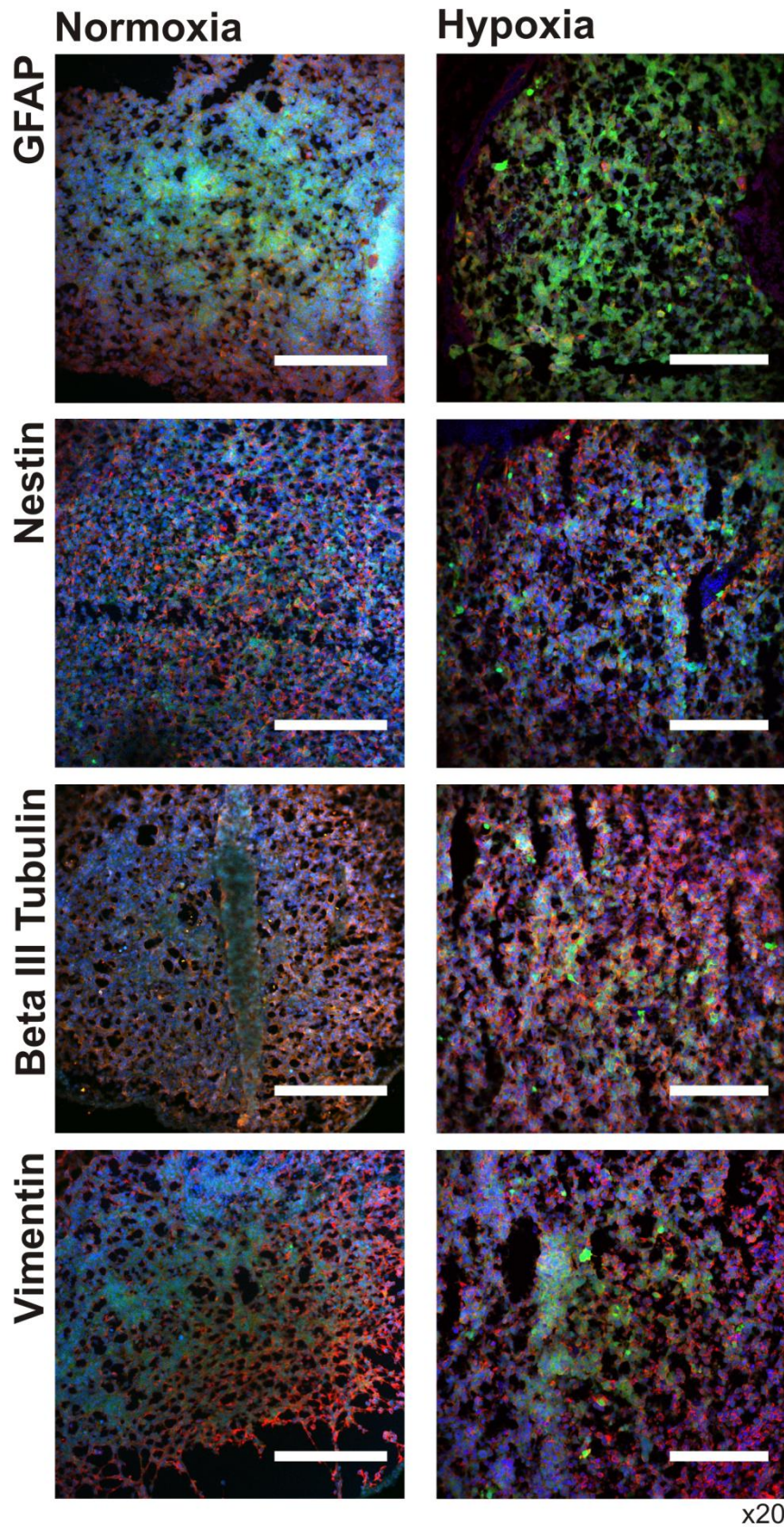


Figure 32. Immunohistochemical Staining of Frozen Tumour samples. Tumour samples are labelled with GFP (green). GFAP, Nestin, β III-Tubulin and Vimentin (red) were used to identify differences between normoxia (21% O_2) and hypoxia (1% O_2) precultured cells. Again nuclei are blue. No significant differences were recorded. Images captured at x20 zoom, Scale Bar - 100 μ m.

4. Discussion

This study aimed to identify whether different neuroblastoma cell lines proliferate upon the chick chorioallantoic membrane to establish a primary tumour. It also aimed to investigate whether this chick model is appropriate for the study of metastatic invasion in neuroblastoma. Finally, this study investigated the role of hypoxia in the metastatic migration of neuroblastoma cells in order to uncover molecular changes making tumour cells more aggressive.

These goals were addressed using an *in vivo* chick embryo model whereby four different neuroblastoma cell lines – Sk-N-AS; IMR-32; Kelly; Sk-N-BE (2)C – were introduced to the CAM which surrounds chick embryos. Cellular proliferation and migration was observed and the metastatic behaviour of neuroblastoma cells was studied.

4.1. The Chick Embryo Model

In the past the chick embryo CAM model has been employed to highlight tumourigenesis and tumour cell aggression in various different cancers such as: adenocarcinoma, bronchial carcinoma, embryonal rhabdomyosarcoma, glioma, Hodgkin's lymphoma, osteosarcoma, squamous-cell carcinoma, and ovarian cancer (Karnofsky et al. 1952; Korngold and Lipari, 1955; Harris. 1958; Hagedorn et al. 2005; Balke et al. 2010; Lokman et al. 2012). Similarly malignant melanoma cells have been observed forming tumours and establishing metastasis within this model although some cell lines were also shown to be unsuited to survive in this environment (Busch et al. 2013). Many similarities can be drawn between malignant melanoma and neuroblastoma given the common ancestry as neural crest cell derivatives and the shared propensity to form solid tumours, which are often highly metastatic. This could explain why some neuroblastoma cell lines, IMR-32 and Sk-N-AS, were able to carry out tumourigenesis upon the CAM in this study.

Tumour morphology:

Interestingly, tumour morphology was widely variable when comparing IMR-32 to Sk-N-AS cells. The former repeatedly developed as unusual air-filled compartments surrounded by small tumour cell deposits while the latter consistently established tumour structures which resembled neuroblastoma surgically removed from human patients. From a pathologist's perspective, neuroblastoma commonly present in humans as haemorrhagic tumours / tumour surrounded by haematoma (Lack EE. 1997 and 2007). With this in mind, our study also demonstrated the formation of similar haemorrhagic / haematoma-like tumours upon the chick CAM when using Sk-N-AS cells. Importantly this occurred regardless of differences in cellular preconditioning in terms of oxygen levels. These findings highlight similarities between tumour formation in the chick model and the disease state observed in humans, suggesting the chick embryo is an appropriate model for the *in vivo* study of neuroblastoma.

Surprisingly, tumourigenesis was independent of positive MYCN amplification status as neither chemotherapy resistant Sk-N-BE (2)C nor Kelly cell lines were able to develop solid tumours upon the CAM. These observations complement previous findings, which demonstrated tumour cell survival and tumourigenesis using: Sk-N-AS, NB5, NB7, NB8, NB10 and NB16 cell lines, of which NB5, 7, 8 and 10 are MYCN amplified (Stupack et al. 2006). This is interesting as it was expected MYCN amplified cells would be better suited to survival upon the CAM due to the clinical relevance of a positive MYCN status, which is linked to rapid disease progression and acts as an indicator of poor prognosis (Slack et al 2005; Cohn et al. 2009; Ochiai et al. 2010; Carter et al. 2012).

Tumour Invasion:

Concerning tumour cell migration and invasion, all foetal viscera and tissues were thoroughly assessed for cells precultured in each condition. Crucially, the pattern of tumour cell metastasis was almost identical occurring within common organs and tissues such as the liver and intestine regardless of tumour cell preconditioning. The foundation of Sk-N-AS cell secondary tumours in the liver was particularly interesting and highly significant, as this organ is an extremely common site for the formation of metastasis in children suffering neuroblastoma (Carlsen et al. 1985). Secondary

tumour formation in the liver greatly increases the overall size of the organ and frequently results in the onset of abdominal compartment syndrome. This phenomenon is often deadly, especially in neonates (0 - 28 days old) (Web Reference 4), as the paediatric abdomen is extremely limited with regards to available excess space. Tumour metastasis can be extensive and secondary deposits occur throughout the organ forcing it to expand into the lung fields where it severely impedes gas exchange. The rapidly swelling liver also compresses nearby organs such as the kidneys leading to renal failure, and the alimentary canal leading to constipation (Mullassery et al. 2009).

Limitations:

There were several limitations associated with the use of the chick embryo CAM model. Firstly, this study was carried out in line with guidance set by the UK Government, Home Office. Therefore chicks were not permitted to survive beyond the age of embryonic day 14. As such, the metastatic cascade had to be completed within a seven day period from implantation at E7 to dissection at E14. Additionally, this research was required to be completed within 1 year and so time was a substantial limiting factor as chicks were grown for 14 days before results could be collected. Moreover, this is a tested *in vivo* model, therefore it was expected cells would behave in a similar manner to neuroblastoma growing in humans, however by its very nature, this study does not relate exactly to the human condition due to the fact that it has been carried out in a different species.

Finally it was thought the use of fluorescent labels for tumour cell identification may limit the chick embryo model as a particular label might interfere with tumour cell behaviour, however different labels were used – GFP or dTomato – and there was no difference in tumourigenesis, invasion or proliferation. Therefore it was concluded that fluorescent labelling did not affect the behaviour of cell lines used in this study regardless of preculture condition.

4.2. Preculture in Normoxia versus Hypoxia

Preconditioning neuroblastoma cells in normoxia (37°C, 5% CO₂, 21% O₂), resulted in tumourigenesis of IMR-32 and Sk-N-AS cell lines only. Hypoxic preconditioning had an impact on the size of primary tumours. Tumours formed from cells precultured under hypoxia were on average 78% larger than those developing from cells cultured under normoxia. Indeed the largest tumour developed from hypoxia preconditioned cells and was found to have a volume of 531.2mm³. Moreover, cellular preculture in pathological hypoxia (37°C, 5% CO₂, 1% O₂), led to extensive tumour cell migration and the formation of metastatic secondary tumours (Goda et al. 1997; Höckel and Vaupel, 2001; Brown and Wilson, 2004; Simon and Keith, 2008).

Role of HIF:

Hypoxia induced increases in tumour size and completion of the metastatic cascade could be explained by hypoxia driven stabilisation of intracellular HIF, leading to modifications / adaptations within tumour cells (Epstein et al. 2001; Lando et al. 2002; Koivunen et al. 2004). These changes were postulated to influence tumour cell behaviour following introduction to the *in vivo* model and indeed, hypoxia imposed changes enhanced Sk-N-AS cell tumourigenesis whilst enabling tumour cells to invade chick tissues. This finding occurred in accordance with the literature where it is reported hypoxia is associated with increased levels of: angiogenesis, cell proliferation, glucose metabolism, growth factor signalling and local pH (Ryan et al. 1998; Carmeliet et al. 1998; Fukuda et al. 2007; Caniggia et al. 2000; Shimoda et al. 2006). Upregulation in each of these processes supports tumour cell survival and enhances the chances of tumour cells completing the metastatic cascade. Furthermore it has also been reported that hypoxic preculture (12hours at ~ 0% O₂) is linked to a reduction in cellular apoptosis and altered metastatic potential (Leuenroth et al. 2000; Birner et al. 2000).

In order to explain hypoxia induced completion of the metastatic cascade, this study determined if invasion was HIF dependent by pretreating cells with DMOG, a cell permeable prolyl-4-hydroxylase inhibitor which suppresses the action of PHDs and FIH (Bruick and McKnight. 2001; Asikainen et al. 2005). Under normoxic conditions both PHDs and FIH alter HIF-1 α subunits with the former hydroxylating proline

residues later leading to degradation via coupling with von Hippel-Lindau protein, while the latter hydroxylates asparagine residue 803 in the carboxy-terminal transcriptional activation domain (C-TAD). Therefore DMOG treatment of Sk-N-AS cells stabilises HIF, mimicking aspects of pathological hypoxia. If hypoxia initiated invasion is HIF dependent, DMOG treatment should lead to / cause metastatic behaviour of Sk-N-AS cells and indeed, tumourigenesis and metastasis was observed in several chicks. This was important because the HIF pathway is widely regarded as the principle process enabling cell survival in hypoxia although lesser studied HIF independent processes are also in effect when O₂ was limited and could have influenced tumour cell behaviour. The literature supported these findings by demonstrating that the induction of dedifferentiation, associated with increased neuroblastoma cell aggression, was linked to stabilisation of the HIF transcription factor (Jögi et al. 2004). Moreover, HIF transcription has been further linked to tumour metastasis via amplification / polymorphism of the MDM2 oncogene which degrades the vital tumour suppressor p53 (Carr-Wilkinson et al. 2010). Hence, it can be regarded that hypoxia induced Sk-N-AS metastasis is most likely HIF dependent. Future investigation with a HIF knockdown cell line could be used to confirm these findings. This is significant in neuroblastoma, as inhibition of differentiation may prevent maturation of tumour cells leading to the formation of a less aggressive phenotype such as that seen in ganglioneuroblastoma or ganglioneuroma.

HIF and hypoxic marker expression:

As the DMOG experiments demonstrated, metastasis in this study is most likely HIF dependent. Therefore the HIF subunits, HIF-1 α and HIF-2 α , were studied. It is known that HIF is commonly expressed in some malignant tumours however this is rarely exhibited in normal tissues (Zhong et al. 1999; Talks et al. 2000). Regarding HIF-1 α , previous *in vitro* studies used neuroblastoma cells, Sk-N-BE (2)C, to demonstrate swift upregulation within hours of introduction to hypoxia (1% O₂) although subsequent downregulation also occurred within 72 hours (Holmquist-Mengelbier et al. 2006). In contrast, HIF-2 α followed an opposing pattern, whereby upregulation was more prolonged, peaking after 72 hours of hypoxia and diminishing over a lengthy period of reoxygenation (Holmquist-Mengelbier et al. 2006).

In this study HIF-1 α was not expected to be upregulated after seven days of reoxygenation upon the CAM, however Sk-N-AS tumour sections were uniformly positive for HIF-1 α regardless of preculture condition suggesting that the embryonic chick environment upregulates HIF. Contrastingly, HIF-2 α was not expressed in any of the conditions. This was surprising as evidence in the literature (Noguera et al. 2009) reports HIF-2 α is strongly expressed in well-vascularised regions of hypoxic neuroblastoma (1% and 5% O₂) but also, knockdown of the subunit was shown to reduce neuroblastoma growth in athymic mice (Holmquist-Mengelbier et al. 2006). The same paper finally concluded, abundant HIF-2 α expression correlates with advanced clinical staging and indicates a poor prognostic outlook. Such dissimilarity highlights a contradiction in findings which is yet to be resolved, as the link between HIF expression and clinical disease seems to be complex and highly variable.

Also investigated were GLUT-1 and Ca9 which are tightly regulated and expressed following hypoxia. The expression of GLUT-1 is known to peak after 16 hours of hypoxia (Rafajová et al. 2004) and in the past, was found to resemble the expression of HIF-1 α , with the strongest staining identified further from vasculature among clusters of tumour cells existing close to necrotic tissue (Mayer et al. 2008). Similarly, expression patterns of levels of HIF-1 α and GLUT-1 was found to be identical in this study although each was uniformly expressed throughout all tumour cells regardless of preculture conditions. Moreover intensified staining was not recorded in specific tumour regions. Glucose transporter 1 receptors are known to be upregulated during cancer cell metabolism and following exposure to hypoxia (Ameri et al. 2010; Harrison et al. 2013). With this in mind uniform staining is unlikely to be related to hypoxic exposure in this study, as GLUT-1 was upregulated regardless of preconditioning. Rather it is suggested that expression of HIF and continuous cancer cell metabolism are the likely explanation for uniform expression.

Staining with the Ca9 antibody presented a different picture. The literature indicates Ca9 expression is induced after 6 hours of hypoxia and peaks at 24 hours. In contrast to GLUT-1, which demonstrates a relatively rapid decline, Ca9 expression is known to remain for more than 96 hours reoxygenation (Rafajová et al. 2004; Vordermark et al. 2005). Findings from this study identified Ca9 expression more than 7 days after tumour cells had been removed from an hypoxic environment. Paraffin samples demonstrated uniform staining in tumours grown from hypoxia

precultured cells although other cells precultured in normoxia or treated with DMOG were negative.

Role of hypoxia on cell proliferation:

In order to understand the influence of hypoxia on neuroblastoma at the molecular level, different tumour samples were stained with proliferation marker Ki-67; HIF-1 α and HIF-2 α antibodies; and downstream hypoxic markers Ca 9 and GLUT-1. Proliferation of Sk-N-AS tumours precultured in hypoxia was significantly increased when compared to normoxic counterparts. Therefore hypoxic preconditioning is associated with increased tumour cell proliferation, an observation which had previously been noted in the literature, suggesting stress-induced proliferation occurs in tumours expressing stabilised HIF-1 α (Carmeliet et al. 1998). This further validates the chick embryo model, however it must also be remembered that tumours stained in this study had been reintroduced to physiological oxygen for 7 days upon the CAM, at which point it was thought all signs of previous hypoxia would have been downregulated. The fact that a significant difference remained between cells precultured in hypoxia and normoxia demonstrates that three day preculture in hypoxia results in long-lasting changes to tumour cells. Regardless of preculture conditions it was also observed that some tumour cells were shown to be non-proliferative, this could point to the existence of a 'dormant' cell population.

4.3. Hypoxia and Metastasis

Hypoxia induced Metastasis is general to Neuroblastoma

Despite MYCN amplification and resistance to chemotherapy, Sk-N-BE 2(C) cells possess biological features which are remarkably similar to Sk-N-AS cells. For instance, both cell lines are derived from secondary bone marrow metastasis and each express deletion of chromosome 1p. For such reasons Sk-N-BE (2)C cells were an ideal candidate to investigate the effects of hypoxia on a MYCN amplified cell line within the chick CAM model.

Sk-N-BE (2)C cells were precultured under hypoxia and implanted upon the CAM following the same protocol as used for Sk-N-AS cells. Despite findings from earlier experiments which highlighted failed tumourigenesis and metastatic invasion of Sk-N-BE (2)C cells precultured in normoxia, hypoxic preculture resulted in tumourigenesis and crucially lead to the development of metastatic foci. This was again shown to be HIF dependent with primary and metastatic secondary tumours forming after cells were pretreated with DMOG prior to implantation upon the CAM. Similarly a mixture of tumour cells – precultured in normoxia and hypoxia – also lead to tumourigenesis and the formation of metastatic secondary tumours. Moreover it should be noted Sk-N-BE (2)C tumour morphology was comparable to Sk-N-AS tumours cultivated upon the CAM and the pattern of tumour cell invasion was also similar, affecting the same chick embryo tissues and organs. These results show that the mechanism of hypoxia-induced invasion linked to increased tumour cell aggression is general for neuroblastoma cells and might play an important role in the clinical pathology of disease.

Hypoxia pre-conditioned cells can influence normoxic cells:

In order to investigate if normoxic cells were capable of invasion, they were implanted upon the CAM alongside cells preconditioned in hypoxia. When cells were implanted separately, those precultured in normoxia showed identical behaviour as when they had been previously implanted alone, i.e. tumourigenesis occurred without invasion. This indicates either no signals / diffusing factors were emitted from hypoxic cells co-implanted upon the CAM or, too few signals were present within the egg to appropriately induce metastasis. However, when cells were implanted together and direct contact was permitted, the observed metastasis was extensive. This was intriguing, as previously normoxic cells were consistently identified as being unable to migrate and invade the chick embryo. Also interesting was that metastatic secondary tumours constituted cells which were either precultured under normoxia or hypoxia. It was rare to observe a secondary tumour developing as a combination of different cells.

These findings could indicate cells precultured in hypoxia interact with other less aggressive cells dictating tumour cell aggression and driving metastatic invasion. The idea of coerced invasion would suggest collective tumour cell migration in operation within this *in vivo* model, as it seems likely cells were invading chick tissues as a unit. On the other hand there is also evidence of single-cell migration as from time to time multiple small tumour satellites formed upon the CAM. The idea of patterned tumour cell invasion is important because different tumours tend to utilise specific migration mechanisms. However it has also been suggested that tumour cell invasion could be the result of several different mechanisms of migration occurring in tandem to produce an overriding metastatic effect (Friedl and Wolf, 2003).

On the molecular level is it interesting that mixed tumours expressed Ca9 intermittently in contrast with the uniform pattern shown in hypoxia-only precultured cells. This was an important finding as Ca9 is one of the genes most strongly induced by exposure to hypoxia (Mayer et al. 2006). However, the absence of Ca9 expression in neuroblastoma treated with DMOG demonstrates that Ca9 expression may not be HIF dependent despite previous findings (Wykoff et al. 2000). It is also possible that a link exists between increased pH, expression of Ca9 and enhanced metastatic potential. Recently a group has provided evidence suggesting increased pH is related to increased tumourigenesis, bolstering metastasis and an increase in the overall level of tumour cell aggression (Wojtkowiak et al. 2012). Moreover, it was previously accepted that Ca9 regulates pH, although expression is inhibited in more acidic environments (Sørensen et al. 2005). Supporting this link is work published by others who have identified Ca9 as an adequate marker of tumour cell aggression in studies of human colon cancer, glioblastoma and breast cancer (McIntyre et al. 2012; Tafreshi et al. 2012).

Mechanisms of intravasation:

This study identified the formation of metastatic tumour spheres which suggested invasive tumour cells not only survived 7 days within the chick model, but also proliferated, becoming established as independent secondary tumours. Moreover, the manner in which tumour cells invaded tissues / organs seemed to be highly selective and reminiscent of Paget's theory of cancer metastasis, whereby highly selective invading tumour cells intravasate vasculature and traverse the body in

search of tissues specifically suited for the formation of metastatic secondaries (Paget S. 1889). In terms of tumour cell intravasation, a crucial step in the metastatic cascade, frozen tumour samples were stained with the antibody smooth muscle actin- α . This demarcated blood vessels and capillaries traversing the tumour and also provided an opportunity to identify tumour cells entering the vasculature. As one might expect, cells precultured in hypoxia were observed undergoing intravasation while those preconditioned in normoxia were not witnessed entering the circulation. This implies cells precultured in normoxia did not enter the vasculature when applied to the CAM alone, however it could also be that they did intravasate but this process was completed before E14. An additional explanation is that normoxia precultured cells did intravasate but the phenomenon was missed due to the protocol used when choosing sections for staining.

Regarding a scenario where tumour cells precultured in normoxia failed to carry out intravasation, it is possible these cells did not possess the qualities required to degrade CAM matrix which mostly consists of collagen. Inability to erode surrounding extracellular matrix would inhibit tumour cell migration to nearby blood vessels for intravasation. In the event of a tumour cell being implanted directly adjacent to a blood vessel wall it could be possible that normoxic preculture means cells lack the necessary machinery required to infiltrate vascular lumen which are clad with collagen and developing smooth muscle cells. Nonetheless, cells which managed to complete intravasation may not possess the ability to survive within the circulation and as such could succumb to apoptosis before reaching target organs / tissues. Another theory is that cells were unable to identify suitable targets for extravasation or indeed were unable to adequately adhere to capillary walls in order to carry out extravasation. If cells did progress to invade tissues supporting the formation of metastatic secondary tumours they would then have to contend with the avian immune system which develops rapidly around E13. Lastly tumour cells migrating into the chick embryo must overcome the regular obstacles obstructing survival of any cell, such as ensuring the development of an adequate supply of nutrients. To cap this exhaustive process, cells were required to complete the entire metastatic cascade within seven days as tumour cells were implanted on E7 before embryos were dissected at E14.

4.4. Future Work

This study suggests increased tumour cell aggression, migration and invasion is stimulated by stabilisation of the HIF transcription factor, as degradation was inhibited by DMOG, resulting in tumour cell metastasis. Confirmation of HIF dependent metastasis could be identified by producing a HIF knockdown Sk-N-AS cell line with latter implantation upon the CAM.

More excitingly, this work opens the opportunity to further investigate the roles of hypoxia on neuroblastoma cell migration and invasion. While the influence of HIF on metastasis and neuroblastoma aggression can be shown *in vivo*, a more detailed molecular understanding would be extremely valuable. An in-depth view of the molecular mechanism could enable us to understand the metastatic process and help to design drugs targeted against the hypoxia driven invasion of neuroblastoma cells. This can be undertaken by cultivating tumours on the CAM using normoxia and hypoxia preconditioned cells, removing tumour structures at E14 and running polymerase chain reaction assays or Western blots. These could be used to assess for collagenases, such as matrix metalloproteinases and adhesion molecules, which might disassemble CAM collagen, promoting tumour cell intravasation, further elucidating the molecular mechanisms behind hypoxia induced metastasis.

Rather than sectioning and staining tumour samples, normoxia and hypoxia precultured tumour cells could be implanted upon the CAM and a small blood sample could be removed from easily accessible extraembryonic vasculature at different intervals. This would enable identification of intravasating tumour cells using a FACs (fluorescence activated cell sorting) machine. Using this method one could gain a clearer picture of whether tumour cells precultured in normoxia are capable of undertaking intravasation.

Extravasation and secondary tumour cell formation could be studied in more detail by utilising the experimental method associated with this chick embryo model, whereby cells are injected into extraembryonic vasculature upon the CAM rather than implantation upon the membrane. Another interesting project would be to culture and precondition primary neuroblastoma cells taken from a patient and implant them upon the CAM. Via this method, one could observe any differences seen when using commercial cell lines. It would also be interesting to test cell lines

from other solid tumours to investigate whether the chick embryo is a suitable vessel to investigate metastasis in other cancers.

By gaining a special licence from the UK Home Office one could follow chicks in experiments up to E21, the day of hatching. This would allow more in depth study of the metastatic pathway as both primary and secondary tumours would have the opportunity to further advance and interact with chick immunity. Dissection of chicks throughout each stage would enable a complete view of the tumourigenesis process and the establishment of tumour cell invasion. One could also suggest that a longer incubation would enable events occurring with normoxic cells: will they die or will they continue to grow and proliferate in a manner similar to those preconditioned in hypoxia.

Finally, this study utilised lentiviral vectors for fluorescent tumour labelling. As there exists a possibility of insertional oncogenesis associated with the integration of lentiviral DNA, GFP / dTomato labelling of tumour cells could potentially have affected metastatic data.

4.5. Conclusions

Neuroblastoma is a harrowing and unpredictable disease which often results in the death of a child. As such it is studied worldwide and interest continues to grow however this tumour occurs less regularly than other more famous diseases and so the field remains rather limited. Hence, any understanding of how these cells survive and metastasise is extremely valuable as it could later contribute to a cure or improvements in patient care. Moreover, successful in utilising the CAM model may later lead to its use as an *in vivo* model for novel drug trials.

Hypoxia drives invasion in neuroblastoma, which was found in this study to be HIF dependent. Hypoxia was also shown to increase cellular proliferation enabling tumours to develop rapidly and undertake extensive proliferation. Not only that, this study demonstrated that hypoxic cells may impact upon other non-invasive cells, initiating cellular migration and invasion, promoting completion of the metastatic cascade and establishing secondary tumours in a range of organs and tissues. This is a significant finding and has enlightened overall understanding of the metastatic

process. Furthermore, this process is accompanied by an increase in Ca²⁺ which alters environmental pH and may assist in degradation of the extracellular matrix promoting tumour cell migration.

In conclusion, this study has begun to lay the path for a complete understanding of the molecular mechanisms underpinning metastasis of neuroblastoma. This shall help to pave the way for the development of new therapies which can find a way to reprogram these neural crest derived cells to stop invading, eventually aiding the children suffering from this horrific disease.

5. References

Airley R, Loncaster J, Davidson S, Bromley M, Roberts S, Patterson A, et al. Glucose transporter GLUT-1 expression correlates with tumor hypoxia and predicts metastasis-free survival in advanced carcinoma of the cervix. *Clin Cancer Res*. 2001; 7(4):928-34.

An WG, Kanekal M, Simon MC, Maltepe E, Blagosklonny MV, Neckers LM. Stabilization of wild-type p53 by hypoxia-inducible factor 1 α . *Nature*. 1998; 392(6674):405-8.

Ameri K, Luong R, Zhang H, Powell AA, Montgomery KD, Espinosa I, et al. Circulating tumour cells demonstrate an altered response to hypoxia and an aggressive phenotype. *Br J Cancer*. 2010; 102(3):561-9.

Aoki Y, Saint-Germain N, Gyda M, Magner-Fink E, Lee YH, Credidio C, Saint-Jeannet JP. 'Sox10 regulates the development of neural crest-derived melanocytes in *Xenopus*', *Developmental Biology*. 2003; 259 (1), 19-33.

Asada M, Yamada T, Ichijo H, Delia D, Miyazono K, Fukumuro K, et al. Apoptosis inhibitory activity of cytoplasmic p21(Cip1/WAF1) in monocytic differentiation. *EMBO J*. 1999; 18(5):1223-34.

Asikainen TM, Schneider BK, Waleh NS, Clyman RI, Ho WB, Flippin LA, et al. Activation of hypoxia-inducible factors in hyperoxia through prolyl 4-hydroxylase blockade in cells and explants of primate lung. *Proc Natl Acad Sci U S A*. 2005; 102(29):10212-7.

Attiyeh EF, London WB, Mosse YP, Wang Q, Winter C, Khazi D, et al. Chromosome 1p and 11q deletions and outcome in neuroblastoma. *N Engl J Med* 2005; 353:2243–2253.

Auerbach R, Lewis R, Shinnars B, Kubai L, Akhtar N. Angiogenesis assays: a critical overview. *Clin Chem*. 2003; 49:32-40.

Auerbach R, Lu WC, Pardon E, Gumkowski F, Kaminska G, Kaminski M. Specificity of adhesion between murine tumor cells and capillary endothelium: an in vitro correlate of preferential metastasis in vivo. *Cancer Res*. 1987; 47(6):1492-6.

Ausprunk DH, Knighton DR, Folkman J. Differentiation of vascular endothelium in the chick chorioallantois: a structural and autoradiographic study. *Dev Biol*. 1974; 38(2):237-48.

Balke M, Neumann A, Kersting C, Agelopoulos K, Gebert C, Gosheger G, et al. Morphologic characterization of osteosarcoma growth on the chick chorioallantoic membrane. *BMC Res Notes*. 2010; 3:58.

- Bang AG, Papalopulu N, Kintner C, Goulding MD. Expression of Pax-3 is initiated in the early neural plate by posteriorizing signals produced by the organizer and by posterior non-axial mesoderm. *Development*. 1997; 124:2075–2085.
- Berra E, Benizri E, Ginouvès A, Volmat V, Roux D, Pouyssegur J. HIF prolyl-hydroxylase 2 is the key oxygen sensor setting low steady-state levels of HIF-1alpha in normoxia. *EMBO J*. 2003; 22(16):4082-90.
- Bhargava R, Oppenheimer O, Gerald W, Jhanwar SC, Chen B. Identification of MYCN gene amplification in neuroblastoma using chromogenic in situ hybridization (CISH): an alternative and practical method. *Diagn Mol Pathol*. 2005 Jun; 14(2):72-6.
- Birner P, Schindl M, Obermair A, Plank C, Breitenecker G, Oberhuber G. Overexpression of hypoxia-inducible factor 1alpha is a marker for an unfavorable prognosis in early-stage invasive cervical cancer. *Cancer Res*. 2000; 60(17):4693-6.
- Blagosklonny MV, An WG, Romanova LY, Trepel J, Fojo T, Neckers L. p53 inhibits hypoxia-inducible factor-stimulated transcription. *J Biol Chem*. 1998; 273(20):11995-8.
- Blouw B, Song H, Tihan T, Bosze J, Ferrara N, Gerber HP et al. The hypoxic response of tumors is dependent on their microenvironment. *Cancer Cell*. 2003; 4(2):133-46.
- Bown N, Cotterill S, Lastowska M, O'Neill S, Pearson AD, Plantaz D, et al. Gain of chromosome arm 17q and adverse outcome in patients with neuroblastoma. *N Engl J Med* 1999; 340:1954–1961.
- Brahimi-Horn MC, Pouyssegur J. HIF at a glance. *J Cell Sci*. 2009; 122(Pt 8):1055-7.
- Brodeur GM, Minturn JE, Ho R, Simpson AM, Iyer R, Varela CR, et al. Trk receptor expression and inhibition in neuroblastomas. *Clin Cancer Res* 2009; 15:3244–3250.
- Brodeur GM, Pritchard J, Berthold F, Carlsen NLT, Castel V, Castleberry RP, et al. Revisions of the International Criteria for Neuroblastoma Diagnosis, Staging, and Response to Treatment. *J Clin Oncol* 1993; 11:1466-1477
- Brown JM, Wilson WR. Exploiting tumour hypoxia in cancer treatment. *Nat Rev Cancer*. 2004; 4(6):437-47.
- Bruick RK. Expression of the gene encoding the proapoptotic Nip3 protein is induced by hypoxia. *Proc Natl Acad Sci U S A*. 2000 Aug 1;97(16):9082-7.
- Bruick RK, McKnight SL. A conserved family of prolyl-4-hydroxylases that modify HIF. *Science*. 2001 Nov 9;294(5545):1337-40.
- Busch C, Krochmann J, Drews U. The chick embryo as an experimental system for melanoma cell invasion. *PLoS One*. 2013; 8(1):e53970.
- Caniggia I, Mostachfi H, Winter J, Gassmann M, Lye SJ, Kuliszewski M, Post M. Hypoxia-inducible factor-1 mediates the biological effects of oxygen on human trophoblast differentiation through TGFbeta(3) *J Clin Invest*. 2000; 105(5):577-87.
- Carlsen NL, Schroeder H, Bro PV, Erichsen G, Hamborg-Pedersen B, Jensen KB, et al. Neuroblastomas treated at the four major child oncologic clinics in Denmark 1943–1980: an evaluation of 180 cases. *Med Pediatr Oncol* 1985; 13:180–186.
- Carmeliet P, Dor Y, Herbert JM, Fukumura D, Brusselmans K, Dewerchin M, et al. Role of HIF-1alpha in hypoxia-mediated apoptosis, cell proliferation and tumour angiogenesis. *Nature*. 1998; 394(6692):485-90.
- Caron H, van Sluis P, van Hoeve M, de Kraker J, Bras J, Slater R, et al. Allelic loss of chromosome 1p36 in neuroblastoma is of preferential maternal origin and correlates with N-myc amplification. *Nat Genet* 1993; 4:187–190.

Carr-Wilkinson J, O'Toole K, Wood KM, Challen CC, Baker AG, Board JR, et al. High Frequency of p53/MDM2/p14ARF pathway abnormalities in relapsed neuroblastoma. *Clin Cancer Res* 2010; 16:1108–1118.

Carrero P, Okamoto K, Coumailleau P, O'Brien S, Tanaka H, Poellinger L. Redox-regulated recruitment of the transcriptional coactivators CREB-binding protein and SRC-1 to hypoxia-inducible factor 1alpha. *Mol Cell Biol*. 2000; 20(1):402-15.

Carter R, Mullassery D, See V, Theocharatos S, Pizer B, Losty PD, et al. Exploitation of chick embryo environments to reprogram MYCN-amplified neuroblastoma cells to a benign phenotype, lacking detectable MYCN expression. *Oncogenesis*. 2012; 1:e24.

Chambers AF, Sharif R, Ling V. A model system for studying metastasis using the embryonic chick. *Cancer Res*. 1982; 42:4018-4025.

Chen CT, Yamaguchi H, Lee HJ, Du Y, Lee HH, Xia W, et al. Dual targeting of tumor angiogenesis and chemotherapy by endostatin-cytosine deaminase-uracil phosphoribosyltransferase. *Mol Cancer Ther*. 2011; 10(8):1327-36.

Chen EY, Fujinaga M, Giaccia AJ. Hypoxic microenvironment within an embryo induces apoptosis and is essential for proper morphological development. *Teratology*. 1999; 60(4):215-25.

Chen Z, Trotman LC, Shaffer D, Lin HK, Dotan ZA, Niki M, et al. Crucial role of p53-dependent cellular senescence in suppression of Pten-deficient tumorigenesis. *Nature*. 2005; 436(7051):725-30.

Cimpean AM, Ribatti D. The chick embryo chorioallantoic membrane as a model to study tumour metastasis. *Angiogenesis*. 2008; 11:311-319.

Cohn SL, Pearson AD, London WB, Monclair T, Ambros PF, Brodeur GM, et al. INRG Task Force. The International Neuroblastoma Risk Group (INRG) classification system: an INRG Task Force report. *J Clin Oncol*. 2009; 27(2):289-97.

Coldman AJ, Fryer CJ, Elwood JM, Sonley MJ. Neuroblastoma: influence of age at diagnosis, stage, tumor site, and sex on prognosis. *Cancer* 1980;46:1896–1901.

Conte M, Parodi S, De Bernardi B, Milanaccio C, Mazzocco K, Angelini P, et al. Neuroblastoma in adolescents: the Italian experience. *Cancer* 2006; 106:1409–1417.

Castleberry RP. Biology and treatment of neuroblastoma. *Pediatr Clin North Am* 1997; 44:919–937.

Dayan F, Roux D, Brahimi-Horn MC, Pouyssegur J, Mazure NM. The oxygen sensor factor-inhibiting hypoxia-inducible factor-1 controls expression of distinct genes through the bifunctional transcriptional character of hypoxia-inducible factor-1alpha. *Cancer Res*. 2006; 66(7):3688-98.

De Amicis F, Perri A, Vizza D, Russo A, Panno ML, Bonfiglio D, et al. Epigallocatechin gallate inhibits growth and epithelial-to-mesenchymal transition in human thyroid carcinoma cell lines. *J Cell Physiol*. 2013; 228(10):2054-62.

De Bernardi B, Gerrard M, Boni L, Rubie H, Cañete A, Di Cataldo A, et al. Excellent outcome with reduced treatment for infants with disseminated neuroblastoma without MYCN gene amplification. *J Clin Oncol*. 2009; 27(7):1034-40.

Deryugina EI, Quigley JP. Chick embryo chorioallantoic membrane model systems to study and visualize human tumour cell metastasis. *Histochem Cell Biol*. 2008; 130:1119-1130.

Deryugina EI, Zijlstra A, Partridge JJ, Kupriyanova TA, Madsen MA, Papagiannakopoulos T, et al. Unexpected effect of matrix metalloproteinase down-regulation on vascular intravasation and metastasis of human fibrosarcoma cells selected in vivo for high rates of dissemination. *Cancer Res*. 2005; 65(23):10959-69.

Dings J, Meixensberger J, Jäger A, Roosen K. Clinical experience with 118 brain tissue oxygen partial pressure catheter probes. *Neurosurgery*. 1998; 43(5):1082-95.

- Dorsky RI, Moon RT, Raible DW. Control of neural crest cell fate by the Wnt signalling pathway. *Nature*. 1998; 396:370–372.
- Dungwa JV, Hunt LP, Ramani P. HIF-1 α up-regulation is associated with adverse clinicopathological and biological factors in neuroblastomas. *Histopathology*. 2012; 61(3):417-27.
- Ebert BL, Gleadle JM, O'Rourke JF, Bartlett SM, Poulton J, Ratcliffe PJ. Isoenzyme-specific regulation of genes involved in energy metabolism by hypoxia: similarities with the regulation of erythropoietin. *Biochem J*. 1996; 313 (Pt 3):809-14.
- Ebos JM, Lee CR, Cruz-Munoz W, Bjarnason GA, Christensen JG, Kerbel RS. Accelerated metastasis after short-term treatment with a potent inhibitor of tumor angiogenesis. *Cancer Cell*. 2009; 15(3):232-9.
- Ema M, Hirota K, Mimura J, Abe H, Yodoi J, Sogawa K, et al. Molecular mechanisms of transcription activation by HLF and HIF1 α in response to hypoxia: their stabilization and redox signal-induced interaction with CBP/p300. *EMBO J*. 1999; 18(7):1905-14.
- Epstein AC, Gleadle JM, McNeill LA, Hewitson KS, O'Rourke J, Mole DR, et al. C. elegans EGL-9 and mammalian homologs define a family of dioxygenases that regulate HIF by prolyl hydroxylation. *Cell*. 2001; 107(1):43-54.
- Esiashvili N, Goodman M, Ward K, Marcus RB Jr, Johnstone PA. Neuroblastoma in adults: Incidence and survival analysis based on SEER data. *Pediatr Blood Cancer*. 2007; 49(1):41-6.
- Essex LJ, Mayor R, Sargent MG. Expression of Xenopus Snail in mesoderm and prospective neural fold ectoderm *Dev. Dyn*. 1993, 198, 108–122.
- Ferronha T, Rabadán MA, Gil-Guiñon E, Le Dréau G, de Torres C, Martí E. LMO4 is an essential cofactor in the Snail2-mediated epithelial-to-mesenchymal transition of neuroblastoma and neural crest cells. *J Neurosci*. 2013; 33(7):2773-83.
- Fidler IJ, Gruys E, Cifone MA, Barnes Z, Bucana C. Demonstration of multiple phenotypic diversity in a murine melanoma of recent origin. *J Natl Cancer Inst*. 1981; 67(4):947-56.
- Fidler IJ, Kripke ML. Metastasis results from preexisting variant cells within a malignant tumor. *Science*. 1977; 197(4306):893-5.
- Flamant L, Roegiers E, Pierre M, Hayez A, Sterpin C, De Backer O, et al. TMEM45A is essential for hypoxia-induced chemoresistance in breast and liver cancer cells. *BMC Cancer*. 2012; 12:391.
- Folkman J. What is the evidence that tumors are angiogenesis dependent? *J Natl Cancer Inst*. 1990; 82(1):4-6.
- Forsythe JA, Jiang BH, Iyer NV, Agani F, Leung SW, Koos RD, Semenza GL. Activation of vascular endothelial growth factor gene transcription by hypoxia-inducible factor 1. *Mol Cell Biol*. 1996; 16(9):4604-13
- Fredlund E, Ovenberger M, Borg K, Pählman S. Transcriptional adaptation of neuroblastoma cells to hypoxia. *Biochem Biophys Res Commun*. 2008; 366(4):1054-60.
- Friedl P, Wolf K. Tumour-cell invasion and migration: diversity and escape mechanisms. *Nat Rev Cancer*. 2003; 3(5):362-74.
- Fuchs A, Lindenbaum ES. The two- and three-dimensional structure of the microcirculation of the chick chorioallantoic membrane. *Acta Anat (Basel)*. 1988; 131(4):271-5.
- Fukata M, Kaibuchi K. 'Rho-family GTPases in cadherin-mediated cell-cell adhesion', *Nature Reviews Molecular Cell Biology*. 2001; 2 (12).

- Fukuda R, Zhang H, Kim JW, Shimoda L, Dang CV, Semenza GL. HIF-1 regulates cytochrome oxidase subunits to optimize efficiency of respiration in hypoxic cells. *Cell*. 2007; 129(1):111-22.
- Genbacev O, Joslin R, Damsky CH, Polliotti BM, Fisher SJ. Hypoxia alters early gestation human cytotrophoblast differentiation/invasion in vitro and models the placental defects that occur in preeclampsia. *J Clin Invest*. 1996; 97(2):540-50.
- Gestblom C, Hoehner JC, Hedborg F, Sandstedt B, Pålman S. In vivo spontaneous neuronal to neuroendocrine lineage conversion in a subset of neuroblastomas. *Am J Pathol*. 1997; 150(1):107-17.
- Goda F, O'Hara JA, Liu KJ, Rhodes ES, Dunn JF, Swartz HM. Comparisons of measurements of pO₂ in tissue in vivo by EPR oximetry and microelectrodes. *Adv Exp Med Biol*. 1997; 411:543-9.
- Graeber TG, Peterson JF, Tsai M, Monica K, Fornace AJ Jr, Giaccia AJ. Hypoxia induces accumulation of p53 protein, but activation of a G1-phase checkpoint by low-oxygen conditions is independent of p53 status. *Mol Cell Biol*. 1994; 14(9):6264-77.
- Greene HS, Harvey EK. The relationship between the dissemination of tumour cells and the distribution of metastasis. *Cancer Res*. 1964; 24:799-811.
- Hagedorn M, Javerzat S, Gilges D, Meyre A, de Lafarge B, Eichmann A, et al. Accessing key steps of human tumor progression in vivo by using an avian embryo model. *Proc Natl Acad Sci U S A*. 2005; 102(5):1643–1648.
- Hamburger V, Hamilton HL. A series of normal stages in the development of the chick embryo. *Dev Dyn*. 1951; 195(4):231-72.
- Hart IR, Fidler IJ. Role of organ selectivity in the determination of metastatic patterns of B16 melanoma. *Cancer Res*. 1980; 40(7):2281-7.
- Harris JJ. The human tumor grown in the egg. *Ann N Y Acad Sci*. 1958; 76(3):764-9.
- Harrison H, Rogerson L, Gregson HJ, Brennan KR, Clarke RB, Landberg G. Contrasting hypoxic effects on breast cancer stem cell hierarchy is dependent on ER- α status. *Cancer Res*. 2013; 73(4):1420-33.
- Henderson TO, Bhatia S, Pinto N, London WB, McGrady P, Crotty C, et al. Racial and ethnic disparities in risk and survival in children with neuroblastoma: A Children's Oncology Group study. *J Clin Oncol* 29:76-82, 2011
- Höckel M, Vaupel P. Tumor hypoxia: definitions and current clinical, biologic, and molecular aspects. *J Natl Cancer Inst*. 2001; 93(4):266-76.
- Holmquist-Mengelbier L, Fredlund E, Löfstedt T, Noguera R, Navarro S, Nilsson H, et al. Recruitment of HIF-1 α and HIF-2 α to common target genes is differentially regulated in neuroblastoma: HIF-2 α promotes an aggressive phenotype. *Cancer Cell*. 2006; 10(5):413-23.
- Huang Y, Yuan J, Righi E, Kamoun WS, Ancukiewicz M, Nezivar J, et al. Vascular normalizing doses of antiangiogenic treatment reprogram the immunosuppressive tumor microenvironment and enhance immunotherapy. *Proc Natl Acad Sci U S A*. 2012; 109(43):17561-6.
- Huber K, Combs S, Ernsburger U, Kalcheim C, Unsicker K. Generation of neuroendocrine chromaffin cells from sympathoadrenal progenitors: beyond the glucocorticoid hypothesis. *Ann N Y Acad Sci* 2002; 971: 554-9.
- Humphries JD, Byron A, Humphries MJ (2006) 'Integrin ligands at a glance', *Journal of Cell Science*. 2006; 119(19).
- Hussein D, Estlin EJ, Dive C, Makin GW. Chronic hypoxia promotes hypoxia-inducible factor-1 α -dependent resistance to etoposide and vincristine in neuroblastoma cells. *Mol Cancer Ther*. 2006 Sep; 5(9):2241-50.

- Hutchison R. On suprarenal sarcoma in children with metastases to the skull. *Q J Med* 1907; 1:33–38.
- Iehara T, Hiyama E, Tajiri T, Yoneda A, Hamazaki M, Fukuzawa M, et al. Is the prognosis of stage 4s neuroblastoma in patients 12 months of age and older really excellent? *European Journal of Cancer* 2012;48:1707– 1712.
- Jaakkola P, Mole DR, Tian YM, Wilson MI, Gielbert J, Gaskell SJ, et al. Targeting of HIF- α to the von Hippel-Lindau ubiquitylation complex by O₂-regulated prolyl hydroxylation. *Science*. 2001; 292(5516):468-72.
- Jin YH, Yoo KJ, Lee YH, Lee SK. Caspase 3-mediated cleavage of p21WAF1/CIP1 associated with the cyclin A-cyclin-dependent kinase 2 complex is a prerequisite for apoptosis in SK-HEP-1 cells. *J Biol Chem*. 2000; 275(39):30256-63.
- Jögi A, Øra I, Nilsson H, Lindeheim A, Makino Y, Poellinger L, Axelson H, Pålman S. Hypoxia alters gene expression in human neuroblastoma cells toward an immature and neural crest-like phenotype. *Proc Natl Acad Sci U S A*. 2002; 99(10):7021-6.
- Jögi A, Vallon-Christersson J, Holmquist L, Axelson H, Borg A, Pålman S. Human neuroblastoma cells exposed to hypoxia: induction of genes associated with growth, survival, and aggressive behaviour. *Exp Cell Res*. 2004; 295(2):469-87.
- Johnson KA, Aplenc R, Bagatell R. Survival by race among children with extracranial solid tumors in the United States between 1985 and 2005. *Pediatr Blood Cancer*. 2011; 56(3):425-31.
- Juárez-Ocaña S, Palma-Padilla V, González-Miranda G, Siordia-Reyes AG, López-Aguilar E, Aguilar-Martínez M, et al. Epidemiological and some clinical characteristics of neuroblastoma in Mexican children (1996-2005). *BMC Cancer*. 2009; 9:266.
- Kaneko Y, Kobayashi H, Watanabe N, Tomioka N, Nakagawara A. Biology of neuroblastomas that were found by mass screening at 6 months of age in Japan. *Pediatric Blood and Cancer* 2006; 46:285–291.
- Karnofsky DA, Ridgway LP, Patterson PA. Tumor transplantation to the chick embryo. *Ann N Y Acad Sci*. 1952; 55(2):313-29.
- Katzenstein HM, Bowman LC, Brodeur GM, Thorner PS, Joshi VV, Smith EI, et al. Prognostic significance of age, MYCN oncogene amplification, tumor cell ploidy, and histology in 110 infants with stage D(S) neuroblastoma: The pediatric oncology group experience—a pediatric oncology group study. *J Clin Oncol* 1998; 16:2007–2017
- Kee Y, Bronner-Fraser M. 'To proliferate or to die: role of Id3 in cell cycle progression and survival of neural crest progenitors', *Genes & Development*, 2005; 19 (6).
- Khayat R, Patt B, Hayes D Jr. Obstructive sleep apnea: the new cardiovascular disease. Part I: Obstructive sleep apnea and the pathogenesis of vascular disease. *Heart Fail Rev*. 2009; 14(3):143-53.
- Kim JW, Tchernyshyov I, Semenza GL, Dang CV. HIF-1-mediated expression of pyruvate dehydrogenase kinase: a metabolic switch required for cellular adaptation to hypoxia. *Cell Metab*. 2006; 3(3):177-85.
- Koivunen P, Hirsilä M, Günzler V, Kivirikko KI, Myllyharju J. Catalytic properties of the asparaginyl hydroxylase (FIH) in the oxygen sensing pathway are distinct from those of its prolyl 4-hydroxylases. *J Biol Chem*. 2004; 279(11):9899-904.
- Koop S, Schmidt EE, MacDonald IC, Morris VL, Khokha R, Grattan M, et al. Independence of metastatic ability and extravasation: metastatic ras-transformed and control fibroblasts extravasate equally well. *Proc Natl Acad Sci U S A*. 1996; 93(20):11080-4.

- Korngold L, Lipari R. Tissue antigens of human tumors grown in rats, hamsters, and eggs. *Cancer Res.* 1955; 15(3):159-61.
- Kozakewich HPW, Perez-Atayde AR, Donovan MJ, Fletcher JA, Estroff JA, Shamberger RC, et al. Cystic neuroblastoma: emphasis on gene expression, morphology and pathogenesis. *Pediatr Dev Pathol* 1998; 1: 17-28.
- Krishnan J, Ahuja P, Bodenmann S, Knapik D, Perriard E, Krek W, et al. Essential role of developmentally activated hypoxia-inducible factor 1alpha for cardiac morphogenesis and function. *Circ Res.* 2008; 103(10):1139-46.
- Krull CE, Lansford R, Gale NW, Collazo A, Marcelle C, Yancopoulos GD, et al. 'Interactions of Eph-related receptors and ligands confer rostrocaudal pattern to trunk neural crest migration', *Current Biology*, 1997, 7 (8), 571-580.
- Kulesa PM, Kasemeier-Kulesa JC, Teddy JM, Margaryan NV, Seftor EA, Seftor RE et al. Reprogramming metastatic melanoma cells to assume a neural crest cell-like phenotype in an embryonic microenvironment. *Proc Natl Acad Sci USA* 2006; 103: 3752–3757.
- Kung AL, Wang S, Kico JM, Kaelin WG, Livingston DM. Suppression of tumor growth through disruption of hypoxia-inducible transcription. *Nat Med.* 2000; 6(12):1335-40.
- Kushner BH, Kramer K, LaQuaglia MP, Modak S, Cheung NK. Neuroblastoma in adolescents and adults: The Memorial Sloan-Kettering experience. *Med Pediatr Oncol* 2003; 41:508–515.
- Lack EE. Tumors of the adrenal gland and extra-adrenal paraganglia. Atlas of tumor pathology, series 3, fascicle 19. Armed Forces Institute of Pathology, Washington DC, 1997.
- Lack EE. Tumors of the autonomic nervous system (including paraganglia). In, CDM Fletcher. Third Edition, *Diagnostic Histopathology of Tumours Vol 2. Neuroblastoma and related tumors, Neuroblastoma and ganglioneuroblastoma.* Elsevier Limited 2007; 28: 1771-1775.
- Lando D, Peet DJ, Gorman JJ, Whelan DA, Whitelaw ML, Bruick RK. FIH-1 is an asparaginyl hydroxylase enzyme that regulates the transcriptional activity of hypoxia-inducible factor. *Genes Dev.* 2002; 16:1466–1471
- Le Douarin N, Fontaine J, Le Lièvre C. New studies on the neural crest origin of the avian ultimobranchial glandular cells--interspecific combinations and cytochemical characterization of C cells based on the uptake of biogenic amine precursors. *Histochemistry.* 1974; 38(4):297-305.
- Le Douarin NM, Teillet M-A. Experimental analysis of the migration and differentiation of neuroblasts of the autonomic nervous system and of neuroectodermal mesenchyme derivatives, using a biological cell marking technique. *Dev. Biol.* 1974; 41:162–184.
- Lee PJ, Jiang BH, Chin BY, Iyer NV, Alam J, Semenza GL, et al. Hypoxia-inducible factor-1 mediates transcriptional activation of the heme oxygenase-1 gene in response to hypoxia. *J Biol Chem.* 1997; 272(9):5375-81.
- Leuenroth SJ, Grutkoski PS, Ayala A, Simms HH. Suppression of PMN apoptosis by hypoxia is dependent on Mcl-1 and MAPK activity. *Surgery.* 2000; 128(2):171-7.
- Li K, Dong K, Gao J, Yao W, Xiao X, Zheng S. Neuroblastoma management in Chinese children. *J Invest Surg.* 2012; 25(2):86-92.
- Light JE, Koyama H, Minturn JE, Ho R, Simpson AM, Iyer R, et al. Clinical significance of NTRK family gene expression in neuroblastomas. *Pediatr Blood Cancer.* 2012; 59(2):226-32.
- Lokman NA, Elder ASF, Ricciardelli C, Oehler MK. Chick Chorioallantoic Membrane (CAM) Assay as an In Vivo Model to Study the Effect of Newly Identified Molecules on Ovarian Cancer Invasion and Metastasis. *Int. J. Mol. Sci.* 2012; 13:9959-9970.

- Lill NL, Grossman SR, Ginsberg D, DeCaprio J, Livingston DM. Binding and modulation of p53 by p300/CBP coactivators. *Nature*. 1997; 387(6635):823-7.
- Luo T, Matsuo-Takasaki M, Sargent TD. Distinct roles for Distal-less genes Dlx3 and Dlx5 in regulating ectodermal development in *Xenopus*. *Mol Reprod Dev*. 2001; 60:331–337.
- MacDonald IC, Schmidt EE, Morris VL, Chambers AF, Groom AC. Intravital videomicroscopy of the chorioallantoic microcirculation: a model system for studying metastasis. *Microvasc Res*. 1992; 44(2):185-99.
- Marión RM, Strati K, Li H, Murga M, Blanco R, Ortega S, et al. A p53-mediated DNA damage response limits reprogramming to ensure iPS cell genomic integrity. *Nature*. 2009; 27;460(7259):1149-53.
- Maris JM, Hogarty MD, Bagatell R, Cohn SL. Neuroblastoma. *Lancet* 2007; 369:2106–20.
- Mascorro JA, Yates RD. Mitotic cell division in the extraadrenal chromaffin system of various species. *J Electron Microscop Tech*. 1989; 12(4):323-30
- Matthay KK, Reynolds CP, Seeger RC, Shimada H, Adkins ES, Haas-Kogan D, et al. Long-term results for children with high-risk neuroblastoma treated on a randomized trial of myeloablative therapy followed by 13-cis-retinoic acid: a children's oncology group study. *J Clin Oncol*. 2009; 27(7):1007-13.
- Maxwell PH, Wiesener MS, Chang GW, Clifford SC, Vaux EC, Cockman ME, et al. The tumour suppressor protein VHL targets hypoxia-inducible factors for oxygen-dependent proteolysis. *Nature*. 1999; 399(6733):271-5.
- Mayer A, Höckel M, Vaupel P. Endogenous Hypoxia Markers: Case Not Proven! In: Kang K A, Harrison DK, Bruley DF. Oxygen Transport to Tissue, XXIX Edition, Vol. 614, Chapter 15, Adv. Exp. Med. Biol. January 2008.
- Mayer A, Höckel M, Vaupel P. Endogenous hypoxia markers in locally advanced cancers of the uterine cervix: reality or wishful thinking? *Strahlenther Onkol*. 2006; 182(9):501-10.
- Mayor R, Morgan R, Sargent MG. Induction of the prospective neural crest of *Xenopus* Development, *Development*. 1995; 121(3):767-77.
- McIntyre A, Patiar S, Wigfield S, Li JL, Ledaki I, Turley H, et al. Carbonic anhydrase IX promotes tumor growth and necrosis in vivo and inhibition enhances anti-VEGF therapy. *Clin Cancer Res*. 2012; 18(11):3100-11.
- McLennan R, Krull CE. 'Ephrin-As cooperate with EphA4 to promote trunk neural crest migration', *Gene Expression*, 2002; 10, 5-6.
- Meulemans D, Bronner-Fraser M. Gene-regulatory interactions in neural crest evolution and development. *Developmental Cell*. 2004; 7(3):291-299.
- Michaelis M, Hinsch N, Michaelis UR, Rothweiler F, Simon T, ilhelm Doerr HW, et al. Chemotherapy-associated angiogenesis in neuroblastoma tumours. *Am J Pathol*. 2012; 180(4):1370-7.
- Mitchell WG, Davalos-Gonzalez Y, Brumm VL, Aller SK, Burger E, Turkel SB, et al. Opsoclonus-ataxia caused by childhood neuroblastoma: developmental and neurologic sequelae. *Pediatrics* 2002; 109:86–98.
- Mohyeldin A, Garzón-Muvdi T, Quiñones-Hinojosa A. Oxygen in stem cell biology: a critical component of the stem cell niche. *Cell Stem Cell*. 2010; 7(2):150-61.

- Mole DR, Schödel J, Oikonomopoulos S, Ragoussis J, Pugh CW, Ratcliffe PJ. High-resolution genome-wide mapping of HIF-binding sites by ChIP-seq. *Blood*. 2011; 117(23):207-17.
- Monclair T, Brodeur GM, Ambros PF, Brisse HJ, Cecchetto G, Holmes K, et al. The International Neuroblastoma Risk Group (INRG) Staging System: An INRG Task Force Report. *J Clin Oncol*. 2009; 27(2):298–303
- Moody AM, Norma AR, Tait D. Paediatric tumours in the adult population: The experience of the Royal Marsden Hospital 1974–1990. *Med Pediatr Oncol*. 1996; 26(3):153-9.
- Mueller BM, Romerdahl CA, Gillies SD, Reisfeld RA. Enhancement of antibody-dependent cytotoxicity with a chimeric anti-GD2 antibody. *J Immunol*. 1990; 144(4):1382-6.
- Mukhopadhyay CK, Mazumder B, Fox PL. Role of hypoxia-inducible factor-1 in transcriptional activation of ceruloplasmin by iron deficiency. *J Biol Chem*. 2000; 275(28):21048-54.
- Mullassery D, Dominici C, Jesudason EC, McDowell HP, Losty PD. Neuroblastoma: contemporary management. *Arch Dis Child Educ Pract Ed*. 2009; 94(6):177-85.
- Nakagawara A, Arima-Nakagawara M, Scavarda NJ, Azar CG, Cantor AB, Brodeur GM. Association between high levels of expression of the TRK gene and favorable outcome in human neuroblastoma. *N Engl J Med*. 1993; 328:847–854.
- Nakagawara A. Molecular basis of spontaneous regression of neuroblastoma: role of neurotrophic signals and genetic abnormalities. *Hum Cell*. 1998; 11:115–124.
- Nakagawara, A. "Neural crest development and neuroblastoma: the genetic and biological link." *Prog Brain Res*. 2004; 146: 233-42.
- Nickerson HJ, Matthay KK, Seeger RC, Brodeur GM, Shimada H, Perez C, et al. Favorable biology and outcome of stage IV-S neuroblastoma with supportive care or minimal therapy: A Children's Cancer Group study. *J Clin Oncol* 2000;18:477–486.
- Noguera R, Fredlund E, Piqueras M, Pietras A, Beckman S, Navarro S, Pålman S. HIF-1alpha and HIF-2alpha are differentially regulated in vivo in neuroblastoma: high HIF-1alpha correlates negatively to advanced clinical stage and tumor vascularization. *Clin Cancer Res*. 2009; 15(23):7130-6.
- Ochiai H, Takenobu H, Nakagawa A, Yamaguchi Y, Kimura M, Ohira M, et al. Bmi1 is a MYCN target gene that regulates tumorigenesis through repression of KIF1B beta and TSLC1 in neuroblastoma. *Oncogene*. 2010; 29:2681–2690.
- Ohira M, Morohashi A, Inuzuka H, Shishikura T, Kawamoto T, Kageyama H, et al. "Expression profiling and characterization of 4200 genes cloned from primary neuroblastomas: identification of 305 genes differentially expressed between favorable and unfavorable subsets." *Oncogene* 2003; 22(35): 5525-36.
- Oppitz M, Busch C, Schriek G, Metzger M, Just L, Drews U. Non-malignant migration of B16 mouse melanoma cells in the neural crest and invasive growth in the eye cup of the chick embryo. *Melanoma Res* 2007; 17: 17–30.
- Ossowski L, Reich E. Experimental model for quantitative study of metastasis. *Cancer Res*. 1980; 40(7):2300-9.
- Owens C, Irwin M. Neuroblastoma: The impact of biology and cooperation leading to personalized treatments. *Critical Reviews in Clinical Laboratory Sciences*. 2012; 49(3): 85–115
- Pàez-Ribes M, Allen E, Hudock J, Takeda T, Okuyama H, Viñals F, et al. Antiangiogenic therapy elicits malignant progression of tumours to increased local invasion and distant metastasis. *Cancer Cell*. 2009; 15(3):220-31.

- Paget S. The distribution of secondary growths in cancer of the breast. *Lancet* 1889; 1:571–573.
- Palma-Padilla V, Juárez-Ocaña S, González-Miranda G, Siordia-Reyes AG, Mejía-Aranguré JM, Carreón-Cruz R, et al. Incidence and trends of neuroblastoma in Mexican children attending at Instituto Mexicano del Seguro Social. *Rev Med Inst Mex Seguro Soc*. 2010; 48(2):151-8.
- Pantel K, Denève E, Nocca D, Coffy A, Vendrell JP, Maudelonde T, et al. Circulating epithelial cells in patients with benign colon diseases. *Clin Chem*. 2012; 58(5):936-40.
- Papandreou I, Cairns RA, Fontana L, Lim AL, Denko NC. HIF-1 mediates adaptation to hypoxia by actively downregulating mitochondrial oxygen consumption. *Cell Metab*. 2006; 3(3):187-97.
- Park JR, Eggert A, Caron H. Neuroblastoma: biology, prognosis, and treatment. *Pediatr Clin North Am*. 2008; 55(1):97-120.
- Pelengaris S, Khan M, Evan G. c-MYC: more than just a matter of life and death. *Nat Rev Cancer*. 2002; 2(10):764-76.
- Petitjean A, Mathe E, Kato S, Ishioka C, Tavtigian SV, Hainaut P, et al. Impact of mutant p53 functional properties on TP53 mutation patterns and tumor phenotype: lessons from recent developments in the IARC TP53 database. *Hum Mutat*. 2007; 28(6):622-9.
- Pfander D, Cramer T, Schipani E, Johnson RS. HIF-1alpha controls extracellular matrix synthesis by epiphyseal chondrocytes. *J Cell Sci*. 2003; 116(Pt 9):1819-26.
- Philip T, Zucker JM, Bernard JL, Lutz P, Bordigoni P, Plouvier E, et al. Improved survival at 2 and 5 years in the LMCE1 unselected group of 72 children with stage IV neuroblastoma older than 1 year of age at diagnosis: is cure possible in a small subgroup? *J Clin Oncol*. 1991; 9(6):1037-44.
- Pilgrim HI. The kinetics of the organ-specific metastasis of a transplantable reticuloendothelial tumour. *Cancer Res*. 1969; 29(6):1200-5.
- Podsypanina K, Du YC, Jechlinger M, Beverly LJ, Hambardzumyan D, Varmus H. Seeding and propagation of untransformed mouse mammary cells in the lung. *Science*. 2008; 321(5897):1841-4.
- Pohl KR, Pritchard J, Wilson J. Neurological sequelae of the dancing eye syndrome. *Eur J Pediatr*. 1996; 155: 237–244.
- Pui CH, Pei D, Pappo AS, Howard SC, Cheng C, Sandlund JT, et al. Treatment outcomes in black and white children with cancer: results from the SEER database and St Jude Children's Research Hospital, 1992 through 2007. *J Clin Oncol*. 2012; 30(16):2005-12.
- Rabadán MA, Usieto S, Lavarino C, Martí E. Identification of a putative transcriptome signature common to neuroblastoma and neural crest cells. *Dev Neurobiol*. 2013 Jun 14. doi: 10.1002/dneu.22099.
- Rafajová M, Zatovicová M, Kettmann R, Pastorek J, Pastoreková S. Induction by hypoxia combined with low glucose or low bicarbonate and high posttranslational stability upon reoxygenation contribute to carbonic anhydrase IX expression in cancer cells. *Int J Oncol*. 2004; 24(4):995-1004.
- Ravi R, Mookerjee B, Bhujwala ZM, Sutter CH, Artemov D, Zeng Q, et al. Regulation of tumor angiogenesis by p53-induced degradation of hypoxia-inducible factor 1alpha. *Genes Dev*. 2000; 14(1):34-44.
- Ribatti D, Nico B, Vacca A, Presta M. The gelatin sponge-chorioallantoic membrane assay. *Nat Protoc*. 2006; 1(1):85-91.
- Rabatti D, Nico B, Vacca A, Roncali L, Burri PH, Djonov V. Chorioallantoic membrane capillary bed: a useful target for studying angiogenesis and anti-angiogenesis in vivo. *Anat Rec*. 2001; 264:317-324.

- Ribatti D, Vacca A, Roncali L, Dammacco F. The chick chorioallantoic membrane as a model for in vivo research on anti-angiogenesis. *Curr Pharm Biotechnol.* 2000; 1:73-82
- Ries LAG, Smith MA, Gurney JG, et al. Cancer incidence and survival among children and adolescents: United States SEER program 1975–1995. NIH publication no. 99-4649. Bethesda, Maryland, USA: National Cancer Institute, SEER Program, 1999.
- Rolfs A, Kvietikova I, Gassmann M, Wenger RH. Oxygen-regulated transferrin expression is mediated by hypoxia-inducible factor-1. *J Biol Chem.* 1997; 272(32):20055-62.
- Romanoff AL. *The avian embryo: structural and functional development.* The Macmillan Company, New York, 1960.
- Rous P, Murphy JB. Tumour implantations in the developing embryo. *J Am Med Assoc* 1911; 56:741.
- Rudnick E, Khakoo Y, Antunes NL, Seeger RC, Brodeur GM, Shimada H, et al. Opsoclonus-myoclonus-ataxia syndrome in neuroblastoma: clinical outcome and antineuronal antibodies—a report from the Children’s Cancer Group Study. *Med Pediatr Oncol* 2001; 36:612–622.
- Ryan HE, Lo J, Johnson RS. HIF-1 alpha is required for solid tumor formation and embryonic vascularization. *EMBO J.* 1998; 17(11):3005-15.
- Santiago, A. & Erickson, C.A. 'Ephrin-B ligands play a dual role in the control of neural crest cell migration', *Development.* 2002; 129(15):3621-3632.
- Schackert G, Fidler IJ. Development of in vivo models for studies of brain metastasis. *Int J Cancer.* 1988; 41(4):589-94.
- Schilling FH, Spix C, Berthold F, Erttmann R, Fehse N, Hero B, et al. Neuroblastoma screening at one year of age. *N Engl J Med.* 2002; 346(14):1047-53.
- Schmidt ML, Lukens JN, Seeger RC, Brodeur GM, Shimada H, Gerbing RB, et al. Biologic factors determine prognosis in infants with stage IV neuroblastoma: a prospective Children’s Cancer Group study. *Journal of Clinical Oncology* 2000; 18:1260–1268.
- Scotting PJ, Walker DA, Perilongo G, et al. "Childhood solid tumours: a developmental disorder." *Nat Rev Cancer.* 2005; 5(6):481-8.
- Semenza GL, Nejfelt MK, Chi SM, Antonarakis SE. Hypoxia-inducible nuclear factors bind to an enhancer element located 3' to the human erythropoietin gene. *Proc Natl Acad Sci U S A.* 1991; 88(13):5680-4.
- Semenza GL, Wang GL. A nuclear factor induced by hypoxia via de novo protein synthesis binds to the human erythropoietin gene enhancer at a site required for transcriptional activation. *Mol Cell Biol.* 1992; 12(12):5447-54.
- Sermeus A, Genin M, Maincent A, Fransolet M, Notte A, Leclere L, et al. Hypoxia-induced modulation of apoptosis and BCL-2 family proteins in different cancer cell types. *PLoS One.* 2012; 7(11):e47519. doi: 10.1371/journal.pone.0047519. Epub 2012 Nov 5.
- Shimada H, Chatten J, Newton WA Jr, Sachs N, Hamoudi AB, Chiba T, et al. Histopathologic prognostic factors in neuroblastic tumors: definition of subtypes of ganglioneuroblastoma and an age-linked classification of neuroblastomas. *J Natl Cancer Inst.* 1984; 73(2):405-16.
- Shimada H, Umehara S, Monobe Y, Hachitanda Y, Nakagawa A, Goto S, et al. International neuroblastoma pathology classification for prognostic evaluation of patients with peripheral neuroblastic tumors: a report from the Children’s Cancer Group. *Cancer.* 2001; 92(9):2451-61.
- Shimoda LA, Fallon M, Pisarcik S, Wang J, Semenza GL. HIF-1 regulates hypoxic induction of NHE1 expression and alkalinization of intracellular pH in pulmonary arterial myocytes. *Am J Physiol Lung Cell Mol Physiol.* 2006; 291(5):L941-9.

- Shuangshoti S, Shuangshoti S, Nuchprayoon I, Kanjanapongkul S, Marrano P, Irwin MS, et al. Natural course of low risk neuroblastoma. *Pediatr Blood Cancer*. 2012; 58(5):690-4.
- Shweiki D, Itin A, Soffer D, Keshet E. Vascular endothelial growth factor induced by hypoxia may mediate hypoxia-initiated angiogenesis. *Nature*. 1992; 359(6398):843-5.
- Simon MC, Keith B. The role of oxygen availability in embryonic development and stem cell function. *Nat Rev Mol Cell Biol*. 2008; 9(4):285-96.
- Slack A, Lozano G, Shohet JM. MDM2 as MYCN transcriptional target: implications for neuroblastoma pathogenesis. *Cancer Lett*. 2005; 228:21–27.
- Sørensen BS, Hao J, Overgaard J, Vorum H, Honoré B, Alsner J, et al. Influence of oxygen concentration and pH on expression of hypoxia induced genes. *Radiother Oncol*. 2005; 76(2):187-93.
- Sowter HM, Ratcliffe PJ, Watson P, Greenberg AH, Harris AL. HIF-1-dependent regulation of hypoxic induction of the cell death factors BNIP3 and NIX in human tumors. *Cancer Res*. 2001; 61(18):6669-73.
- Spix C, Pastore G, Sankila R, Stiller CA, Steliarova-Foucher E. Neuroblastoma incidence and survival in European children (1978–1997): Report from the Automated Childhood Cancer Information System project. *Eur J Cancer*. 2006; 42(13):2081-91
- Squire JA, Thorner P, Marrano P, Parkinson D, Ng YK, Gerrie B, et al. Identification of MYCN Copy Number Heterogeneity by Direct FISH Analysis of Neuroblastoma Preparations. *Mol Diagn*. 1996; 1(4):281-289.
- Stiller CA, Parkin DM. International variations in the incidence of Neuroblastoma. *Int J Cancer*. 1992; 52(4):538-43.
- Stupack DG, Teitz T, Potter MD, Mikolon D, Houghton PJ, Kidd VJ, et al. Potentiation of neuroblastoma metastasis by loss of caspase-8. *Nature*. 2006; 439(7072):95-9.
- Tafreshi NK, Bui MM, Bishop K, Lloyd MC, Enkemann SA, Lopez AS, et al. Noninvasive detection of breast cancer lymph node metastasis using carbonic anhydrases IX and XII targeted imaging probes. *Clin Cancer Res*. 2012; 18(1):207-19.
- Talks KL, Turley H, Gatter KC, Maxwell PH, Pugh CW, Ratcliffe PJ, et al. The expression and distribution of the hypoxia-inducible factors HIF-1alpha and HIF-2alpha in normal human tissues, cancers, and tumor-associated macrophages. *Am J Pathol*. 2000; 157(2):411-21.
- Teitz T, Lahti JM, Kidd VJ. Aggressive childhood neuroblastomas do not express caspase-8: an important component of programmed cell death. *J Mol Med (Berl)*. 2001; 79(8):428-36.
- Thiele CT. Neuroblastoma Cell Lines. In (Ed.) Masters, J. *Human Cell Culture*. Lancaster, UK: Kluwer Academic Publishers. 1998, Vol 1, p 21-53.
- Thiery JP, Duband JL, Delouvee A. 'PATHWAYS AND MECHANISMS OF AVIAN TRUNK NEURAL CREST CELL-MIGRATION AND LOCALIZATION'. *Developmental Biology*. 1982; 93(2):324-343.
- Thiery, J. P. Epithelial–mesenchymal transitions in tumour progression. *Nature Rev*. 2002; Cancer 2, 442–454.
- Thurston G, Suri C, Smith K, McClain J, Sato TN, Yancopoulos GD, et al. Leakage-resistant blood vessels in mice transgenically overexpressing angiopoietin-1. *Science*. 1999; 286(5449):2511-4.
- Tian H, Hammer RE, Matsumoto AM, Russell DW, McKnight SL. The hypoxia-responsive transcription factor EPAS1 is essential for catecholamine homeostasis and protection against heart failure during embryonic development. *Genes Dev*. 1998; 12(21):3320-4.

Tribulo C, Aybar MJ, Nguyen VH, Mullins MC, Mayor R. Regulation of Msx genes by a Bmp gradient is essential for neural crest specification. *Development*. 2003;130:6441–6452.

Tufan AC, Satiroglu-Tufan NL. The chick embryo choriallantoic membrane as a model system for the study of tumour angiogenesis, invasion and development of anti-angiogenic agents. *Curr Cancer Drug Targets*. 2005; 5(4):249-66.

Ullah MS, Davies AJ, Halestrap AP. The plasma membrane lactate transporter MCT4, but not MCT1, is up-regulated by hypoxia through a HIF-1 α -dependent mechanism. *J Biol Chem*. 2006; 281(14):9030-7.

Volm M, Koomägi R. Hypoxia-inducible factor (HIF-1) and its relationship to apoptosis and proliferation in lung cancer. *Anticancer Res*. 2000; 20(3A):1527-33.

Vordermark D, Kaffer A, Riedl S, Katzer A, Flentje M. Characterization of carbonic anhydrase IX (CA IX) as an endogenous marker of chronic hypoxia in live human tumor cells. *Int J Radiat Oncol Biol Phys*. 2005; 61(4):1197-207.

Waldman T, Kinzler KW, Vogelstein B. p21 is necessary for the p53-mediated G1 arrest in human cancer cells. *Cancer Res*. 1995; 55(22):5187-90.

Wang GL, Jiang BH, Rue EA, Semenza GL. Hypoxia-inducible factor 1 is a basic-helix-loop-helix-PAS heterodimer regulated by cellular O₂ tension. *Proc Natl Acad Sci U S A*. 1995; 92(12):5510-4

Wang GL, Semenza GL. Desferrioxamine induces erythropoietin gene expression and hypoxia-inducible factor 1 DNA-binding activity: implications for models of hypoxia signal transduction. *Blood*. 1993; 82(12):3610-5.

Wenger RH, Stiehl DP, Camenisch G. Integration of oxygen signaling at the consensus HRE. *Sci STKE*. 2005;2005 (306):re12.

Wiangnon S, Kamsa-Ard S, Jetsrisuparb A, Sriplung H, Sontipong S, Sumitsawan Y, et al. Childhood cancer in Thailand: 1995-1997. *Asian Pac J Cancer Prev*. 2003; 4(4):337-43.

Wikenheiser J, Doughman YQ, Fisher SA, Watanabe M. Differential levels of tissue hypoxia in the developing chicken heart. *Dev Dyn*. 2006; 235(1):115-23.

Wilting J, Birkenhäger R, Eichmann A, Kurz H, Martiny-Baron G, Marmé D, et al. VEGF121 induces proliferation of vascular endothelial cells and expression of flk-1 without affecting lymphatic vessels of chorioallantoic membrane. *Dev Biol*. 1996; 176(1):76-85.

Wojtkowiak JW, Rothberg JM, Kumar V, Schramm KJ, Haller E, Proemsey JB, et al. Chronic autophagy is a cellular adaptation to tumor acidic pH microenvironments. *Cancer Res*. 2012; 72(16):3938-47.

Woods WG, Gao RN, Shuster JJ, Robison LL, Bernstein M, Weitzman S, et al. Screening of infants and mortality due to neuroblastoma. *N Engl J Med*. 2002; 346(14):1041-6.

Wu X, Bayle JH, Olson D, Levine AJ. The p53-mdm-2 autoregulatory feedback loop. *Genes Dev*. 1993; 7(7A):1126-32

Wykoff CC, Beasley NJ, Watson PH, Turner KJ, Pastorek J, Sibtain A, et al. Hypoxia-inducible expression of tumor-associated carbonic anhydrases. *Cancer Res*. 2000; 60(24):7075-83.

Yamamoto K, Ohta S, Ito E, Hayashi Y, Asami T, Mabuchi O, et al. Marginal decrease in mortality and marked increase in incidence as a result of neuroblastoma screening at 6 months of age: cohort study in seven prefectures in Japan. *J Clin Oncol*. 2002; 20(5):1209-14.

Yamamoto T, Seino Y, Fukumoto H, Koh G, Yano H, Inagaki N, et al. Over-expression of facilitative glucose transporter genes in human cancer. *Biochem Biophys Res Commun*. 1990; 170(1):223-30.

Yu AL, Gilman AL, Ozkaynak MF, London WB, Kreissman SG, Chen HX, et al. Anti-GD2 antibody with GM-CSF, interleukin-2, and isotretinoin for neuroblastoma. *N Engl J Med*. 2010; 363(14):1324-34.

Zelzer E, Levy Y, Kahana C, Shilo BZ, Rubinstein M, Cohen B. Insulin induces transcription of target genes through the hypoxia-inducible factor HIF-1alpha/ARNT. *EMBO J*. 1998; 17(17):5085-94.

Zhang H, Pu J, Qi T, Qi M, Yang C, Li S, et al. MicroRNA-145 inhibits the growth, invasion, metastasis and angiogenesis of neuroblastoma cells through targeting hypoxia-inducible factor 2 alpha. *Oncogene*. 2012. doi: 10.1038/onc.2012.574. [Epub ahead of print]

Zhong H, De Marzo AM, Laughner E, Lim M, Hilton DA, Zagzag D, et al. Overexpression of hypoxia-inducible factor 1alpha in common human cancers and their metastases. *Cancer Res*. 1999; 59(22):5830-5.

Zijlstra A, Aimes RT, Zhu D, Regazzoni K, Kupriyanova T, Seandel M, et al. Collagenolysis-dependent angiogenesis mediated by matrix metalloproteinase-13 (collagenase-3). *J Biol Chem*. 2004; 279(26):27633-45.

Zijlstra A, Seandel M, Kupriyanova TA, Partridge JJ, Madsen MA, Hahn-Dantona EA, et al. Proangiogenic role of neutrophil-like inflammatory heterophils during neovascularization induced by growth factors and human tumor cells. *Blood*. 2006; 107(1):317-27.

Zimling ZG, Rechnitzer C, Rasmussen M, Petersen BL. Familial neuroblastoma – different histological manifestations in a family with three affected individuals. *APMIS: Acta Pathologica, Microbiologica et Immunologica Scandinavica* 2004; 112:153–158.

5.1. Web References

1. German Childhood Cancer Registry, accessed 24th October 2012. <http://www.kinderkrebsregister.de/english/content08.html>
2. The Sympathetic Nervous System – Regions commonly affected by neuroblastoma, accessed 19th July 2013. http://drugline.org/img/term/system-sympathetic-nervous-14642_3.jpg
3. Microscopic picture of Homer Wright Rosettes taken by the US Armed Forces Institute of Pathology, published online by Wikipedia 7th July 2008, accessed 19th July 2013. <http://commons.wikimedia.org/wiki/File:Rosette.jpg>
4. World Health Organisation, Health topics, Infant, Newborn. Accessed 14th October 2013. http://www.who.int/topics/infant_newborn/en/